

**IMPROVED SAFETY PERFORMANCE
FUNCTIONS FOR SIGNALIZED
INTERSECTIONS**

Final Report

SPR 756



Oregon Department of Transportation

IMPROVED SAFETY PERFORMANCE FUNCTIONS FOR SIGNALIZED INTERSECTIONS

Final Report

SPR 756

by

Karen Dixon, Texas A&M Transportation Institute
Chris Monsere, Portland State University
Raul Avelar, Texas A&M Transportation Institute
Joel Barnett, Portland State University
Paty Escobar, Texas A&M Transportation Institute
Sirisha Kothuri, Portland State University
Yi Wang, Portland State University

for

Oregon Department of Transportation
Research Section
555 13th Street NE, Suite 1
Salem OR 97301

and

Federal Highway Administration
400 Seventh Street, SW
Washington, DC 20590-0003

August 2015

<p>1. Report No. FHWA-OR-RD-16-03</p>	<p>2. Government Accession No.</p>	<p>3. Recipient's Catalog No.</p>
<p>4. Title and Subtitle Improved Safety Performance Functions for Signalized Intersections</p>		<p>5. Report Date -August 2015-</p>
<p>7. Author(s) Karen Dixon, Texas A&M Transportation Institute Chris Monsere, Portland State University Raul Avelar, Texas A&M Transportation Institute Joel Barnett, Portland State University Paty Escobar, Texas A&M Transportation Institute Sirisha Kothuri, Portland State University Yi Wang, Portland State University</p>		<p>6. Performing Organization Code</p> <p>8. Performing Organization Report No.</p>
<p>9. Performing Organization Name and Address Oregon Department of Transportation Research Section 555 13th Street NE, Suite 1 Salem, OR 97301</p>		<p>10. Work Unit No. (TRAIS)</p>
<p>12. Sponsoring Agency Name and Address Oregon Dept. of Transportation Research Section and Federal Highway Admin. 555 13th Street NE, Suite 1 400 Seventh Street, SW Salem, OR 97301 Washington, DC 20590-0003</p>		<p>11. Contract or Grant No. SPR 756</p>
		<p>13. Type of Report and Period Covered Final Report</p>
		<p>14. Sponsoring Agency Code</p>
<p>15. Supplementary Notes</p>		

16. Abstract

For this effort, the research team developed new safety performance functions (SPFs) for signalized intersections in Oregon. The modeling dataset consisted of 964 crashes from a total of 73 intersections that were randomly selected based on the presence of a traffic signal (identified through the crash data records). The SPFs were developed using a Poisson-lognormal Generalized Linear Mixed model framework for total crashes and severe injury crashes (coded as KAB). Three SPFs were developed: 1) an SPF for total crashes, which relies on both major and minor AADTs to predict the expected number of crashes; 2) an SPF for KAB crashes, whose predictions derive from both AADTs as well as from the speed limit on the major road; and (3) a severity model to predict the proportion of KAB crashes to be used in combination with the SPF for total crashes. The research analyses determined that the speed limit variable significantly improved the quality of the SPFs and severity model, and as expected, suggests increasing severity with speed differentials. The models were validated spatially and temporally based on additional sites and using an additional year of data. The models all performed well during the validation; however enhanced models to improve model reliability were developed based on the larger dataset. As part of the model development, this research also explored a variety of rules to identify crashes as intersection-related based on the crash geo-location (including the common 250 feet rule). Crashes were manually classified from the combined data available from the geo-location of crashes, the geometric database, and the various fields in the Oregon crash database. These classifications were then compared to a number of rule options for classifying them as intersection crashes. The analysis revealed that the best performing rule is to use crashes that were geo-located within 300 feet of the centerline intersection at signalized locations plus crashes where the crash report indicates that they were associated with a traffic control device (i.e. traffic signal). Finally, this research effort developed models to estimate minor road AADT for use in safety analysis where this exposure information is not available. These models were developed from data from 66 intersections with known minor and major AADT volumes and validated with data from another 25 intersections. Significant model variables included major AADT, number of approach lanes, functional class, presence of a two-way left-turn lane, and parallel road AADT.

17. Key Words

18. Distribution Statement

Copies available from NTIS, and online at http://www.oregon.gov/ODOT/TD/TP_RES/

19. Security Classification
(of this report)
Unclassified

20. Security Classification
(of this page)
Unclassified

21. No. of Pages
174

22. Price

SI* (MODERN METRIC) CONVERSION FACTORS

APPROXIMATE CONVERSIONS TO SI UNITS					APPROXIMATE CONVERSIONS FROM SI UNITS				
Symbol	When You Know	Multiply By	To Find	Symbol	Symbol	When You Know	Multiply By	To Find	Symbol
<u>LENGTH</u>					<u>LENGTH</u>				
in	inches	25.4	millimeters	mm	mm	millimeters	0.039	inches	in
ft	feet	0.305	meters	m	m	meters	3.28	feet	ft
yd	yards	0.914	meters	m	m	meters	1.09	yards	yd
mi	miles	1.61	kilometers	km	km	kilometers	0.621	miles	mi
<u>AREA</u>					<u>AREA</u>				
in ²	square inches	645.2	millimeters squared	mm ²	mm ²	millimeters squared	0.0016	square inches	in ²
ft ²	square feet	0.093	meters squared	m ²	m ²	meters squared	10.764	square feet	ft ²
yd ²	square yards	0.836	meters squared	m ²	m ²	meters squared	1.196	square yards	yd ²
ac	acres	0.405	hectares	ha	ha	hectares	2.47	acres	ac
mi ²	square miles	2.59	kilometers squared	km ²	km ²	kilometers squared	0.386	square miles	mi ²
<u>VOLUME</u>					<u>VOLUME</u>				
fl oz	fluid ounces	29.57	milliliters	ml	ml	milliliters	0.034	fluid ounces	fl oz
gal	gallons	3.785	liters	L	L	liters	0.264	gallons	gal
ft ³	cubic feet	0.028	meters cubed	m ³	m ³	meters cubed	35.315	cubic feet	ft ³
yd ³	cubic yards	0.765	meters cubed	m ³	m ³	meters cubed	1.308	cubic yards	yd ³
NOTE: Volumes greater than 1000 L shall be shown in m ³ .									
<u>MASS</u>					<u>MASS</u>				
oz	ounces	28.35	grams	g	g	grams	0.035	ounces	oz
lb	pounds	0.454	kilograms	kg	kg	kilograms	2.205	pounds	lb
T	short tons (2000 lb)	0.907	megagrams	Mg	Mg	megagrams	1.102	short tons (2000 lb)	T
<u>TEMPERATURE (exact)</u>					<u>TEMPERATURE (exact)</u>				
°F	Fahrenheit	(F-32)/1.8	Celsius	°C	°C	Celsius	1.8C+32	Fahrenheit	°F

*SI is the symbol for the International System of Measurement

ACKNOWLEDGEMENTS

The research included in this report was sponsored by the Oregon Department of Transportation (ODOT). The project team would like to thank the research staff at ODOT and the members of the Technical Advisory Committee for their oversight and guidance in the performance of this research effort.

DISCLAIMER

This document is disseminated under the sponsorship of the Oregon Department of Transportation and the United States Department of Transportation in the interest of information exchange. The State of Oregon and the United States Government assume no liability of its contents or use thereof.

The contents of this report reflect the view of the authors who are solely responsible for the facts and accuracy of the material presented. The contents do not necessarily reflect the official views of the Oregon Department of Transportation or the United States Department of Transportation.

The State of Oregon and the United States Government do not endorse products of manufacturers. Trademarks or manufacturers' names appear herein only because they are considered essential to the object of this document.

This report does not constitute a standard, specification, or regulation.

EXECUTIVE SUMMARY

This *Final Report* documents a research effort to develop improved safety performance functions (SPFs) for signalized intersections in the State of Oregon. In particular, this research effort focused on the relationship between the physical characteristics of the signalized intersection, the crash history at each location, and the approach speed (represented by speed limit). In addition to developing SPFs for signalized intersection crash prediction for total crashes and severe injury crashes, the research also included an estimation procedure for minor road annual average daily traffic (AADT) values. The research team also re-assessed and ultimately developed a reliable procedure as to how to define an intersection-related crash.

Chapter 1 introduces the project and reviews the specific objectives of this research effort. Chapter 2 of this report includes a literature review summarizing the many known factors that influence crashes at signalized intersections as well as current estimation procedures for crashes and AADT values. Chapter 3 then presents an overview of the site selection and final sites selected for the SPF development and validation activities. Chapter 4 reviews the method developed for estimating minor road traffic volumes, and Chapter 5 similarly presents the analysis method and findings for defining intersection-related crashes and then developing SPFs for total and severe injury crashes. The report concludes with Chapter 6 (summary of findings), Chapter 7 (references), and Appendices A - D.

TABLE OF CONTENTS

1.0	EACH CHAPTER HEADING USES STYLE HEADING 1	1
2.0	LITERATURE REVIEW	3
2.1	CALIBRATION OF HSM MODELS	3
2.2	DEPENDENT VARIABLES	4
2.2.1	<i>Spatial Level of Aggregation</i>	4
2.2.2	<i>Crash Type</i>	5
2.2.2.1	Angle Crashes	5
2.2.2.2	Left-Turning Crashes	6
2.2.2.3	Rear-End	6
2.2.2.4	Crash Severity	6
2.3	INFLUENCING FACTORS	7
2.3.1	<i>Traffic Characteristics</i>	7
2.3.1.1	Volume.....	8
2.3.1.2	Vehicle Type.....	8
2.3.1.3	Functional Classification.....	8
2.3.2	<i>Traffic Control and Operational Features</i>	8
2.3.2.1	Speed Limit.....	9
2.3.2.2	Lighting.....	10
2.3.2.3	Signal Head Visibility	11
2.3.2.4	Presence of Advanced Warning Signs.....	11
2.3.2.5	Traffic Signal Phasing.....	11
2.3.3	<i>Geometric Characteristics</i>	12
2.3.3.1	Approach Lane.....	12
2.3.3.2	Distance / Spatial.....	13
2.3.3.3	Land Use	13
2.3.4	<i>Other</i>	14
2.3.4.1	Driver Characteristics.....	14
2.3.4.2	Environmental	14
2.4	MODELING TECHNIQUES	15
2.4.1	<i>Negative Binomial</i>	15
2.4.2	<i>Probit</i>	15
2.4.3	<i>Generalized Additive Model</i>	15
2.4.4	<i>Generalized Estimating Equations</i>	16
2.4.5	<i>Logit</i>	16
2.4.6	<i>Multilevel</i>	16
2.5	ESTIMATING MINOR VOLUMES.....	17
2.5.1	<i>Travel Demand Modeling</i>	17
2.5.2	<i>Geospatial Methods</i>	17
2.5.3	<i>Regression Methods</i>	17
2.5.3.1	Ordinary Least Squares	17
2.5.3.2	Geographically Weighted Regression	18
2.6	SUMMARY OF LITERATURE FINDINGS	18
3.0	DATA AND DATA COLLECTION	21
3.1	SITE IDENTIFICATION AND SELECTION	21
3.1.1	<i>Identifying Candidate Intersections</i>	21
3.1.2	<i>Study Sample</i>	23
3.1.3	<i>Study Sample for Model Validation</i>	26
3.2	DATA COLLECTION FOR SPF DEVELOPMENT	28
3.2.1	<i>Candidate Roadway Variables</i>	29
3.2.2	<i>Crash Data</i>	32

3.3	DATA COLLECTION FOR MINOR ROAD AADT ESTIMATION	33
4.0	ESTIMATING MINOR VOLUMES	35
4.1	DATA.....	35
4.1.1	<i>Average Annual Daily Traffic</i>	35
4.1.2	<i>Functional Class</i>	36
4.1.3	<i>Land Use and Demographic</i>	36
4.1.4	<i>Network</i>	36
4.2	MODELING APPROACH	37
4.3	RESULTS.....	39
4.3.1	<i>Descriptive Statistics</i>	39
4.3.2	<i>Models to Estimate Total Minor Entering Volume (AADT)</i>	41
4.3.3	<i>Models to Estimate Minor Volume by Leg</i>	44
4.4	REVIEW OF AADT MODEL VALIDATION	47
4.5	SUMMARY	48
4.5.1	<i>Sample Application</i>	49
5.0	SAFETY ANALYSIS FOR SIGNALIZED INTERSECTIONS	51
5.1	MATCHING CRASHES AND INTERSECTIONS.....	51
5.1.1	<i>Investigating a Threshold for Distance from Intersection for Crash Classification in Oregon</i>	51
5.2	METHODOLOGY	52
5.2.1	<i>Manual Classification of Intersection Crashes</i>	53
5.2.2	<i>Manual Classification of Intersection Related Crashes</i>	54
5.2.3	<i>Statistical Analysis on Distance, Speed Limit and Max IFA for Intersection Crash Classification</i>	56
5.2.3.1	<i>Developing Screening Rules based on Statistical Models</i>	57
5.2.4	<i>Evaluation of Crash Screening Methods using the Validation Subset</i>	58
5.2.4.1	<i>Measures of Effectiveness</i>	58
5.2.4.2	<i>Classic Crash Screening Method Validation Analysis</i>	59
5.2.4.3	<i>Leave-One-Out Cross Validation Analysis</i>	60
5.2.5	<i>Summary of Evaluation of IR Screening Methods</i>	62
5.3	SPF DEVELOPMENT	63
5.3.1	<i>Statistical Methodology for Initial Model Development</i>	63
5.3.1.1	<i>Implications of Selected Statistical Methodology for Crash Prediction</i>	64
5.3.1.2	<i>Dataset Characteristics</i>	65
5.3.2	<i>Initial SPF for Total Crashes</i>	68
5.3.3	<i>Initial SPF for KAB Crashes</i>	73
5.4	INITIAL PROBABILITY-BASED SEVERITY MODEL	78
5.5	SPF VALIDATION OVERVIEW	81
5.5.1	<i>Temporal Transferability</i>	82
5.5.2	<i>Spatial Transferability</i>	82
5.5.3	<i>Spatial Temporal Transferability</i>	83
5.6	DEVELOPING ENHANCED SPF MODELS	83
5.6.1	<i>Characteristics of Assembled Dataset for Model Updates</i>	83
5.6.2	<i>Enhanced SPF for Total Crashes</i>	84
5.6.2.1	<i>Fit Assessment</i>	85
5.6.3	<i>Enhanced Probability-Based Severity Model</i>	87
5.7	EXAMPLE PROBLEMS APPLYING SPFS.....	88
5.7.1	<i>Example Use of Total Crash Model</i>	88
5.7.2	<i>Example Use of the Crash Severity Model</i>	89
5.8	SUMMARY OF WORK.....	90
6.0	CONCLUSIONS AND RECOMMENDATIONS.....	93
7.0	REFERENCES.....	97

APPENDICES

- APPENDIX A: SUPPLEMENTAL TABLES AND EXAMPLE DATA COLLECTION
- APPENDIX B: AADT CONVERSION METHODOLOGY
- APPENDIX C: AADT MODEL VALIDATION
- APPENDIX D: PREDICTIVE METHOD VALIDATION
- APPENDIX E: INTERSECTION SITE INFORMATION (SEPARATE DOCUMENT)
- APPENDIX F: VALIDATION SITE INFORMATION (SEPARATE DOCUMENT)

LIST OF TABLES

Table 3.1: Preliminary Random Sample of Intersections	22
Table 3.2: Region 1 Random Sample of Sites	24
Table 3.3: Region 2 Random Sample of Sites	25
Table 3.4: Region 3 Random Sample of Sites	25
Table 3.5: Region 4 Random Sample of Sites	26
Table 3.6: Region 5 Random Sample of Sites	26
Table 3.7: Region 1 Validation Sites	27
Table 3.8: Region 2 Validation of Sites	27
Table 3.9: Region 3 Validation Sites	28
Table 3.10: Region 4 Validation Sites	28
Table 3.11: Region 5 Validation Sites	28
Table 3.12: Site Data and Corresponding Collection Method	29
Table 3.13: Location and Geometric Configuration for Intersection #1	31
Table 3.14: Lane Geometry – Intersection #1	32
Table 4.1: Types of Intersection Approaches Minor Volume Models	40
Table 4.2: Descriptive Statistics for Minor Volume Models	40
Table 4.3: Summary of Categorical Variables for Minor Volume Models	41
Table 4.4: Model Outputs for Total Minor Entering Volume, Two-way Major and Minor Roads (with Parallel Facility)	42
Table 4.5: Model Outputs Total Minor Entering Volume, Two-way Major and Minor Roads (without Parallel Facility)	43
Table 4.6: Model Outputs for Minor Volume Estimation Model By Leg (with Parallel Facility AADT)	45
Table 4.7: Model Outputs for Minor Volume Estimation Model By Leg (without Parallel Facility AADT)	46
Table 5.1: Predictors included in Probability Models Developed	57
Table 5.2: Performance of Screening Methods on Validation Data	59
Table 5.3: Performance of Screening Methods using LOOCV	61
Table 5.4: Yearly Statistics for Complete Intersection-year Data. Years 2010-2012	66
Table 5.5: Analysis of Deviance for Full and Reduced Models	69
Table 5.6: Coefficient Estimates for Reduced Model	69
Table 5.7: Analysis of Deviance for Full and Reduced Models	74
Table 5.8: AIC, BIC, LogLikelihood and Deviance Comparisons for Mod3 and Mod4	75
Table 5.9: Coefficient Estimates for Recommended KAB SPF	75
Table 5.10: Analysis of Deviance for Parsimonious and Extended Models	78
Table 5.11: Coefficient Estimates for Initial Probability-Based Severity Model	79
Table 5.12: Yearly Statistics for Complete 2010-2013 Dataset for Updating the Models	84
Table 5.13: Updated Coefficient Estimates for Total Crashes SPF	84
Table 5.14: Coefficient Estimates for Reduced Model	87
Table 5.15: Table of Road Characteristics for an Example Intersection	88
Table 6.1: Equations to Estimate the Minor Road Volume	94
Table 6.2: Enhanced SPFs to Estimate Crashes at Signalized Intersections in Oregon	95

LIST OF FIGURES

Figure 3.1: Stratified Random Sample (50 Intersections).....	23
Figure 3.2: Validation Stratified Random Sample (35 Intersections).....	27
Figure 3.3: Data Collection Form Photos	30
Figure 4.1: Example Parallel Facility AADT	36
Figure 4.2: Sample Images Showing GIS Network Information.....	37
Figure 4.3: Adjusted AADT for Use in the Volume by Leg Models.....	39
Figure 4.4: Diagnostic Plots for Total Minor Entering Volume (with Parallel Facility AADT)	44
Figure 4.5: Diagnostic Plots for Total Minor Entering Volume (without Parallel Facility AADT)	44
Figure 4.6: Summary Diagnostic Plots for Minor Volume Estimate by Leg (with Parallel Facility AADT).....	47
Figure 4.7: Summary Diagnostic Plots for Minor Volume Estimate by Leg (without Parallel Facility AADT).....	47
Figure 5.1: Sample Sites with Buffers at Various Radii	52
Figure 5.2: Sample Sites of various IFA Radii	53
Figure 5.3: Sample Site at Low Speed Limit Urban Area	54
Figure 5.4: Probability curves from DS mod (left) and SL mod (right)	57
Figure 5.5: Performance Comparison of Screening Methods.....	62
Figure 5.6: Correlations Among Variables in Complete Dataset	67
Figure 5.7: Scatter Plot of ln(KAB Crashes) and Critical Variables in the Complete Dataset	68
Figure 5.8: Q-Q Plot of Intersection Random Effect.....	70
Figure 5.9: Marginal Distribution Fit of Model Parameters Specific to Modeling Data	71
Figure 5.10: Marginal Distribution Fit of Model Parameters Projected to the Population	71
Figure 5.11: Marginal Distribution of Data and the Two Fits of Proposed SPF.....	72
Figure 5.12: CURE Plots for Major and Minor AADTs.....	73
Figure 5.13: Q-Q Plot of Intersection Random Effect in KAB Model	76
Figure 5.14: Marginal Distribution Fit of KAB SPF to Data and Population Projection	77
Figure 5.15: CURE Plots for Major SpLim and ModAADT.....	77
Figure 5.16: KAB Proportion of Crashes vs. Severity Model Prediction by Minor AADT	80
Figure 5.17: Severity Model Prediction vs Major AADT	81
Figure 5.18: Original and Updated SPFs for Minor AADT of 7,000 vpd	85
Figure 5.19: Q-Q Plot of Intersection Random Effect in Updated Model	86
Figure 5.20: Theoretical and Observed Marginal Distributions of Sites by Total Crash Frequencies for Period 2010-2013	86
Figure 5.21: CURE Plots for Updated Total Crashes SPF	87
Figure 5.22: Original and Updated Severity Models for Minor Speed Limit of 30 mph.....	88

1.0 EACH CHAPTER HEADING USES STYLE HEADING 1

The effective identification, prioritization, and application of safety treatments will each require an understanding of the complex interaction between the elements of roadway design, infrastructure, and traffic. This is particularly true in an environment of limited funding, since large scale improvements will be increasingly difficult to implement and lower cost targeted solutions will be more common. Techniques available in the American Association of Highway and Transportation Officials (AASHTO) *Highway Safety Manual* (HSM) are helping the Oregon Department of Transportation (ODOT) staff complete the analysis needed to identify solutions suitable to address the causes of crashes. Due to the high percentage of crashes occurring at signalized intersections, considerable attention is required for the effective selection of improvement strategies that will result in the greatest reduction in crashes for dollars invested at these critical locations. ODOT has been researching the data needs and implementing the HSM within current procedures when possible but has identified limitations that affect the reliability of the results when the study site is a signalized intersection.

The HSM includes Safety Performance Functions (SPFs) to assess options for improving the safety of intersections. These are statistically-derived equations that use traffic volumes and other factors to predict crash reductions for various types of improvements. Since the SPFs do not allow for certain features such as turn lanes and lane widths, Crash Modification Factors (CMFs) can then be used to adjust the results of the equations to address these factors. Currently the available safety assessment SPF tools do not explicitly include consideration of approach speeds, yet it is widely accepted that speed affects both the frequency and the severity of crashes. The initial predictive models upon which the HSM procedure is based focused on rural two-lane highways and the approach speed at those intersections was not deemed to be significant. This foundation work then was used to define the SPF format for future models for the first edition of the HSM, so speed was excluded as a critical input variable in subsequent studies where SPFs were developed for other types of facilities.

The question of including speed in the SPF process is frequently raised by the engineering community. The research effort summarized in this *Final Report* focuses on determining the safety impact of different speed limits at signalized intersections in Oregon.

The research includes three key efforts:

- Estimating minor road traffic volumes at signalized intersections (see Chapter 4),
- Determining if a crash should be identified as intersection-related (see Chapter 5), and
- Developing updated SPFs for Oregon signalized intersections (also included in Chapter 5).

The overall objective of this research effort, therefore, is to develop more reliable ways to assess signalized intersection safety in Oregon so that ODOT and other agencies can allocate funding resources towards effective intersection safety configurations for both new and existing facilities. This Final Report summarizes the models developed for this purpose. Chapter 2.0 of this report presents a brief literature review. Chapter 3.0 next addresses the site selection and data collection sampling effort. Chapter 4.0 reviews the minor road AADT estimation analysis. Chapter 5.0 then presents the intersection-related crash evaluation followed by the SPF development. Chapter 6.0 then summarized the findings. Finally, cited references are summarized in Chapter 7.0. The report appendices (Chapters 8.0 through 13.0) include a list of abbreviations used in this report, the key for the data collection form, a review of AADT conversion methodology, an overview of the AADT model validation, a similar overview of the SPF validation, the detailed site information for the 50 study sites identified for initial SPF development, and the detailed site information for the 35 study sites used for model validation activities.

2.0 LITERATURE REVIEW

A variety of methods have been used to estimate crash frequency at signalized intersections. Most notably, the HSM (*AASHTO 2010*) provides SPFs derived from negative binomial regression that, once calibrated for local conditions, can be used in any jurisdiction. The first edition of the HSM included four types of signalized intersection SPFs:

- Rural Two-Lane Four-Legged Signalized Intersections (R4SG2),
- Rural Multi-Lane Highway Signalized Intersections (R4SG4),
- Urban/Suburban Arterial Three-Legged Signalized Intersections (U3SG), and
- Urban/Suburban Arterial Four-Legged Signalized Intersections (U4SG).

Each of the HSM signalized intersection SPFs is associated with a set of defined base conditions. Any features that differ from these established base conditions must be considered explicitly through the application of multiplicative CMFs. The R4SG2 models have base conditions that assume no lighting, skew of zero degrees, and no left and right turn lanes that are not stop-controlled. The U3SG and U4SG intersections have base conditions that assume no left-turn lane, no right-turn lane, permissive left turn phase, right turn permitted on red, and no lighting. The R4SG4 does not have specified base conditions. The HSM base condition SPFs are based on data from multiple states and for similar intersections.

The purpose of this literature review is to identify the key decision and predictor variables for generation of jurisdiction specific SPFs for ODOT. A prior report (SPR 667) studied the safety performance of Oregon's intersections (*Monsere et al. 2011*). This report included a thorough review of relevant work published prior to 2005. This literature review, therefore, focuses on any research related to intersection safety performance modeling or safety effect estimation published since 2005. The review is organized around the modeling framework. The first section reviews other efforts to calibrate the HSM models. The second section review the various approaches used to establish candidate dependent variables. This review is then followed by a summary of influencing variables that have been included in the models or analysis. Finally, the review identifies the various statistical approaches that have been used for these studies.

2.1 CALIBRATION OF HSM MODELS

Recent studies in Virginia and Ohio suggest that the SPFs included in the HSM can under predict crashes in these jurisdictions even after calibration (*Garber et al. 2010; Young and Park 2012*). For these and other reasons, some agencies have elected to develop their own SPFs rather than calibrate the HSM models. Young and Park (*Young and Park 2012*) calibrated the HSM's SPFs and compared them to jurisdiction specific SPFs for the city of Regina, Saskatchewan. Models

were developed using volume and road characteristics as predictors for total collisions, fatal/injury collisions, and property damage only collisions occurring in 2005 through 2009. Comparison of the calibrated HSM SPFs and the jurisdiction specific SPFs suggested that calibrated HSM SPFs under predicted the crashes for Regina.

Garber et al. (*Garber et al. 2010*) used negative binomial models to calibrate SPFs developed using Ohio data for the Virginia Department of Transportation. The jurisdiction specific SPFs predicted crash frequency better than the Ohio data generated functions used in the AASHTOWare software program SafetyAnalyst.

Dixon et al. (*Dixon et al. 2012*) calibrated the HSM SPFs for both segments and intersections based on the HSM calibration procedures. The authors concluded that the use of severity-based calibration factors were more appropriate due to the current crash reporting procedures in Oregon. Also, the calibration factor for urban four-lane divided facilities should not be used due to the small available sample size of this type of road segment in Oregon. For SPFs that use proportional adjustments for crash severity and unique CMFs, the Oregon researchers also recommended using locally computed proportions rather than the HSM default values.

2.2 DEPENDENT VARIABLES

The development of SPFs often requires that total crashes be modeled due to sample size issues; however, the literature and practice suggest that improved safety performance models may be feasible if models for specific crash types can be estimated. At intersections, multi-vehicle crashes are the most common crash types (e.g. rear-end and angle crashes) that might merit unique sub-models. The models in the HSM urban and suburban chapter model multiple and single vehicle crashes separately. In the HSM approach, severity and collision-type are estimated with proportioning factors that convert the frequency predictions into severity or collision-type predictions. For modeling purposes, the dependent variable is some form of crash frequency. The majority of studies reviewed total crashes, crash type, and/or crash severity.

2.2.1 Spatial Level of Aggregation

Crash prediction models are typically based on crashes that have been grouped to a common spatial unit (e.g. intersection or approach leg). In the studies reviewed, grouping crashes by intersection helped researchers to capture the influences of various intersection features (*Miller et al. 2011; Jonsson et al. 2007; Abdel-Aty and Haleem 2011; Wang and Abdel-Aty 2006; Wang and Abdel-Aty 2007; Wang and Abdel-Aty 2008; Kim and Washington 2006; Yan et al. 2005; Chen et al. 2012a; Mitra and Washington 2012; Qi et al. 2013; Chen et al. 2012b; Yan et al. 2008; Davis and Aul 2007; Souleyrette et al. 2007; Li and Tarko 2011; Bullough et al. 2013; Das and Abdel-Aty 2008; Wang et al. 2008; Li and Lee 2011*). Researchers studying advanced warning, speed limit reductions, lane width, and signal visibility used intersection approach as a way of grouping crashes (*Potts et al. 2013; Potts et al. 2007; Sayed et al. 2008; Wu et al. 2013; Sharma et al. 2012; Appiah et al. 2011*). Two studies involving segments were reviewed: Stephan and Newstead (*Stephan and Newstead 2012*) studied the natural and built environment along signalized urban arterials and Ma et al. (*Ma et al. 2010*) examined the severity of crashes along rural two-lane highways. Finally, Wang and Abdel-Aty (*Wang and Abdel-Aty 2007*) grouped crashes by associating the crash to the major or minor roadway approach.

2.2.2 Crash Type

Miller et al. (*Miller et al. 2011*) explored crash causality at intersections using a disaggregated approach to crash prediction. In the study, the researchers used six years of crash data (2000-2005) to mine patterns at 72,218 crashes at more than 6,000 signalized and unsignalized intersections in Virginia. Vehicle speed, driver action, alignment, lighting, weather, traffic control, driver visibility obstruction, volume, shoulder width, and surface conditions were identified as important crash factors in 25 of 51 classification trees. The researchers also generated negative binomial generalized linear models to investigate total crashes, injury crashes, rear-end crashes, and angle crashes concluding that disaggregating by crash type was generally more accurate when compared to models generated using total crashes.

Jonsson et al. (*Jonsson et al. 2007*) estimated crash prediction models to investigate the effects of traffic and geometry on four different crashes types in rural California: opposite direction, same direction, intersecting (angle), and single-vehicle. Traffic characteristics, geometric features, and crash data from 1993-2002 for 264 four-leg stop-controlled intersections and 378 three-leg stop-controlled intersections resulting in 2,676 crashes were modeled with negative binomial regression. As a result of the modeling effort, the researchers found that when prediction models are categorized by the defined crash-types, they will have different significant variables for both three-leg intersections and four-leg intersections.

2.2.2.1 Angle Crashes

Abdel-Aty and Haleem (*Abdel-Aty and Haleem 2011*) compared multinomial adaptive regression splines (MARS) and negative binomial regression techniques to estimate angle crash frequency at 2,475 three- and four-legged unsignalized intersections located in six different counties in Florida. The researchers found that significant predictors of angle crashes included the major traffic volume, distance to nearest upstream signal, distance to nearest intersection, median type, percentage of heavy vehicles, size of intersection, and geographic location. In prior work, Wang and Abdel-Aty (*Wang and Abdel-Aty 2007*) investigated collisions involving two through movement vehicles conflicting at a right-angle. They evaluated a total of 197 signalized intersections located in central Florida and used generalized estimating equations to account for site correlation. The research determined that significant predictors of right-angle crashes were the product of through volumes, number of through lanes, and late night and early morning traffic signal flashing-mode operations. The research also identified speed limit, skew, yellow and all-red intervals, and the presence of left-turn bay offset as significant predictors of right-angle crashes.

Kim and Washington (*Kim and Washington 2006*) used a limited-information maximum likelihood estimation approach to account for endogeneity between left-turn lanes and angle crashes using data collected at 155 rural intersections in 38 counties of Georgia. A total of 155 intersections (113 unsignalized intersections and 42 signalized intersections) experienced 317 angle crashes within 250 feet of the intersection. The study found that when accounting for endogeneity between left-turn lanes and angle crashes, left-turn lanes reduced angle crashes. The study also determined that when endogeneity is not accounted for, left-turn lanes appear to increase angle crashes.

2.2.2.2 Left-Turning Crashes

Wang and Abdel-Aty (*Wang and Abdel-Aty 2008*) investigated left-turn crash frequency at 197 four-legged signalized intersections located in Orange and Hillsborough counties in Florida. The researchers assembled and modeled crash data (2000-2005), traffic data, and intersection characteristics in an effort to evaluate the causality of left-turn crashes. The modeling effort for left-turn crash occurrence by pattern type consistently indicated that crash occurrence was related to entering flows of the colliding vehicles, and not the total entering volume at the intersection. Wang and Adbel-Aty determined that for four of the nine crash patterns approach speed limit was a significant predictor of left-turn crash occurrence.

Yan and Radwan (*Yan and Radwan 2008*) studied 72,912 crashes that occurred during the years 1999 through 2001 in Florida to identify crash risk associated with unprotected left-turn crashes at signalized intersections using logistic regression. Results indicated that type of vehicle (excluding van) and driver age (under the age of 65) had negative effects. Driver-related factors, non-local versus local, driver age (greater than 65 compared to less than 18), alcohol, physical defect, and gender had positive effects on crashes.

2.2.2.3 Rear-End

Wang and Abdel-Aty (*Wang and Abdel-Aty 2006*) used generalized estimating equations (GEE) with a negative binomial link function to investigate the temporal and spatial relationships of rear-end crashes. The Florida researchers collected geometric, traffic exposure, traffic control, and crash data at 208 signalized intersections for the time period of 2001-2003. They performed spatial analysis by grouping 476 intersections along 41 corridors based on density in central Florida and modeling total rear-end crashes from 1999 and 2000. The analysis identified traffic volume, number of turn lanes, number of phases per cycle, speed limits, and higher population areas as items significantly correlated with rear-end crash frequencies.

Yan et al. (*Yan et al. 2005*) investigated the relationship of rear-end crashes at signalized intersections using multiple logistic regression. Their analysis of 7666 rear-end crashes suggested significant relationships between rear-end crashes and road environmental factors, as well as vehicle type, driver age, driver residence, and gender for both the struck vehicle role and the striking vehicle role. Additionally, they found that driver factors such as alcohol or drug use were significant.

2.2.2.4 Crash Severity

Crash severity can be modeled by separate models that estimate frequency (such as in the HSM approaches for some models). In other modeling approaches, the risk factors can be explored using logistic approaches. Savolainen et al. (*Savolainen et al. 2011*) reviewed 133 previous research efforts describing logit, probit, neural networks, and classification trees used to model crash severity. In their review, the authors concluded that

endogeneity, underreporting, and the correlation effects of multiple injuries within the same crash or within a small period of time are concerns in modeling severity.

In models particular to intersections, Chen et al. (*Chen et al. 2012a*) used logistic regression to study severity of injuries to vehicle occupants and intersection crashes using nine years of crash data (n=12,144 crashes) from Victoria, Australia. Chen et al. identified seven significant independent variables for the prediction of crash severity: driver gender, driver age, speed zone, traffic control, time of day, crash type, and seat belt usage. Sayed et al. (*Sayed et al. 2008*) conducted a before-and-after study investigating the safety impacts of improved signal visibility at 175 four-legged signalized intersections. The study sites each had an approach speed of approximately 30 miles per hour (mph) (50 kilometers per hour (kph)). Visibility improvements included increasing the signal lens size, new backboards, addition of reflective tape, and providing additional signal heads. They then used five generalized linear models to predict crash severity based on major and minor average annual daily traffic (AADT). Signal visibility did not have a significant effect on combined fatal and injury crashes. Property Damage Only (PDO), daytime, nighttime, and total collisions each experienced significant decreases in crash frequency.

Anastasopoulos and Mannering (*Anastasopoulos and Mannering 2011*) compared the use of random parameter logit models with fixed parameter logit models. They predicted crash severity using geometrics, traffic characteristics, socioeconomic, and collision characteristics. The fixed parameters model performed better in predicting crash severity than the random parameters models, though the random parameters predicted within five percent of the fixed parameters.

Finally, Ye and Lord (*Ye and Lord 2011*) modeled crash severity using multinomial logit (MNL), mixed logit (ML), and ordered probit methodologies to compare the effects of underreporting. Ye and Lord used simulated crash data and the Monte Carlo approach for four years (1998-2001) of observed crashes (26,175 usable records). Results indicated that underreporting occurred in all three model methodologies. The authors recommended using fatalities as the baseline for MNL and ML models, while the ordered probit model should use a descending order from fatal to PDO.

2.3 INFLUENCING FACTORS

The research team reviewed the published literature and identified several safety performance factors to consider. These items include traffic characteristics, traffic control and operational features, geometric characteristics, and select other factors. These items are reviewed in the following sections.

2.3.1 Traffic Characteristics

Key influential traffic characteristics identified in the literature included traffic volume, vehicle type, and functional classification as reviewed in the following sections.

2.3.1.1 Volume

A large body of work confirmed a positive relationship between increasing traffic volume and crashes. Specifically related to intersection research, major and minor volumes were most often used as separate independent variables (*Li and Lee 2011; Bullough et al. 2013; Davis and Aul 2007; Appiah et al. 2011; Sayed et al. 2008; Jonsson et al. 2007; Kim and Washington 2006; Wang and Abdel-Aty 2006*). Other studies included the major volumes or entering volumes only (*Abdel-Aty and Haleem 2011; Wang and Abdel-Aty 2007; Wang and Abdel-Aty 2008; Stephan and Newstead 2012; Potts et al. 2007; Sharma et al. 2012; Souleyrette et al. 2007; Li and Tarko 2011; Wang et al. 2008*). Several studies that only examined crashes in approach lanes or where crashes were due to turning movements included turning movement counts in the models (*Wang et al. 2008; Wu et al. 2013; Potts et al. 2013*).

2.3.1.2 Vehicle Type

Yan et al. (*Yan et al. 2005*) used logistic regression to contrast heavy vehicles, light trucks, and vans to the reference category of cars. They observed that all three larger vehicle types were more likely to be involved in rear-end crashes than the more prevalent passenger car. Abdel-Aty and Haleem (*Abdel-Aty and Haleem 2011*) found that angle crash frequency was predicted to increase with an increase in heavy vehicle traffic. Similarly, Sharma et al. (*Sharma et al. 2012*) and Wu et al. (*Wu et al. 2013*) found a positive relationship between heavy vehicles and crash frequency. However, Bullough et al. (*Bullough et al. 2013*) found that an increase in the percentage of heavy vehicles during daylight hours had a negative effect on crash frequency as did an increase during the nighttime hours.

2.3.1.3 Functional Classification

Miller et al. (*Miller et al. 2011*) compared crash experience based on road functional classification for arterials and roads that were not arterial. The researchers identified a significant positive relationship between principal arterials and total crashes, injury crashes, and angle crashes. Stephan and Newstead (*Stephan and Newstead 2012*) studied the effects of urban natural and built environments on segment crashes finding that principal arterials were more likely to have a crash than non-principal arterials. Ma et al. (*Ma et al. 2010*) used multivariate Poisson lognormal methods to expose a positive relationship for collectors on possible injuries, non-disabling injuries, disabling injuries, and fatalities. In comparison, minor arterials were found to have smaller positive effects on crash severity.

2.3.2 Traffic Control and Operational Features

Traffic control and operational features, as identified in the published literature, that have been determined to influence safety performance include speed, lighting, signal head visibility, presence of advanced warning signs, and traffic signal phasing.

2.3.2.1 Speed Limit

Speed is an important descriptor of traffic operations that has an effect on crash severity and frequency but this variable is difficult to accurately capture in aggregate models. In particular, the exact speed of the crash involved vehicle is rarely known with certainty. To attempt to capture speed effects, most researchers have used posted speed by approach. Mitra and Washington (*Mitra and Washington 2012*) studied 15,245 crashes occurring at 291 intersections in Tuscon, Arizona between 2001 and 2004. Spatial proximity to schools and drinking establishments, weather, and demographic data were used to explore the relationship between crashes and these often omitted variables in crash prediction models. They found that higher posted speed along the minor approach had an increasing effect on crash frequency. Conversely, Mitra and Washington observed that elevated major road speeds had a significant negative relationship with crash frequency. The authors suggest that tandem effects are likely due to differences between actual and posted speeds, as well as the effects of different design standards of facilities associated with posted speeds.

Das and Abdel-Aty (*Das and Abdel-Aty 2008*) developed models by aggregating crashes by varying the intersection influence area by 50 feet intervals. They determined that speed limit had a positive relationship with crash severity at all modeled influence areas. Yan and Radwan (*Yan and Radwan 2008*) found left-turn crash occurrence was highest at intersections with a posted speed limit of 45 mph when compared to other speed limits. Davis and Aul (*Davis and Aul 2007*) concluded that signalized intersections converted from stop-controlled intersections with approach speeds greater than 40 mph experienced a significant increase in rear-end crashes, and a decrease in right-angle crashes. Souleyrette et al. (*Souleyrette et al. 2007*) found that implementation of all-red intervals did not have a significant increase in safety benefit for signalized intersections with an approach speed of 30 mph or greater.

Using multivariate Poisson-lognormal techniques, Ma et al. (*Ma et al. 2010*) found that an increase in the posted speed limit of 10 mph would result in an increase in fatal and disabling-injury types. Intuitively, PDO crashes were found to decrease suggesting an overall increase in severity with an increase of intersection speed.

Abdel-Aty and Haleem (*Abdel-Aty and Haleem 2011*) included a predictor in the MARS analysis of three-leg and four-leg unsignalized intersections categorizing speed limit as equal to or greater than 45 mph or less than 45 mph. Results indicated that at three-leg intersections speed limits of 45 mph or greater were more likely to result in angle crashes.

Wang and Abdel-Aty (*Wang and Abdel-Aty 2007*) found that an increase in speed limit has an insignificant positive relationship with right-angle crashes. In further work, Wang and Abdel-Aty (*Wang and Abdel-Aty 2008*) found that speed limit was a significant positive predictor of left-turn crashes involving opposing direction vehicles. Results from this study also suggested a positive but not statistically significant relationship between speed limit and crashes involving vehicles approaching from the left. Yan et al. (*Yan et al. 2005*) found that rear-end crashes were more likely to occur with increasing

likelihood at posted speed limits from 35 mph to 55 mph than intersections with a posted speed limit of 25 mph.

Sharma et al. (*Sharma et al. 2012*) studied the effect of speed limit reductions in the vicinity of 28 high-speed signalized Nebraska intersections equipped with advanced warning flashers to understand the safety impacts of five and ten mph speed limit reductions. Quantile regression analysis indicated that a signed 15 mph reduction was not statistically significant. A five mph posted reduction was not statistically significant in reducing crash severity, but was found to have significant decreasing effect of 0.6 crashes per approach.

Wu et al. (*Wu et al. 2013*) investigated the safety impacts of implemented speed reductions with advanced flashers on approach to signalized intersections located on 56 major approaches. Nested-logit models were developed using ten years of crash data from 2001 through 2010. Contradictory results were found with a posted static speed reduction on the intersection approach of five mph. Results indicated that the smaller reduction decreased the probability of visible injury, but increased the probability of no injury, possible injury, incapacitating injuries, and fatalities. Reductions of ten mph significantly increased the probability of no injury.

Finally, El-Shawarby et al. (*El-Shawarby et al. 2011*) studied driver running behavior of yellow and red phases at high-speed intersections. Male drivers were observed to be less likely to proceed at the onset of the yellow phase when compared to female drivers. Also, drivers aged 60 years or older were significantly less likely to clear the intersection with shorter detection distances.

2.3.2.2 Lighting

Bullough et al. (*Bullough et al. 2013*) studied the safety effects of lighting at 5,578 unsignalized and 886 signalized intersections in Pennsylvania. The expected crashes per year for daytime and nighttime were calculated using a negative binomial model with independent categorical variables of signalization, land-use, lighting, skew, speed, access control, depressed median, and paved-left shoulder. Lighting was found to have a negative relationship to crash frequency, but it was observed that daytime crash frequency increased by five to eight percent. The authors suggest this is due to the presence of light poles near the intersection. Similar results were found by Shankar et al. (*Shankar et al. 2010*) who used negative binomial models to predict crash frequency with crash data from Minnesota and California at signalized and unsignalized intersections. Results suggest that the presence of lighting had a decreasing effect on crashes for both urban/suburban and rural signalized intersections.

In similar, sometimes parallel, research authors controlled for day and night conditions finding a lower likelihood of crashes at intersections in daylight conditions (*Yan and Radwan 2008; Das and Abdel-Aty 2008*). Other reviewed studies considered only the presence of lighting, and found that lighting had a negative relationship with crash occurrence (*Yan and Radwan 2008; Souleyrette et al. 2007; Jonsson et al. 2007*).

2.3.2.3 Signal Head Visibility

Souleyrette et al. (*Souleyrette et al. 2007*) found a positive relationship between total crashes and all configurations other than overhead signals in one direction in a study of the safety impacts of all-red intervals at low speed, urban intersections. Sayed et al. (*Sayed et al. 2008*) conducted a before-and-after study investigating the safety impacts of improved signal visibility at 175 four-legged signalized intersections with an approach speed of approximately 30 mph (50 kph). Visibility improvements included increasing the signal lens size, new backboards, addition of reflective tape, and providing additional signal heads. Five generalized linear models were used to predict crash severity using major and minor AADT. Signal visibility did not have a significant effect on combined fatal and injury crashes. PDO, daytime, nighttime, and total collisions were all found to have significant decreases in crash frequency.

2.3.2.4 Presence of Advanced Warning Signs

Appiah et al. (*Appiah et al. 2011*) studied the behavior of drivers approaching dilemma zones at intersections with actuated advanced warning system to determine if the system promotes decreases in crash rates over time. The study included 26 system implemented intersections compared to 29 control intersections in Nebraska. The researchers used Bayesian techniques in a before-after study of crash frequency at the high-speed intersections. The application of the advanced warning system suggested an improvement in safety, especially in right-angle crashes which experienced a 43.6 percent reduction in occurrence at the implemented intersections. In similar research, Wu et al. (*Wu et al. 2013*) addressed the safety impacts at signalized intersections equipped with advanced warning flashers and speed reductions finding that flashing time of the warning signs was not significant in predicting crashes.

2.3.2.5 Traffic Signal Phasing

Various crash prediction studies have included traffic signal phasing and phasing components. Mitra and Washington (*Mitra and Washington 2012*) found that the number of signal phases at an intersection have a positive relationship with total intersection crashes. Three of the studies addressed or included left-turn phases. Chen et al. (*Chen et al. 2012b*) conducted a before and after study investigating the safety impacts of changing permissive left-turn signal phasing to protective at 68 signalized intersections using negative binomial regression with the GEE technique. Chen et al. determined that no significant decreases in crashes occurred when left-turn phasing was changed to protected/permissive left-turn phasing as compared to permissive-only signal phasing. Davis and Aul (*Davis and Aul 2007*) studied the safety impacts of different left-turn phases at two major approaches and four minor approaches with an approach speed greater than 40 mph and concluded that a changing of the left-turn phase from permissive/protective to protected had a decreasing effect on total left-turn crashes and major approach left-turn crashes. Conversely, Wang et al. (*Wang et al. 2008*) found that protected left-turns were positively related to crash occurrence. The authors suggest that the positive relationship could explain an increase in rear-end crash types.

Souleyrette et al. (*Souleyrette et al. 2007*) explored the safety impacts of all-red intervals on 104 signalized intersections in Minneapolis, Minnesota. The study intersections had an approach speed of 30 mph. They used a generalized linear mixed model to predict crash frequency. Results of the model found no safety benefit with the overall use of all-red intervals but safety benefits were observed at individual sites. Li and Tarko (*Li and Tarko 2011*) developed multinomial logit models to estimate probability of crashes at signalized intersections along corridors with coordinated phases. Three coordinated systems (encompassing 18 intersections that experienced a total of 1,345 crashes between 2003 and 2006 in Indiana) were the focus of the evaluation. Higher concentrations of arrivals in the first half of the red phase, in the presence of short yellow intervals, and within the first two seconds of green were associated with an increase in the likelihood of rear-end and right-angle crashes. Additionally, variables based on the maximum green were significant for the second-half of green phase arrivals, first half of red phase arrivals, and traffic for the first two seconds of the green phase while no minimum green phase, or mid-point variables were significant allowing the authors to postulate that signals that reach the force-off may be related to an increase in the likelihood of crashes. Also, right angle crashes are more likely to occur at the beginning of the red phase. Wang et al. (*Wang et al. 2008*) found that signal coordination also had a positive effect on crashes when modeled at a fixed influence zone of 250 feet and then at a varied influence distance determined by intersection features and furthest crash distance. Finally, Wang and Abdel-Aty (*Wang and Abdel-Aty2008*) found that late night and early morning yellow flashing operations had a positive effect on right angle crashes.

2.3.3 Geometric Characteristics

Geometric characteristics that influence safety performance include the approach lane features, the intersection influence areas, and the adjacent land use.

2.3.3.1 Approach Lane

Potts et al. (*Potts et al. 2013*) studied 400 intersection approaches in Toronto, Canada evaluating the safety of the channelized right-turn lanes, shared through/right-turn, and conventional right-turn lanes. The research results suggested that all right-turn treatment types exhibited similar safety performance. As part of a larger study, Potts et al. (*Potts et al. 2007*) studied the safety impact of lane widths on arterial intersection approaches in Minnesota (707 intersections) and North Carolina (635 intersections). They designed a cross-sectional modeling approach using average daily traffic (ADT) and lane width to develop negative binomial models. Results indicated that increasing lane width had a significant negative effect on fatal-injury single and multiple vehicle crashes for three-legged signalized intersections.

Jonson et al. (*Jonson et al. 2007*) found that left-turn channelization and number of lanes were significant variables in models predicting same direction crashes for four-leg intersections. Other research controlled for number of lanes as a continuous variable and found that the likelihood of crashes increases with an increase in the number of lanes (*Stephan and Newstead 2012; Chen et al. 2012b*).

In another approach, Wang and Abdel-Aty (*Wang and Abdel-Aty 2007*) grouped lanes into four different subsets: two and three lanes; four and five lanes; six lanes; and seven, eight, and nine lanes. They observed a negative relationship with right-angle crash occurrence with an increase in the number of lanes. Yan et al. (*Yan et al. 2005*) also found a negative relationship between roadways with an increasing number of lanes and rear-end crashes. Qi et al. (*Qi et al. 2013*) investigated a total of 235 crashes at 21 intersections with and without turn lane queue overflow problems in Houston and Austin, Texas. Crash rates at intersections were predicted using negative binomial models. Results indicated that intersections with turn lane queue overflow problems had 35 percent higher predicted rear-end crash rates than intersections without overflow problems. Simulation-based analysis reflected that extension of left-turn lanes would have resulted in a decrease in rear-end crash occurrence.

2.3.3.2 Distance / Spatial

Das and Abdel-Aty (*Das and Abdel-Aty 2008*) used influence areas varying from zero to 200 feet to study the impacts of surface, weather, and traffic conditions on crash severity. Results suggested that the magnitude of effect on crash severity increased with an increased influence area for roadway width and median width.

Wang et al. (*Wang et al. 2008*) studied 177 signalized intersections in Florida with the objective of investigating the safety influence area for four-legged intersections. The study intersections had 7,758 observed crashes over a period of 2000-2005. The authors concluded that the influence area varies depending on intersection features (i.e. length of left-turn lane, speed limit, etc.) thus all features should be taken into consideration when determining the influence distance at the intersection. Li and Lee (*Li and Lee 2011*) used geographically-weighted regression models to estimate crash severity at urban intersections in Chicago, Illinois. The models incorporated spatial distribution of the intersections by assigning higher weights to decreasing distances between intersections. Li and Lee tested the geographically weighted regression (GWR) models assuming lognormal and negative binomial distributions against global models concluding that GWR models (lognormal) better predict crash severity.

2.3.3.3 Land Use

Stephan and Newstead (*Stephan and Newstead 2012*) studied 141 road segments near strip shopping malls in the Melbourne, Australia metropolitan area to investigate the impacts of complex urban environments on safety. They developed crash prediction models to study the relationship between total number of crashes and segment characteristics. Results indicated that increasing complexity (measured as traffic density, number of lanes, and higher access densities) had a positive relationship with increased crash risk, defined by the total crashes within each segment. Reduced crash risk was associated with the presence of median or traffic islands and less complex roadside environments such as natural areas buffering pedestrians and motor vehicles.

Ma et al. (*Ma et al. 2010*), in a study of 108 signalized intersections and 123.5 kilometers of roadway segments in Beijing, China, investigated urban environment effects on crash

severity. They observed that crashes on sharper horizontal curves were more likely to result in severe crashes, and increased shoulder widths were more likely to result in less severe crashes. The authors suggested that less complex road designs tend to decrease crash severity.

2.3.4 Other

In addition to the built environment, researchers have studied a variety of other items including driver demographics, socioeconomic characteristics, and the natural environment.

2.3.4.1 Driver Characteristics

Chen et al. (*Chen et al. 2012a*) found that male drivers and lack of seat belt usage were more likely to be involved in fatal crashes in a study of risk factors associated with crash severity at signalized intersections. The research also indicated that drivers age 65 years or older were more likely to be involved in fatal crashes than younger drivers. Yan et al. (*Yan et al. 2008*) found that crashes involving male drivers were less likely to be involved in left-turn crashes. The researchers also found that ages 56-65 were less likely to be involved in a left-turn crash compared to drivers less than 18 years of age, but less of a decrease in likelihood when compared to drivers of ages 18-55. Drivers 66 years of age or older were more likely than drivers less than 18 years of age of being involved in left-turn crashes.

Wu et al. (*Wu et al. 2013*) used a nested logit model to examine safety impacts of dynamic warning message signs at high-speed signalized intersections. Severity level was described by four variables in the upper nest; no injury, lower intermediate injury, incapacitating injury, and fatal injury. The lower nest further defined 'lower intermediate injury' as possible injury and visible injury. Crashes involving at-fault male drivers were less likely to result in crash severity level of lower intermediate injury, specifically visible injury. Additionally, alcohol was found to have a higher likelihood of incapacitating injury and fatal injury. Das and Abdel-Aty (*Das and Abdel-Aty 2008*) also found that alcohol had a positive relationship with crash severity.

2.3.4.2 Environmental

Yan and Radwan (*Yan and Radwan 2008*) evaluated factors involved with left-turn crashes at signalized intersections and found that crashes during rainy weather are less likely than during clear weather. The authors suggest that the reported decrease in crash risk was due to more cautious driver behavior.

Jonsson et al. (*Jonsson et al. 2007*) used type of terrain to model single vehicle crashes at three-leg and four-leg intersections. They determined that when compared to flat terrain, mountainous terrain was found to have a significant positive influence on single vehicle crashes at three-leg intersections while rolling and mountainous terrain had a significant positive influence on single vehicle crashes at four-leg intersections.

Ma et al. (*Ma et al. 2010*) found that a two degree increase in roadway gradient contributed to a decrease of 12.41 percent in fatal crashes, but increased disabling (24.88 percent), non-disabling (30.93 percent), possible (27.62 percent), PDO (24.07 percent), and total crashes (24.86 percent). Also, a two degree increase in degree of curvature contributed to an increase in crashes for all severity levels. In comparison, mountainous terrain typically associated with steep gradients and sharp degrees of curvature were found to have a positive relationship on PDO and fatal crash severity levels. In addition, the researchers identified negative but statistically insignificant relationships were found for possible and non-disabling severity levels, but were statistically insignificant.

2.4 MODELING TECHNIQUES

Various methodologies have been explored to improve or account for correlations between variables. Novel approaches, such as generalized additive models, were attempted to apply non-linear modeling techniques to predict crashes. In other research, techniques such as generalized estimating equations, multilevel, probit, and logit techniques were utilized and compared to the state of the practice count models (Poisson and negative binomial techniques).

2.4.1 Negative Binomial

Kweon (*Kweon 2011*) investigated four-legged signalized intersections with the objective of developing a tool for identifying high-risk intersections by traffic movements and time of day. Using crash data from 2001 through 2004, Kweon developed negative binomial and Poisson model based safety performance functions using crash patterns, flow, and time of day for data at 35 signalized intersections.

Lord and Park (*Lord and Park 2008*) compared varying and fixed parameters negative binomial approaches on rural three-legged intersections in California. Comparison between the traditional negative binomial models and generalized negative binomial model suggested that generalized negative binomial models can rank some sites as more hazardous when compared to the traditional negative binomial and may not be suitable for empirical Bayes (EB) methods.

2.4.2 Probit

Chiou et al. (*Chiou et al. 2013*) comparatively fit a bivariate generalized ordered probit (BGOP) with a bivariate ordered probit (BOP) model to two-vehicle crashes at signalized intersections in Taipei, Taiwan. The BGOP was found to predict crash severity better than the conventional BOP. Castro et al. (*Castro et al. 2012*) used a special case generalized ordered response probit model to estimate crash frequency in Arlington, Texas using a latent continuous variable divided into intervals to account for time-varying and spatial effects.

2.4.3 Generalized Additive Model

Xie and Zhang (*Xie and Zhang 2008*) compared generalized linear models (GLMs) and generalized additive models (GAMs) using crash data from 59 signalized intersections in Toronto, Canada. Negative binomial distributions for both methodologies were assumed to

account for over dispersion. The authors concluded that GAMs can generate statistically interpretable results and offer useful nonlinear modeling techniques.

2.4.4 Generalized Estimating Equations

Wang and Abdel-Aty (*Wang and Abdel-Aty 2007, 2008*) used GEE to account for correlation in repeated observations. Negative binomial regression and GEE with negative binomial regression were used to model left-turn crash occurrence at signalized intersections to account for site correlation.

2.4.5 Logit

Anastasopoulos and Mannering (*Anastasopoulos and Mannering 2011*) compared the use of random parameter logit models with fixed parameter logit models. Geometrics, traffic characteristics, socioeconomic, and collision characteristics were used to predict crash severity. The fixed parameters model performed better in predicting crash severity than the random parameters models, though the random parameters predicted within five percent of the fixed parameters.

Ye and Lord (*Ye and Lord 2011*) modeled crash severity using MNL, ML, and ordered probit (OP) methodologies to compare the effects of underreporting. Simulated crash data was used using the Monte Carlo approach as well as four years (1998-2001) of observed crashes (26,175 usable records). Results indicated that underreporting occurred in all three model methodologies. The authors recommend using fatalities as baseline for MNL and ML models, whilst the OP model should use a descending order from fatal to PDO.

2.4.6 Multilevel

Multilevel models have also been used to predict crashes in recent years. Kim et al. (*Kim et al. 2007*) explored the application of binomial multilevel models using 548 crashes from 91 two-lane rural intersections in Georgia. A multilevel model was developed for each of five crash types (angle, head-on, rear-end, sideswipe-same direction, sideswipe-opposite direction) to study the interactions between observed and environmental factors and the crash type. The authors found that rural intersections can be modeled using a multilevel techniques to overcome the correlation between crashes at each hierarchy.

Huang et al. (*Huang et al. 2008*) used a Bayesian hierarchical approach to crash prediction to account for the multilevel structure of crash information within datasets. Geographic region, traffic, crash, driver-vehicle, and vehicle-occupant were the proposed levels for the employed methodology. The results demonstrate that accounting for the heterogeneity between the groups is important in crash prediction models and can be accomplished through Bayesian hierarchical methods.

A study in Shanghai, China of 195 signalized intersections within 22 urban corridors was conducted using hierarchical models to predict crashes to account for the correlation between signalized intersections within a corridor. Xie et al. (*Xie et al. 2012*) suggest that the hierarchical negative binomial performed better than the Poisson hierarchical in predicting crashes. Results

also suggested that increasing exposure elements at the intersection level as well as increasing average speeds at the corridor level contributed to higher crash occurrence.

2.5 ESTIMATING MINOR VOLUMES

This section provides a comprehensive discussion of the methods used to estimate traffic volumes on roadways that are not traditionally part of counting programs.

2.5.1 Travel Demand Modeling

One approach towards estimating volumes is to employ the four step travel demand modeling processes. Zhong and Hanson (*Zhong and Hanson 2009*) estimated volumes using TransCAD's built-in four step model for New Brunswick, Canada and found that traffic assignment to only 65 percent of the network forced overestimated traffic on the roadway network. Wang (*Wang 2012*) estimated AADT for local roads using parcel-level travel demand analysis with Institute of Transportation Engineering (ITE) trip generation rates, the gravity model for trip distribution, and equilibrium assignment.

2.5.2 Geospatial Methods

Generally, spatial methods approach estimation of AADT values by attaching weights that decrease with an increase in Euclidean or network distance between the measured traffic count and the estimation location. Wang and Kockelman (*Wang and Kockelman 2009*) used short term program counts to test the ability of Kriging to estimate AADT in Texas. They identified an overall median error percentage of 33 percent with larger errors on low volume roadways and underestimation on high volume roadways. The error was attributed to the non-inclusion of variables such as number of lanes, speed limit, and functional class. Selby and Kockelman (*Selby and Kockelman 2011*) explored the same data set accounting for speed, number of lanes, employment per acre, population per acre, and functional class as covariates. While these variables decreased the absolute error within mini-regions, they had limited effect on the high error percentages associated with low-volume counts.

Pulugurtha and Kasam (*Pulugurtha and Kasam 2012*) investigated the effects of polygon-based network buffers compared to Euclidean distances in Charlotte, North Carolina. Bandwidths of one, one and a half, two, three, four, and five mile distances were compared to similar circular buffers defined by Euclidean radii. Minor thoroughfare volumes were estimated by urban indicator, upstream link speed limit, and rural district indicator. The researchers concluded that negative binomial regression performed better than Poisson, and modeling by functional class performed better than an overall model.

2.5.3 Regression Methods

2.5.3.1 Ordinary Least Squares

Mohamad et al. (*Mohamad et al. 1998*) used multiple regression to estimate AADT on urban and rural county roads using county population, the number of occupied housing units (number of households), county vehicle registration, county employment, and per

capita income at the county level. The final model contained four variables: location, accessibility, county arterial road mileage, and county population accounting for 75 percent of the variation in traffic volumes.

Xia et al. (Xia et al. 1999) used ordinary least squares (OLS) regression to estimate the volumes of 450 non-state urbanized roads in Florida. The resultant model included number of lanes, functional class, land-use, auto-ownership, proximity to county roads, and service employment. Seaver et al. (Seaver et al. 2000) developed regression models using traffic volumes collected on 1213 local roads in Georgia. They evaluated 45 independent variables covering population demographics, education, transportation, income, employment, farming, and urbanization using principal component analysis and regression. Ultimately they developed two sets of models to account for road-types within and outside of a metropolitan statistical area. Of the three models for rural paved roads outside of metropolitan statistical areas, the prediction R^2 values were 0.74, 0.81, and 0.96 with small sample sizes used to calibrated the models ($n=17$, $n=19$, and $n=22$, respectively).

Zhao and Chung (Zhao and Chung 2001) estimated volumes using OLS for roads in Broward County, Florida. The independent variables used were number of lanes, functional class, direct access to expressways, employment within varying Euclidean distances, and accessibility. The Florida researchers generated four models with the best model performance of $R^2 = 0.818$. Dixon et al. (Dixon et al 2012) estimated minor AADT for rural roadways using county and nearest city populations, regional average per capita income, distance to the freeway, functional classification, within a city boundary, presence of a minor and/or major right turn lane, land-use, centerline, and striped edge lines. The resulting analysis generated two models, one model for rural roadways ($R^2=0.62$), and another for use when estimating minor volumes at minor road four-leg signalized intersections ($R^2=0.64$).

2.5.3.2 Geographically Weighted Regression

Zhao and Park (Zhao and Park 2004) developed geographically weighted regression models to estimate AADT in Broward County, Florida. They used five independent variables: number of lanes, population concentration, employment concentration, regional accessibility, whether or not the road that had the count station was directly connected to an expressway. The authors concluded that GWR models predict better than OLS regression due to the ability of the models to better explain the variation in data by accounting for spatial variation in the predictor variables.

2.6 SUMMARY OF LITERATURE FINDINGS

This chapter provided an overview of recent safety research related to the development and calibration of signalized intersection safety performance models. Three critical crash types common to these intersections and as summarized in the literature included angle, left-turning, and rear-end crashes. In addition, much of the literature addressed the development of crash severity models so that the user can better understand what the expected levels of injury may be for crashes at a specific location. The literature review also highlighted a variety of influencing

factors broadly grouped into the categories of traffic characteristics, traffic control and operational features, geometric characteristics, and various other factors such as driver demographics, socioeconomic characteristics, and the natural environment.

This chapter concluded with an evaluation of recent modeling efforts. This included a wide variety of recent modeling techniques used to assess safety at similar locations and past research modeling efforts for generating AADT values using a variety of approaches. While complex methodologies have the capacity to generate more accurate results than regression methods, they are limited in application for practitioners due to the complex, time-consuming modeling processes. The resulting methodology of preference is OLS regression.

3.0 DATA AND DATA COLLECTION

The initial data collection effort for this study required the identification and selection of candidate study locations. Since the focus of the study is on signalized intersections in Oregon, the research team developed a strategy for identifying potential intersections while minimizing the likelihood of selection bias. Following site identification and selection, the research team collected comprehensive data for each intersection. In a supplemental effort, the research team also acquired data to facilitate the development of an estimation procedure for minor road traffic volumes at signalized locations. Sections 3.1, 3.2, and 3.3 describe these site identification and data collection efforts.

3.1 SITE IDENTIFICATION AND SELECTION

During the initial stages of this project, the research team explored the feasibility of using an existing signalized intersection database for Oregon roadways and determined that this type of comprehensive database does not exist. Consequently, the research team developed a strategy for identifying candidate intersections and selecting potential intersections to study. Upon development of this site identification procedure, the research team then developed a sample of sufficient size to perform the model development activities. These two tasks are reviewed in Sections 3.1.1 and 3.1.2.

3.1.1 Identifying Candidate Intersections

As previously noted, the identification of study sites for this research effort is not straightforward since the researchers could not locate a comprehensive database that identifies all signalized intersections in Oregon. As a result, the project team developed a sampling procedure to locate potential intersections. The following steps summarize this site identification procedure.

1. First, members of the research team hypothesized that it is unlikely that, over a three year period, an Oregon signalized intersection would not have at least one reported crash. It is possible that this assumption could potentially miss a few locations in Oregon; however, the likelihood is great that most intersections would have at least one crash in a three year period. Consequently, the research team used the traffic control device field in the Oregon crash database to locate every intersection that was indicated as a signalized intersection.
2. Next, the researchers randomly selected 31 intersection locations and evaluated their characteristics to determine if the intersections selected were suitable study candidate sites. For this purpose a “suitable study” site would be one that is actually signalized, is not located too close to another intersection, interchange, or railroad crossing, and has typical signalized intersection features. For example, an intersection with five legs would be removed from consideration since there are a very small number of

these types of signalized intersection configurations in Oregon. One-way roads were, however, retained in the data set and subsequent analysis.

As shown in Table 3.1, of the initial 31 randomly selected intersections, 14 of the sites were located in ODOT Region 1, 11 were located in Region 2, five were in Region 3 and one was in Region 4. Region 5 did not have any intersections in this initial random test sample of 31 intersections. This observation provides strong evidence that to successfully evaluate safety at signalized intersections that are representative for the entire State of Oregon, the sampling procedure must be a stratified random sample with each Oregon region treated as a population strata. This approach provides the added benefit that the probability sample for each region can collectively be smaller as this sampling procedure provides greater precision.

Also noted in the final column of Table 3.1, only 14 of the originally sampled 31 intersections can be considered suitable for the purposes of this study. In many cases, the reporting officers and/or self-reporting drivers indicated STOP controlled intersections with flashing red beacons as locations with traffic signals. Other intersections were excluded due to atypical site characteristics (as determined using aerial and video site review). This preliminary random sample provided critical information by informing the research team that using the crash data cannot be the sole basis for site selection, but that additional filters must be included before finalizing site selection.

Table 3.1: Preliminary Random Sample of Intersections

ODOT Region	Total Intersections Identified in Initial Screening of Crash Data		Distribution of Preliminary Random Test Sample of Intersections		Distribution of Suitable Intersections from the Random Test Sample
	Number	Percent (%)	Number	Percent (%)	
1	2635	55	14	45	14
2	1423	30	11	36	0
3	358	8	5	16	0
4	229	5	1	3	0
5	91	2	0	0	0
Total	4736	100	31	100	14

- Following the preliminary sampling test, the research team determined that upon initial selection (using the random sampling process for each region), each site must then be inspected using aerial photographs and video information to confirm that a traffic signal is indeed present. After this initial screening analysis, the intersection must then be further assessed and atypical configurations removed from further analysis.

3.1.2 Study Sample

The use of a stratified random sample helps to insure that any heterogeneous characteristics associated with a region can be directly evaluated. As shown in Table 3.1, the number of potential intersections varies by region. The random sample, therefore, should be somewhat larger for Region 1 and Region 2 where a large percentage of the identified candidate intersections are located; however, each region should be adequately considered in the overall project sample. This resulted in a list of 50 intersections to use for the development of the Oregon signalized intersection SPF.

The study sites are shown in Figure 3.1. In this figure, intersections located in close proximity to other selected intersections may appear as a single star as the GIS tool simply stacks the symbols. This is particularly evident in Region 5 where three of the Hermiston intersections appear as a single star. The specific site locations are also identified in Table 3.2 (Region 1), Table 3.3 (Region 2), Table 3.4 (Region 3), Table 3.5 (Region 4), and Table 3.6 (Region 5). The project team used the “Random Number” shown in these tables for the site selection process and retained this value in the tables so that the sites could be excluded for future sampling efforts (to validate the resulting models). During the data collection and reduction process, approximately 50 percent of the sites initially selected in the random sampling effort that used only the crash database intersection list were ultimately not feasible candidates for this study (generally due to miscoding of a traffic signal). This observation is consistent with the original 31 site test. The final analysis database included 12 sites for Region 1, 16 sites for Region 2, nine sites for Region 3, seven sites for Region 4, and six Region 5 sites for a total of 50 sites.

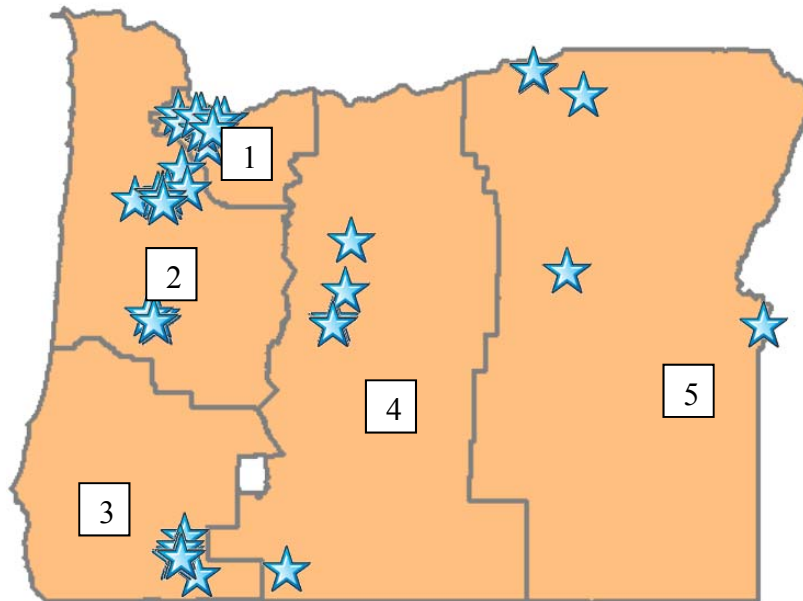


Figure 3.1: Stratified Random Sample (50 Intersections)

Table 3.2: Region 1 Random Sample of Sites

ID	County	City	Road1	Road2
Region 1				
1	Clackamas	Happy Valley	SE Sunnyside Rd.	SE Stevens Rd.
2	Clackamas	Happy Valley	SE Sunnyside Rd.	SE 152 nd Ave.
3	Washington	Hillsboro	NW Evergreen Pkwy.	NW Stucki Place
4	Washington	Beaverton	SW Hart Rd.	SW 155 th Ave.
5	Clackamas	Oregon City	Cascade Hwy (OR 213)	S. Douglas Loop / S. Molalla Ave.
6	Clackamas	Portland	SE Division St.	SE 11 th Ave.
7	Multnomah	Portland	NE Sandy Blvd.	NE 22 nd Ave. / NE Glisan St.
8	Clackamas	Milwaukie	SE McLoughlin Blvd. (OR 99E)	SE Courtney Ave.
9	Multnomah	Gresham	SE Burnside Rd.	SE 3 rd St.
10	Multnomah	Portland	W Burnside St.	21 st Ave.
11	Multnomah	Portland	SE Powell Blvd. (US 26)	SE 174 th Ave.
12	Clackamas	Happy Valley	SE Sunnyside Rd.	SE 132 nd Ave.

Table 3.3: Region 2 Random Sample of Sites

ID	County	City	Road1	Road2
Region 2				
13	Lane	Eugene	Pearl St. / Amazon Pkwy.	19 th Ave.
14	Marion	Salem	Fairgrounds Rd. NE / Portland Rd. NE (OR 99E)	Highland Ave. / Silverton Rd.
15	Marion	Woodburn	N Pacific Hwy. (OR 99E)	Witham Rd. / E Lincoln St.
16	Marion	Salem	Broadway St.	Salem Pkwy. (OR 99E)
17	Marion	Salem	NE Hawthorne Ave.	NE D St.
18	Marion	Salem	NE Commercial St. (OR 99E)	NE Pine St.
19	Lane	Eugene	Pearl St.	13 th Ave.
20	Polk	Dallas	Ellendale Ave.	Kings Valley Hwy.
21	Lane	Eugene	N Delta Hwy.	Green Acres Rd.
22	Marion	Salem	Lancaster Dr.	Cooley Dr.
23	Polk	Salem	NW Doaks Ferry Rd.	NW Orchard Heights Rd.
24	Marion	Silverton	Main St. / Cascade Hwy. (OR 213)	Water St. (OR 214)
25	Marion	Salem	Marion St. (OR 22)	Commercial St.
26	Marion	Salem	Pringle Rd.	Madrona Ave.
27	Lane	Eugene	W Pacific Hwy. (OR 99)	Irving Rd.
28	Lane	Eugene	6 th Ave. (OR 99)	Garfield St. (OR 126)

Table 3.4: Region 3 Random Sample of Sites

ID	County	City	Road1	Road2
Region 3				
29	Jackson	Medford	Main St.	Ross Ln. / Lozier Ln.
30	Jackson	Ashland	Ashland St. (OR 66)	Walker Ave.
31	Jackson	Medford	Crater Lake Ave.	Brookhurst St.
32	Jackson	Eagle Point	Crater Lake Hwy. (OR 62)	Linn Rd.
33	Jackson	Medford	Lozier Ln.	W Stewart Ave.
34	Jackson	Medford	Crater Lake Hwy. (OR 62)	E Vilas Rd.
35	Jackson	Medford	Highland Dr.	Barnett Rd.
36	Jackson	Medford	S Riverside Ave. (OR 99)	E 10 th St.
37	Jackson	Medford	E Barnett Rd.	Ellendale Dr.

Table 3.5: Region 4 Random Sample of Sites

ID	County	City	Road1	Road2
Region 4				
38	Jefferson	Madras	4 th St. (U.S. 26)	B St.
39	Deschutes	Bend	NW Newport Ave. / NW Greenwood Ave.	NW Wall St.
40	Deschutes	Bend	E 8 th St.	Olney Ave. / Penn Ave.
41	Deschutes	Bend	SE 3 rd St. (US 97)	Division St. / Brosterhaus Rd.
42	Deschutes	Redmond	Rimrock Way / NW 19 th St.	Antler Ave.
43	Deschutes	Bend	Bend Pkwy. (US 97)	Powers Rd.
44	Klamath	Klamath Falls	Main St. (US 97)	6 th St.

Table 3.6: Region 5 Random Sample of Sites

ID	County	City	Road1	Road2
Region 5				
45	Umatilla	Pendleton	Court Ave. (US 30)	S Main St.
46	Malheur	Ontario	SW 4 th Ave.	SW 4 th St.
47	Grant	John Day	John Day Hwy. (US 26)	N Canyon Blvd. (US 395)
48	Umatilla	Hermiston	N 1 st St. (US 395)	E Gladys Ave.
49	Umatilla	Hermiston	Umatilla Stanfield Hwy. (US 395)	E 4 th St.
50	Umatilla	Hermiston	Umatilla Stanfield Hwy. (US 395)	Jennie Ave.

3.1.3 Study Sample for Model Validation

To confirm that models developed for the initial evaluation are representative of Oregon conditions at other locations and during additional years, the research team collected site data that they specifically reserved for the model validation effort. Figure 3.2 depicts the 35 randomly selected validation intersections with data available for all study variables. The specific locations are identified in Table 3.7 (Region 1), Table 3.8 (Region 2), Table 3.9 (Region 3), Table 3.10 (Region 4), and Table 3.11 (Region 5). Section 5.5 and Appendix D review the validation procedure used for this analysis.

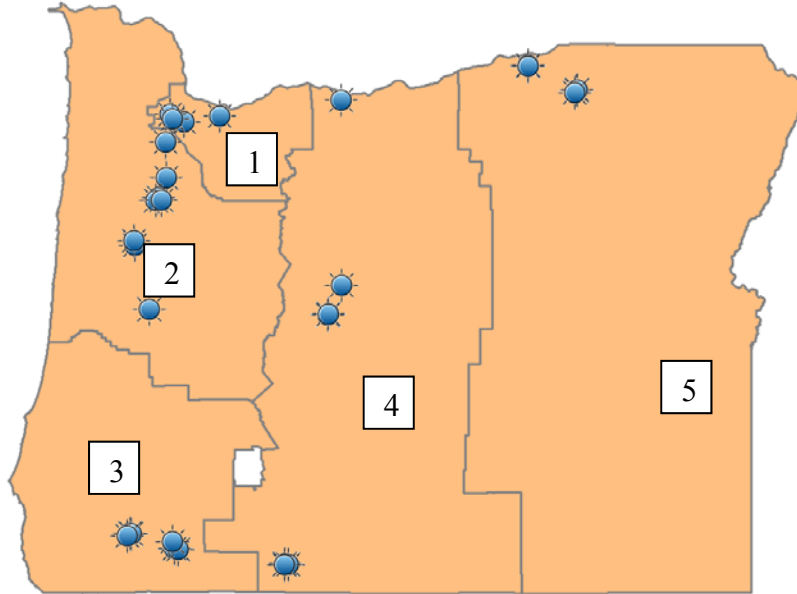


Figure 3.2: Validation Stratified Random Sample (35 Intersections)

Table 3.7: Region 1 Validation Sites

ID	County	City	Road1	Road2
Region 1				
51	Multnomah	Wood Village	NE Arata Rd.	NE 238 th Dr.
52	Washington	Tigard	SW Greenburg Rd.	SW Washington Square Rd.
53	Washington	Hillsboro	SE Century Blvd.	SE Tualatin Valley Hwy.
54	Washington	---	SW Farmington Rd.	SW Grabhorn Rd.
55	Multnomah	Gresham	SE Hogan Ave.	SE Palmquist Rd.

Table 3.8: Region 2 Validation of Sites

ID	County	City	Road1	Road2
Region 2				
56	Yamhill	Newberg	Pacific Hwy. 99W	Villa Rd.
57	Marion	Salem	Madrona Ave. SE	Peck Ave. SE
58	Marion	---	Portland Rd. NE	Brooklake Rd. NE
59	Marion	Salem	Kuebler Blvd. SE	S Liberty Rd.
60	Benton	Corvallis	Western Blvd.	15 th St.
61	Benton	Corvallis	Walnut Blvd.	29 th St.
62	Marion	Salem	Kuebler Blvd. SE	27 th Ave. SE
63	Lane	Eugene	River Rd.	Silver Ln.

Table 3.9: Region 3 Validation Sites

ID	County	City	Road1	Road2
Region 3				
64	Josephine	Grants Pass	D St.	6 th St.
65	Jackson	Medford	Central Ave.	8 th St.
66	Jackson	Medford	Central Ave.	Main St.
67	Josephine	Grants Pass	F St.	Grants Pass Pkwy.
68	Jackson	Medford	Black Oak Dr.	Siskiyou Blvd.
69	Jackson	Central Point	Hamrick Rd.	Pine St.
70	Josephine	Grants Pass	Allen Creek Rd.	Redwood Hwy.

Table 3.10: Region 4 Validation Sites

ID	County	City	Road1	Road2
Region 4				
71	Deschutes	Redmond	Glacier Ave.	SW 9 th St.
72	Klamath	Klamath Falls	Avalon St.	Shasta Way
73	Wasco	The Dalles	Washington St.	3 rd St.
74	Deschutes	Bend	Colorado Ave.	Wall St.
75	Klamath	---	S 6 th St.	Madison St.
76	Deschutes	Bend	NW Portland Ave.	NW Wall St.
77	Deschutes	Bend	Bond St.	Oregon Ave.
78	Klamath	Klamath Falls	Crosby Ave.	Washburn Way

Table 3.11: Region 5 Validation Sites

ID	County	City	Road1	Road2
Region 5				
79	Umatilla	Hermiston	Orchard Ave.	Umatilla-Stanfield Hwy.
80	Umatilla	Pendleton	Court Ave.	SW 10 th St.
81	Umatilla	Hermiston	Main St.	1 st St.
82	Umatilla	Hermiston	Elm Ave.	E 4 th St.
83	Umatilla	Hermiston	Main St.	E 4 th St.
84	Umatilla	Pendleton	Court Ave.	S Main St.
85	Umatilla	Pendleton	Perkins Ave.	Southgate

3.2 DATA COLLECTION FOR SPF DEVELOPMENT

A wide variety of information about an intersection may be needed to adequately evaluate the associated safety performance. The Chapter 2 literature review highlighted many of the common variables used in SPF development. In this section, the roadway variables acquired for the model development are identified. In general, this site-specific data is separated into physical site information (generally represented as roadway variables) and crash data. Sections 3.2.1 and 3.2.2 briefly describe this data collection effort.

3.2.1 Candidate Roadway Variables

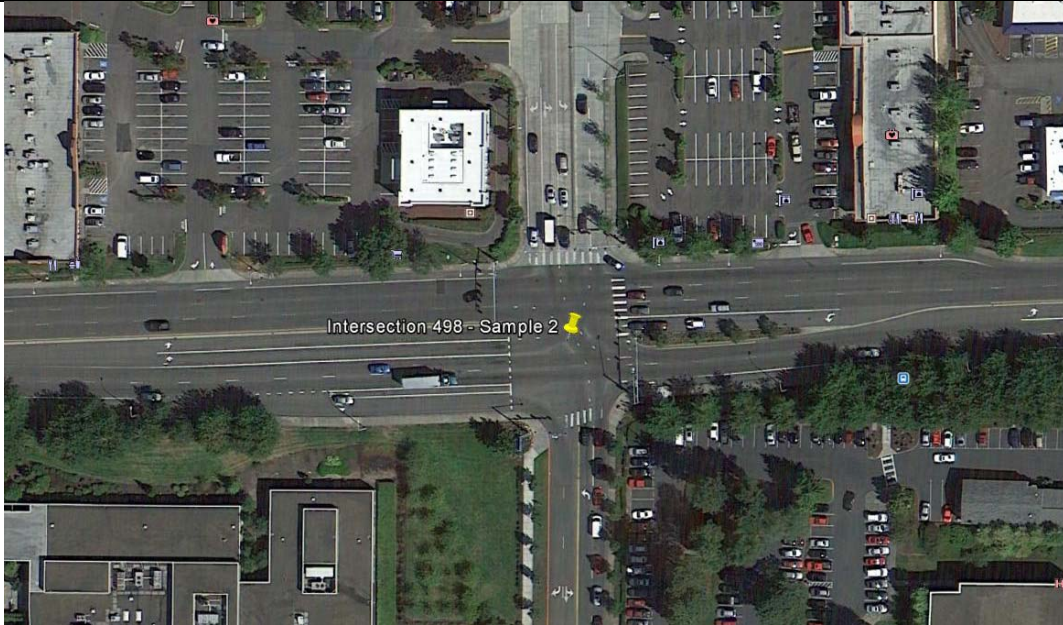
In recent research for Oregon, members of the project team have collected signalized intersection data. From these projects it is clear that a substantial number of candidate variables occur at each location. Consequently, the research team developed a data collection form to summarize information for each individual study site. A completed form for Intersection #1 is shown on the following pages to demonstrate these data collection activities. Table 3.12 summarizes the site data and data collection methods used to date.

Table 3.12: Site Data and Corresponding Collection Method

Intersection Data to Collect	Collection Method
Traffic Volume (represented by AADT)	ODOT Databases
Intersection Location	Google Earth
Intersection Dimensions	Google Earth
Site Characteristics (parking, turn lanes, bicycle facilities, bus stops, etc.)	Google Earth/Video Log
Number of Lanes	Google Earth
Median Configuration	Google Earth/Video Log
Posted Speed	Google Earth/Video Log/ODOT Databases
Traffic Control	Google Earth/Video Log

The first two photos in the data collection form (see Figure 3.3) include an aerial view and a view from the driver’s perspective. Table 3.13 shows the completed location and geometric collection form for Intersection #1. Similarly, Table 3.14 shows the completed lane geometry data collection form. Advisory signs were also acquired, where applicable, but are not shown on the general data collection forms. The project team developed similar data summary figures and tables for all 50 of the selected intersection locations. Due to size constraints, these are included in the stand-alone Appendix C.

Much of the data required to populate this table can be measured using on-line tools such as aerial photographs. For a definition of the various descriptors (shown with footnotes), refer to the data collection key located in Table A.2, Appendix A.



Intersection #1 -- Aerial Photo



Street View Photo

Figure 3.3: Data Collection Form Photos

Table 3.13: Location and Geometric Configuration for Intersection #1

Location	Latitude:	45.433403	Longitude:	-122.561669
Milepost	0.52			
Int. Type ¹	1			
ODOT Region	Region 1			
Road 1 Name	SE Sunnyside	Road 2 Name	SE Stevens Rd.	
No. of lanes ²	5 (2,2,TWLTL)	No. of lanes ²	4 (2,2)	
Road No.	--	Road No.	--	
Description	Road 1			
	Road 1		Road 2	
Direction (NB, SB, WB, EB)	WB	EB	NB	SB
Speed Limit (mph)	40	40	10	35
Road Width ³ (Face-face, ft)	71	88	47	62
Road Width at Int. ³ (Face-face at stop bar, ft)	96	109	47	67
Closest Int. Upstream ⁴ (ft. behind stop bar)	135	481	255	148
Closest Int. Downstream ⁴ (ft. behind stop bar)	332	512	303	423
1 st & 2 nd Closest Dwy. to Int. (ft. behind stop bar)	--	--	--	--
Dwy. Location	0	0	0	0
Dwy. Type	0	0	0	0
Median Type	4	4	1	4
On-Street Parking	4	4	4	4
On-Street Parking Location (ends ft. behind stop bar)	N/A	N/A	N/A	N/A
Bike Lane	3	3	4	4
Bus Stop Near Int.	3	3	3	3
Bus Stops Location (ft. behind stop bar)	N/A	N/A	N/A	N/A
Traffic Control Device ⁵	1	12	12	1
Signs on Traffic Light Pole/Span wire	7, 9, 10	7, 2, 11	1, 4	1, 4, 2
Pedestrian Crossing Light	1	1	1	2

Table 3.14: Lane Geometry – Intersection #1

Description	Road 1	Road 2	Description	Road 1
Exclusive Left Turn Lane per direction ⁶	1	2	1	1
Shared - Left Turn & Thru Lane ⁶	0	0	0	1
Exclusive Thru Lane ⁶	2	2	0	0
Shared - Right Turn & Thru Lane ⁶	1	0	0	0
Exclusive Right Turn Lane ⁶	0	1	0	1
Shared – Left turn / thru / right turn lane ⁶	0	0	1	0
Free Right Turn Lane ⁶	0	0	0	0
Right Turn Lane Length ⁷ (ft. behind stop bar)	N/A	143	N/A	N/A
Right Turn Lane - Taper Length ⁷ (ft)	N/A	132	N/A	N/A
Left Turn Lane Length ⁷ (ft. behind stop bar)	166	279	N/A	175
Left Turn Lane - Taper Length ⁷ (ft.)	74	286	N/A	92
Offset Left Turn Lane ⁸	2	2	2	2
Are chevrons properly oriented? ⁹	3	3	3	3
Channelization ¹⁰	3	3	3	3
Exclusive Left Turn Lane Signalization ¹¹	3	3	3	3
Shared turn & thru lane/Exclusive Thru Lane Signalization ¹¹	1	1	1	4
Exclusive Right Turn Lane Signalization ¹¹	0	5	0	3

3.2.2 Crash Data

The use of crash data for a three year period helps to address minor fluctuations in observed crashes over time. The research team used crash data from 2010 through 2012. In addition to the selection of multi-year crash data, it is important to define which corridor crashes to include in the analysis. Though the crash reports include an option to indicate if an intersection was associated with the crash (these are often upstream queue-related rear-end crashes that may be missed if the sorted crash is solely based on the intersection field). Consequently, the research team performed a sensitivity analysis to determine which crashes should be included as intersection-related crashes. This analysis and resulting procedure are reviewed in Section 5.0 of this report. In addition, there is a need to better understand the level of severity for a specific

crash. Consequently, the model development (also included in Section 5.0) incorporated severe crashes in addition to total crashes.

3.3 DATA COLLECTION FOR MINOR ROAD AADT ESTIMATION

Due to the random nature of the stratified random sampling procedure, recent traffic volume information is not available for every intersection with particular gaps in data for the minor roads. As a result, the research team used a variety of resources to identify the traffic volume. For locations where the traffic volume was not available, the research team developed an estimation procedure for reliably populating this content. Section 4.0 and Section 10.0 (Appendix B) of this report collectively review this process in detail.

4.0 ESTIMATING MINOR VOLUMES

As discussed previously, the volumes on the minor approaches are often missing or not available (even for intersections that are signalized). This chapter explores the possibility of estimating minor volumes based primarily on the data collected as part of the development of the SPFs. This estimation could be useful where it is desirable to apply the SPFs that were developed in this research (or from the HSM) but for which the minor volume is unknown. Based on the reviewed literature, the research team collected additional variables to supplement those gathered for estimating the SPFs. This chapter describes these additional variables, presents the modeling approach, and summarizes the resulting traffic volume estimation model. The chapter concludes with a sample application.

4.1 DATA

This section describes the data used to develop the models. A number of the volume, roadway, and geometric variables are identical to those used in the SPF development so their description is not repeated here unless needed for clarity.

4.1.1 Average Annual Daily Traffic

As described in Section 3.0, the collection of AADT data for both major and minor legs at signalized intersections involved internet searches and public record requests by the research team. The counts were either available as AADT (already factored and converted by reporting agency), ADT, or peak hour counts. The ADT and peak hour counts were factored to AADT using the methods outlined in FHWA Traffic Monitoring Guide (*FHWA 2013*) and factors derived from the nearest suitable automated traffic recording (ATR) station. In addition, the research team computed the AADT for both major and minor legs, for each year from 2007-2013 using time of day, yearly and monthly factors, when appropriate. These factoring methods are described in Appendix B.

For this modeling effort, it was hypothesized that the AADT of facilities that were parallel to the minor facility being modeled and of the same functional class could be a significant predictor. Thus efforts were made to obtain these data. If these parallel facility counts were ADT or peak hour counts, they were factored to AADT using factors derived from the nearest suitable ATR station. If the factored AADTs were obtained for different years, they were all factored to 2013 volumes using time of day, yearly, and monthly factors. Figure 4.1 shows the conceptual drawing of the facility parallel to the minor road whose AADT was gathered and used as a predictor in the analysis.

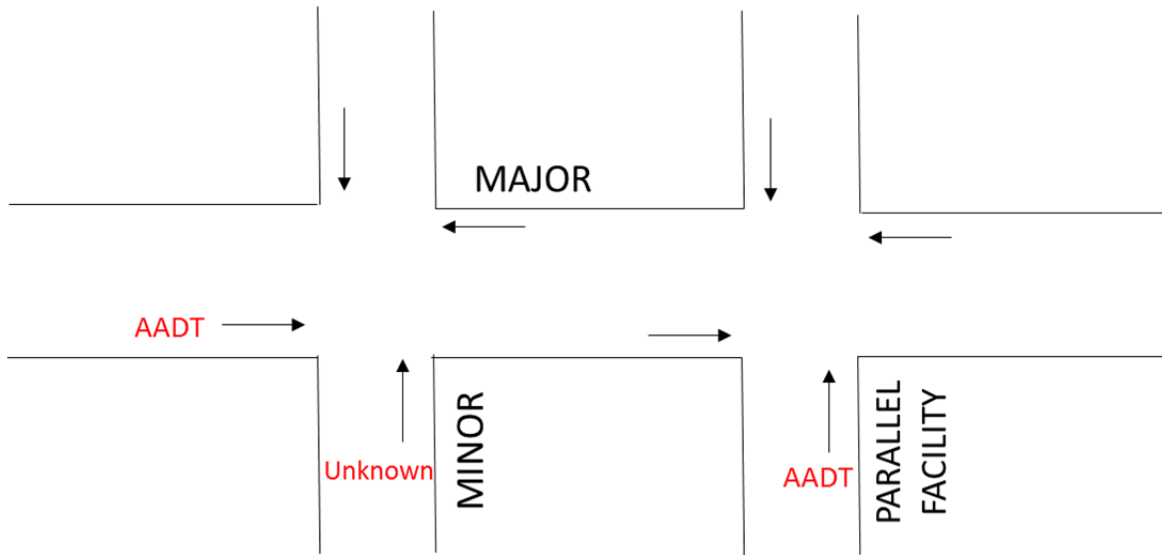


Figure 4.1: Example Parallel Facility AADT

4.1.2 Functional Class

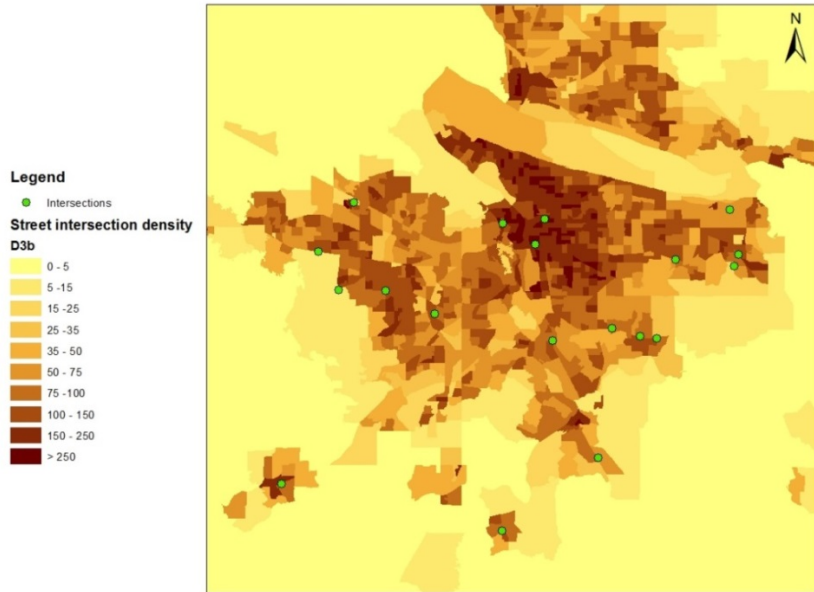
The research team derived the functional classification of major and minor legs at each intersection from the Oregon Department of Transportation’s TransGIS viewer (*ODOT 2014*). Since the sample included signalized intersections only, all the roadways in the sample fell into three functional classes: arterial, collector, and local. For major roadways, the categories of principal arterial, minor arterial, and rural minor arterial were collapsed to arterial. For minor roadways, the categories of minor arterial and principal arterial were collapsed to “arterial.” Major collector and rural major collector were collapsed to “collector.”

4.1.3 Land Use and Demographic

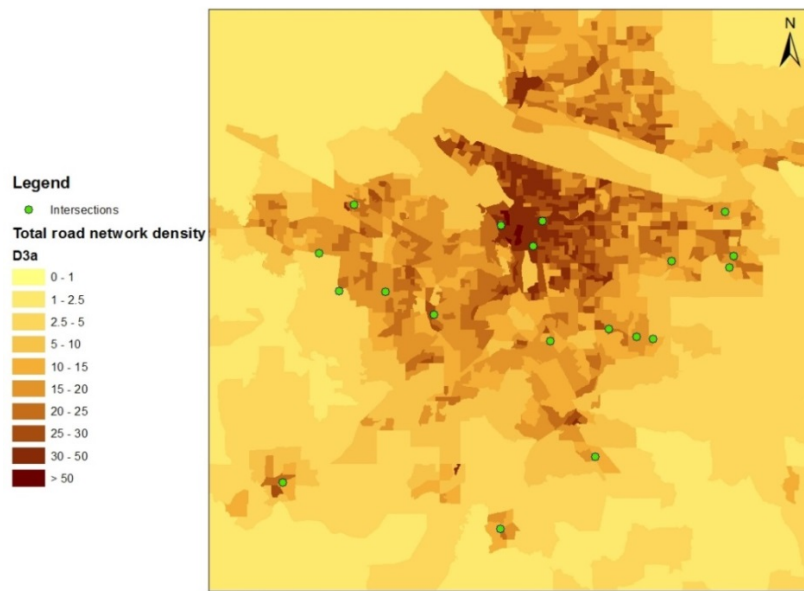
All of the intersections used in this analysis were located in urban areas so it was not possible to include simple variables such as urban/rural/suburban to capture land use. To capture some of the socio-economic variables such as population and income, members of the research team used data from the US Census Bureau (*US Census Bureau 2014*). For each intersection in the sample, population and income data were available by the corresponding county and city where the intersection is located. Therefore, for the appropriate counties and cities, 2013 estimates of population, median income and per capita income were gathered for each intersection.

4.1.4 Network

The research team gathered network related variables such as total road network density and street intersection density for each intersection from the Environmental Protection Agency (EPA)’s Smart Location Database (*EPA 2013*). The street intersection density variable in the EPA database reflected the weighted density of multi-modal intersections. This data was available by census tract. An example of the street network and intersection density variables can be seen in Figure 4.2.



A. Street Intersection Density



B. Total Road Network Density

Figure 4.2: Sample Images Showing GIS Network Information

4.2 MODELING APPROACH

In order to estimate the AADT for the minor approaches, the research team employed multiple linear regressions. Based on prior research by Xie et al. (Xie et al. 2011) and inspection of the data, all the volumes were \log_{10} transformed. The process for model building explored many possible combinations of independent variables including the results from a stepwise search process. During initial model development, the researchers computed correlations between each

pair of predictor variables. Within each pair, if the variables were significantly correlated with each other (correlation coefficient > 0.5), only one variable was retained in subsequent models.

In order to estimate minor volumes, two modeling approaches were applied. The first modeling approach limited the model input data to only intersections that had two-way major and minor roads (i.e. four legs at each intersection). For this model, the AADT for each road was used. The second approach was to model the volumes by leg. The sample of intersections included both one-way and two-way approaches for both major and minor roads. To do this, two-way AADT was converted so that only one leg of the intersection was being modeled. Figure 4.3 shows how the AADT volumes were converted to one leg of the intersection based on one-way or two-way traffic. For major or minor approaches that were two-way, the major AADT was divided by two. For one-way approaches, the AADT is the volume on the leg. This approach assumes that the volumes on the major road are proportional in each direction which may not be necessarily true in reality. However, estimating volumes by leg allows the user to estimate AADT at one-way facilities (and possibly three-leg intersections).

The selection of the final models was based both on the model fit and diagnostics and the ability to readily gather the data for volume estimation. After a preliminary analysis, it was clear that not all roadway-related variables would be predictors of minor road volumes. The analysis indicated that the following variables were at least partially correlated to minor leg AADT and were used in the model building:

- Presence of major and minor exclusive right or left turn lanes,
- Average number of approach thru lanes on major and minor legs,
- Speed limits,
- Presence of center lane (two-way left-turn lane (TWLTL)), and
- Road width.

Despite some initial promise, inclusion of more complicated network variables (e.g. street network density) or the demographic variables (e.g. county and city income levels) did not substantially improve the models. The detailed outputs from the modeling runs are not provided in the chapter text. Rather, only the final models with the significant variables are presented.

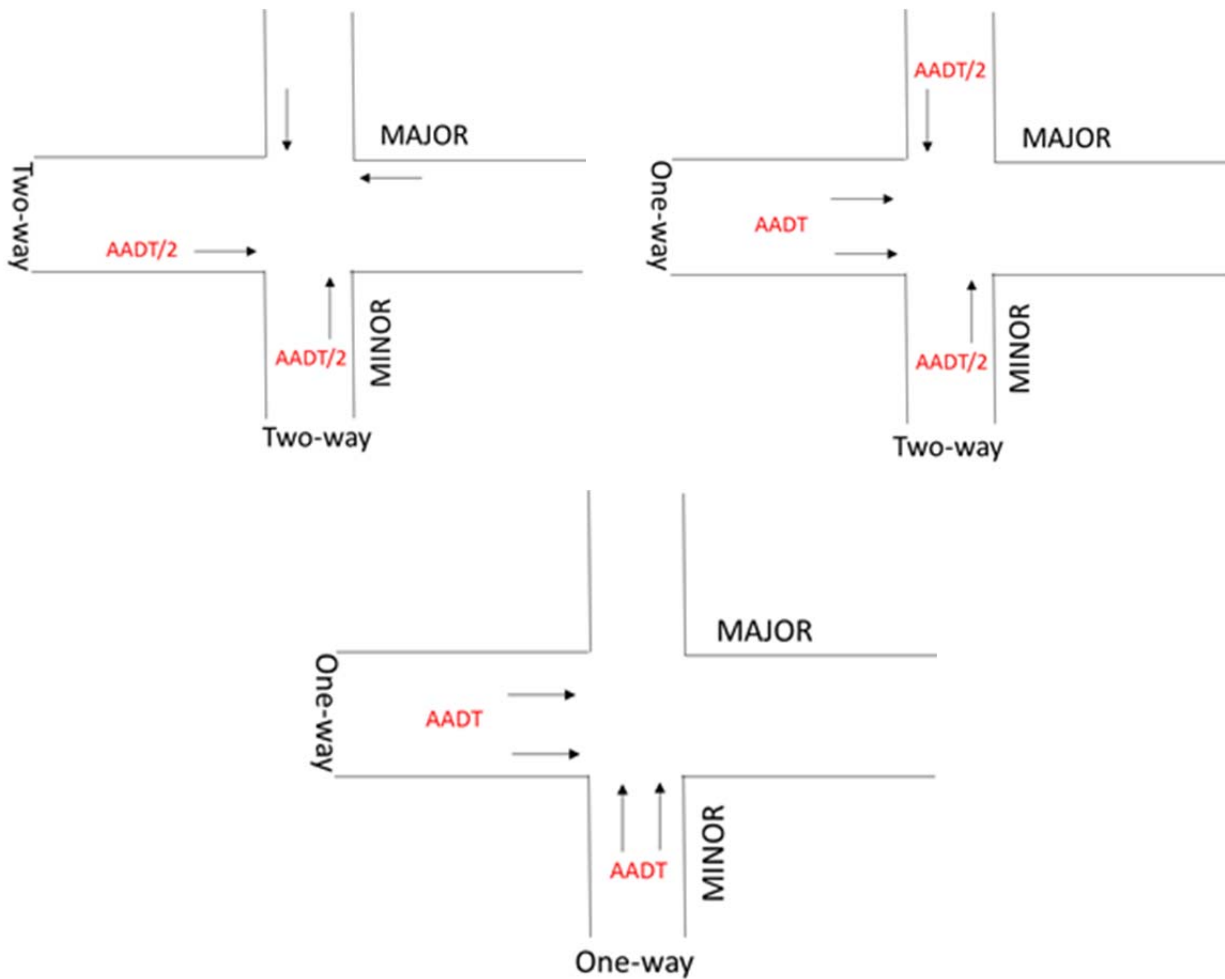


Figure 4.3: Adjusted AADT for Use in the Volume by Leg Models

4.3 RESULTS

The following section presents the analysis and results obtained from the model generation process using the sample sites. As described previously, the results of both models are presented in succession along with model fit parameters.

4.3.1 Descriptive Statistics

The following section presents the descriptive statistics of the variables used in the models. The initial AADT estimation sample consisted of 78 intersections. However, volumes on parallel facilities with the same functional class as the minor road were not available for all intersections. Therefore, the final sample used for AADT modeling consisted of 66 intersections. Table 4.1 shows the distribution of one-way and two-way approaches in the sample.

Table 4.1: Types of Intersection Approaches Minor Volume Models

Major Leg	Minor Leg	
	One-way	Two-way
One-way	6	5
Two-way	4	51
Total	10	56

A majority of the intersections (77 percent) in the sample are two-way facilities on the major and minor roads, while nine percent of the intersections were one-way for both roads. Table 4.2 shows the descriptive statistics for the variables used in modeling the minor road AADT. Within the sample, the major road AADT for 2013 varies from 1806 to 29,500 vehicles per day (vpd). The parallel facility volume also encompasses a wide range of AADT values, varying between a minimum of 733 to a maximum of 18,497 vpd. The average number of approach thru lanes on the major road (sum of the number of through lanes on each major approach divided by 2) varied between one and four, whereas on the minor road they varied between one and three. The speed limit on the major road ranged from 20 to 55 mph and on the minor road it varied between 15 to 45 mph. Similarly, road width for the major road varied from 30 to 83 feet, whereas for the minor the width varied from 30-73 ft. The population and income variables also showed significant variation between various cities and counties as shown in Table 4.2.

Table 4.2: Descriptive Statistics for Minor Volume Models

Parameter		Min	Max	Mean	St.Dev
AADT	Major Road Volume (2013)	3,612	44,464	17,757	8,5551.741
	Log (Major Road Volume) (2013)	3.26	4.47	3.95	0.229
	Parallel Facility Volume (2013)	733	18,497	6,083	4,006.19
	Log (Parallel Facility Volume) (2013)	2.87	4.27	3.69	0.30
Roadway	Average Number of Approach Lanes on Major Road	1	3	1.98	0.63
	Average Number of Approach Lanes on Minor Road	1	3	1.39	0.59
	Speed Limit on Major Road (mph)	20	55	33.26	7.32
	Speed Limit on Minor Road (mph)	15	45	28.98	6.81
	Road Width of Major Road (ft)	30.33	83.36	55.32	15.46
	Road Width of Minor Road (ft)	30.28	72.92	44.65	9.91
Socio-Demographic	County Population	16,018	766,135	281,976	195,025.19
	County Per Capita Income	16,352	32,781	25,564	4,070.84
	County Median Income	35,578	64,352	49,511	12,165.80
	City Population	9,368	609,456	85,360	8,4381.41
	City Per Capita Income	16,441	35,823	24,620	4,412.50
	City Median Income	25,455	92,773	48,384	12,165.80
Network	Road Network Density	4.27	39.87	18.06	6.77
	Intersection Density	6.24	305.49	99.37	60.92

A few variables were coded as dummy variables (either 0 or 1) to be included in the model. A value of zero indicates that the facility (major or minor road) did not have a particular feature, while a value of one indicates the presence of the feature. Table 4.3 shows a list of dummy variables used in the models. A total of 53 intersections in the sample had an exclusive left turn lane on the major road and 43 had left turn lanes on the minor road respectively. Similarly 38 and 52 intersections in the sample did not have the TWLTL for the major and minor roads. While only four major roads in the sample were classified as collectors, 43 minor roads were classified as collectors.

Table 4.3: Summary of Categorical Variables for Minor Volume Models

Parameter	0=No	1=Yes
Exclusive Left Turn Lane of Major Road	13	53
Exclusive Right Turn Lane of Major Road	43	23
TWLTL Lane on Major Road	38	28
Exclusive Left Turn Lane of Minor Road	23	43
Exclusive Right Turn Lane of Minor Road	44	22
TWLTL Lane on Minor Road	52	14
Functional Class of Major Road: Collector	62	4
Functional Class of Minor Road: Collector	23	43

4.3.2 Models to Estimate Total Minor Entering Volume (AADT)

For this set of models, the goal of the AADT estimation effort was to develop a regression model to predict the minor road AADT at intersections where both major and minor roads were two-way facilities. The research team, therefore, estimated two models -- one with the volumes from a parallel facility included as an independent variable and one without. Table 4.4 shows the significant variables for the model that includes values from a parallel facility along with model fit parameters and goodness of fit parameters. The R-squared of the model is 0.63 and the standard error of the residuals is 0.19. Table 4.5 shows the model fit parameters for the model estimated without the parallel volume variable. The R-squared of the model is 0.60 and the standard error of the residuals is 0.1945.

As shown in both tables, major road volume has a positive relationship with minor road AADT, implying that as major road volume increases, minor road AADT also increases. Other variables that show a positive relationship include the nearest parallel road volume, if the major road is a collector or the minor road is a minor arterial. The only variable that exhibited a negative relationship with log (AADT) for the minor road was the average number of approach lanes on the major road.

Further diagnostics of the models are shown in Figure 4.4 and Figure 4.5. To better understand the model outputs, the predicted and observed volumes are transformed back to volumes (rather than log model inputs). In the figures, the plot in the upper left shows the predicted minor volumes on the y-axis with the observed minor volumes on the x-axis. The solid line represents the equal line (where the modeled volume would equal observed volumes). In these plots for both models, it is clear that modeled and observed volumes are in reasonable agreement. To explore any issues with bias by major road volumes, the plot in the upper right shows the residuals on the y-axis with the observed major AADT on the x-axis. The two lower histograms

show two other diagnostics that explain the predictive quality of the models. In the lower left, the histogram shows the absolute percent predicted error as well as the mean absolute percent error (MAPE). Finally, in the lower right the histogram shows the error expressed in vehicles per day as well as the mean error.

Inspection of the goodness of fit parameters presented in the tables and plots in the Figure 4.4 and Figure 4.5 indicate that the final selected models do a reasonable job of estimating the minor road AADT. The mean absolute error is about 36 percent with the majority of the estimates having less than 50 percent error and only a small number of locations have high percent error. The mean error (the difference in the predicted minor volume and actual minor volume) is around 2,000 vpd. As shown in the histogram, the majority of these errors are less than 2,000. The errors (residuals) do not show any trends over the range of major AADT included in the model (3,600 to 44,400 vpd). Given that the models will be used to estimate minor volumes that will be then be applied in SPF for crash prediction, the level of error is acceptable. Finally, there does not seem to be any practical difference between the models estimated (though the model that includes the parallel facility volume has better goodness of fit and diagnostic performance).

Table 4.4: Model Outputs for Total Minor Entering Volume, Two-way Major and Minor Roads (with Parallel Facility)

Parameter	Estimate	Std. Error	t value	Pr(> t)
(Intercept)	0.6837	0.5752	0.68	0.4998
log(Major AADT)	0.686	0.1432	4.79	0.0000**
log(Parallel AADT)	0.1764	0.0991	1.78	0.0818*
Avg. Number of Approach Thru Lanes on Major Road	-0.1636	0.0548	-2.99	0.0046**
Func. Class Major (Arterial=0, Collector=1)	0.2384	0.1141	2.09	0.0423**
Func. Class Minor (Arterial=0, Collector=1)	-0.29235	0.0646	4.53	0.0000**
Residual standard error	0.1900 on 45 degrees of freedom			
R-squared	Multiple R-squared: 0.6268, Adjusted R-squared: 0.5854			
F-statistic	15.12 on 5 and 45 DF, p-value: 1.046e-08			
* Significant at the 90 percent confidence level, ** Significant at the 95 percent confidence level				

The resulting equation associated with Table 4.4 and AADT estimation using traffic volume information from a parallel facility can be represented by the following equation:

$$\begin{aligned} \log(AADT_{Total\ Minor}) &= 0.6837 + 0.686 \log(AADT_{Major}) \\ &+ 0.1764 \log(Parallel\ AADT) - 0.1636(LN_{Major}) + 0.2384(FC_{Major}) \\ &- 0.29235(FC_{Minor}) \end{aligned}$$

Where:

LN_{Major} = Average number of approach thru lanes on the major road

FC_{Major} = Value of 1 if major road is a collector, otherwise a value of 0.

FC_{Minor} = Value of 1 if minor road is a collector, otherwise a value of 0.

Table 4.5: Model Outputs Total Minor Entering Volume, Two-way Major and Minor Roads (without Parallel Facility)

Parameter	Estimate	Std. Error	t value	Pr(> t)
(Intercept)	1.05631	0.5559	1.31	0.197
log(Major AADT)	0.7698	0.1384	5.56	0.0000**
Avg. Number of Approach Thru Lanes on Major Road	-0.1915	0.0537	-3.56	0.0009**
Func. Class Major (Arterial=0, Collector=1)	0.2343	0.1167	2.01	0.0506**
Func. Class Minor (Arterial=0, Collector=1)	-0.32851	0.0627	5.24	0.0000**
Residual standard error	0.1945 on 46 degrees of freedom			
R-squared	Multiple R-squared: 0.6006, Adjusted R-squared: 0.5658			
F-statistic	17.29 on 4 and 46 DF, p-value: 1.009e-08			
* Significant at the 90 percent confidence level, ** Significant at the 95 percent confidence level				

The resulting equation associated with Table 4.5 and AADT estimation without using information from a parallel facility can be represented by the following equation:

$$\begin{aligned} \log(AADT_{Total\ Minor}) &= 1.05631 + 0.7698 \log(AADT_{Major}) - 0.1915(LN_{Major}) + 0.2343(FC_{Major}) \\ &\quad - 0.32851(FC_{Minor}) \end{aligned}$$

Where:

All variables are as previously defined.

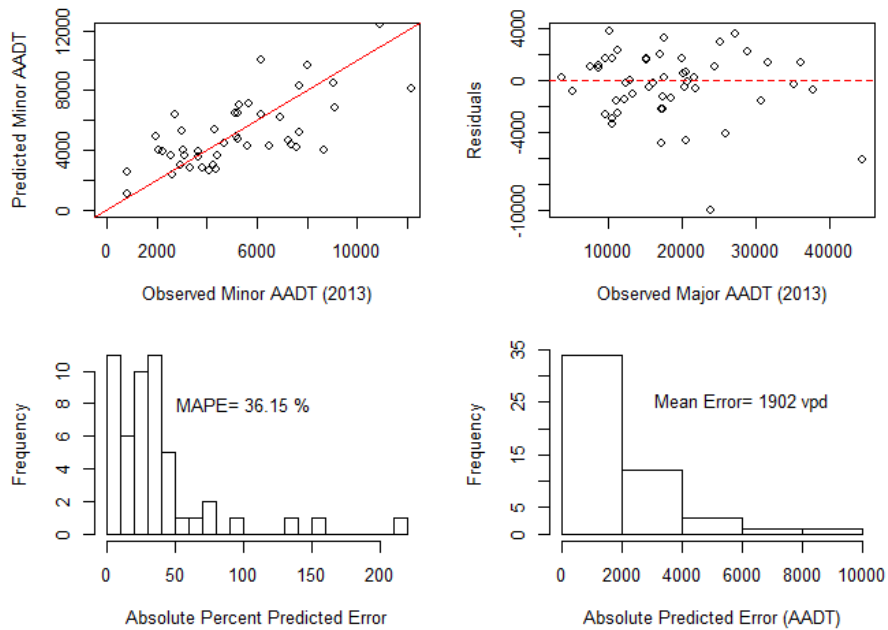


Figure 4.4: Diagnostic Plots for Total Minor Entering Volume (with Parallel Facility AADT)

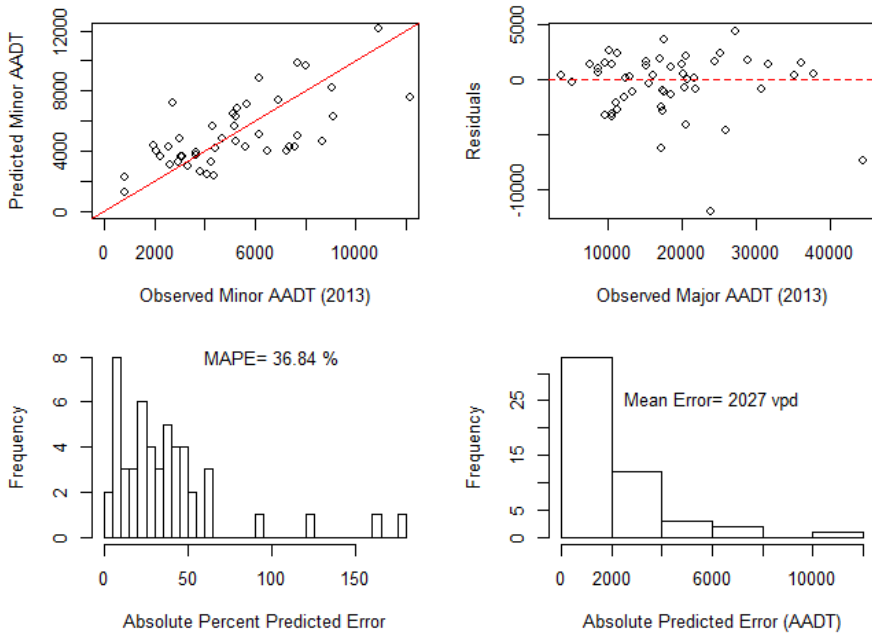


Figure 4.5: Diagnostic Plots for Total Minor Entering Volume (without Parallel Facility AADT)

4.3.3 Models to Estimate Minor Volume by Leg

In this model, both one-way major and minor facilities are estimated. Each two-way facility in the sample included 50 percent of the volume for each leg and 50 percent for the number of approach thru lanes as described previously. Therefore the model was able to incorporate all 66

intersections in the sample. Again, two models were estimated—one with the volumes from parallel facility included as an independent variable and one without. Table 4.6 shows the significant variables along with the associated model fit parameters and goodness of fit parameters. The R-squared of the model is 0.73 and the standard error of the residuals is 0.22. Table 4.7 shows the model fit parameters for the model estimated without the parallel volume variable. The R-squared of the model is 0.69 and the standard error of the residuals is 0.23. As shown in both tables, four variables were significant predictors of the minor AADT. These included log transformed parallel road volume, number of approach thru lanes on minor facility (avg. if two-way), if the minor facility was an arterial, and the presence of a TWLTL on the major facility. Except for the TWLTL variable on the major facility and functional class of the minor road, all the other variables showed a positive relationship with minor facility AADT.

Table 4.6: Model Outputs for Minor Volume Estimation Model By Leg (with Parallel Facility AADT)

Parameter	Estimate	Std. Error	t value	Pr(> t)
(Intercept)	0.9815	0.5542	1.77	0.0816*
log(Major AADT)	0.2318	0.1265	1.83	0.0718*
log(Parallel AADT)	0.3019	0.0981	3.08	0.0031**
Number of Approach Thru Lanes on Minor Road	0.321	0.0568	5.65	0.0000**
Func. Class Minor (Arterial=0, Collector=1)	-0.2511	0.065	-3.86	0.0003**
Major TWLTL (0=No, 1=Yes)	-0.1299	0.058	-2.24	0.0287**
Residual standard error	0.2191 on 60 degrees of freedom			
R-squared	Multiple R-squared: 0.7312, Adjusted R-squared: 0.7088			
F-statistic	32.65 on 5 and 60 DF, p-value: 6.372e-16			

* Significant at the 90 percent confidence level, ** Significant at the 95 percent confidence level

The equation for minor traffic volume estimation **by leg**, as shown in Table 4.6, when traffic volume information is available from a parallel facility can be shown as follows:

$$\begin{aligned} \log(AADT_{Minor\ by\ Leg}) &= 0.9815 + 0.2318 \log(AADT_{Major}) \\ &+ 0.3019 \log(Parallel\ AADT) + 0.321(LN_{Major}) - 0.2511(FC_{Minor}) \\ &- 0.1299(TWLTL_{Major}) \end{aligned}$$

Where:

$TWLTL_{Major}$ = Value of 1 if TWLTL present on major approach, otherwise value of 0.

All other variables are as previously defined.

Table 4.7: Model Outputs for Minor Volume Estimation Model By Leg (without Parallel Facility AADT)

Parameter	Estimate	Std. Error	t value	Pr(> t)
(Intercept)	1.8516	0.5088	3.64	0.0006**
log(Major AADT)	0.2945	0.1332	2.21	0.0308**
Number of Approach Thru Lanes on Minor Road	0.3393	0.0602	5.63	0.0000**
Func. Class Minor (Arterial=0, Collector=1)	-0.2892	0.0681	-4.24	0.0001**
Major TWLTL (0=No, 1=Yes)	-0.1382	0.0618	-2.24	0.029**
Residual standard error	0.2338 on 61 degrees of freedom			
R-squared	Multiple R-squared: 0.6888, Adjusted R-squared: 0.6683			
F-statistic	33.75 on 4 and 61 DF, p-value: 7.627e-15			
* Significant at the 90 percent confidence level, ** Significant at the 95 percent confidence level				

The equation for minor traffic volume estimation **by leg**, as shown in Table 4.7, when traffic volume information is not available from a parallel facility can be shown as follows:

$$\begin{aligned} \log(AADT_{Minor\ by\ Leg}) \\ = 1.8516 + 0.2945 \log(AADT_{Major}) + 0.3393(LN_{Minor}) - 0.2892(FC_{Minor}) \\ - 0.1382(TWLTL_{Major}) \end{aligned}$$

Where:

All variables are as previously defined.

Additional diagnostics of the models are shown in Figure 4.6 and Figure 4.7. Overall, the goodness of fit parameters presented in the tables and inspection of the figures reveal that the final models do a reasonable job of estimating the minor road volume by leg. The mean absolute error is about 43 percent for the models that include the parallel facility volume and about 47 percent for the model that does not. Still, the majority of the estimates have less than 50 percent error and only a small number of locations have a high percent error. The mean error (the difference in the predicted minor volume and actual minor volume) is around 1,000 vpd. This corresponds to the error in the total entering volume since the analysis primarily modelled 50 percent of the AADT for the two-way legs. As shown in the histogram, the majority of these errors are less than 1000. The errors (residuals) do not show any trends over the range of major AADT included in the model (1800 to 29,000 vpd). Finally, there does not seem to be any practical difference between the estimated models, though the model that includes the parallel facility volume does have a better goodness of fit and diagnostic performance.

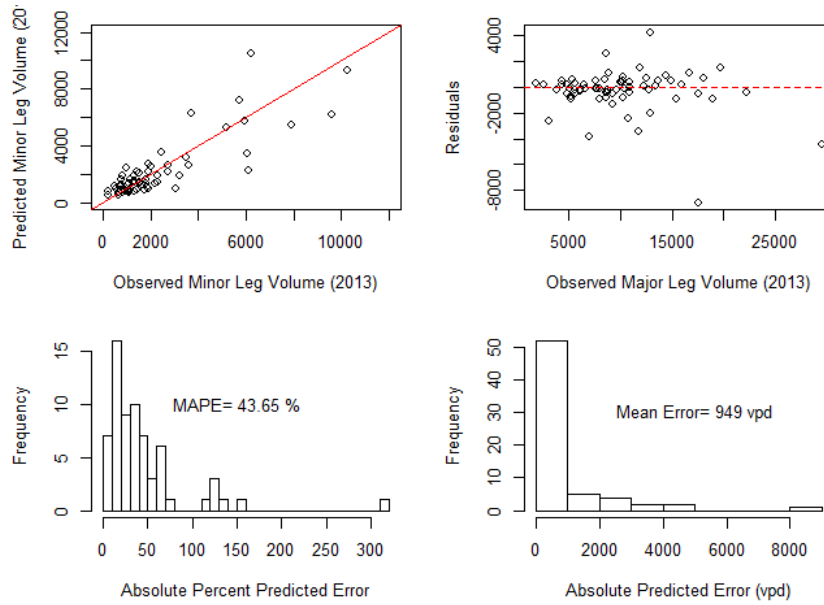


Figure 4.6: Summary Diagnostic Plots for Minor Volume Estimate by Leg (with Parallel Facility AADT)

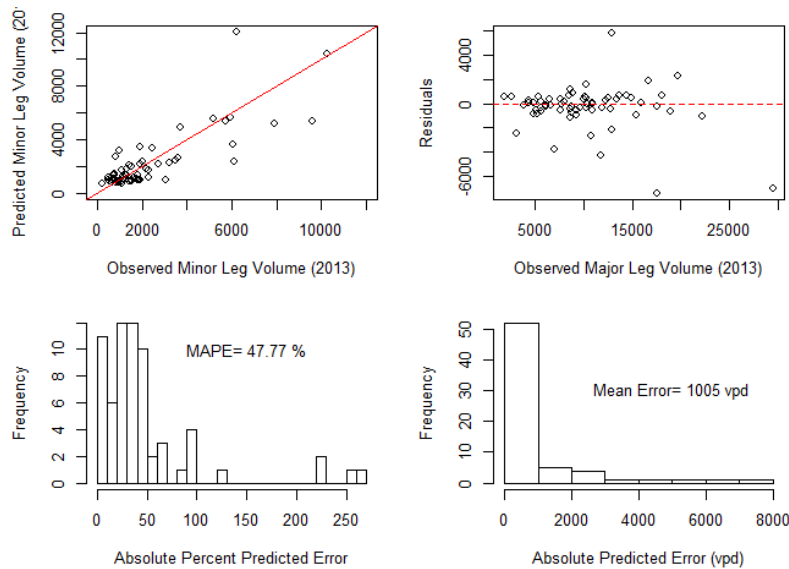


Figure 4.7: Summary Diagnostic Plots for Minor Volume Estimate by Leg (without Parallel Facility AADT)

4.4 REVIEW OF AADT MODEL VALIDATION

The models were validated by applying them to twenty-five new intersections that were not used in model development. These intersections were sampled from across the state. Of the 25 intersections selected for validation, nine were in Region 1 (36 percent), five in Region 2 (20 percent), five in Region 3 (20 percent), four in Region 4 (16 percent), and two in Region 5 (8 percent). A detailed description of the validation effort is presented in Appendix C. The

selection of these intersections was based on available data, including major and minor volumes and the volume on the parallel facility. Overall, the models estimated the minor facility AADT reasonably well. For the models estimating total minor entering volume the mean absolute error was 1,950 vpd and the MAPE was 52.4 percent. For the models estimated by leg, the mean absolute error was 1,400 vpd and the MAPE was 49.1 percent. Thus, the models were judged to produce reasonable estimates of minor volumes when applied to the new data set.

As a further test, the regression models to predict minor facility AADT were re-estimated using a larger set of intersections drawing from both the training and the validation set. The research team used a total of 91 intersections for this re-estimation effort. Two sets of models were estimated for total entering volume and by leg without using parallel facility volume as a predictor. The goodness of fit parameters revealed that these models performed reasonably well in predicting minor road AADT and were similar to the models estimated using training data only. However, as the validation intersections were not chosen randomly, the research team recommends the use of models estimated using the training data only as presented in this chapter.

4.5 SUMMARY

If both approaches to the intersection are two-way streets, the recommended model is the model to estimate total entering volume. The models should not be applied to major roads with AADTs that exceed 30,000 vpd. The models can be applied with or without the nearest parallel facility AADT. This information is relatively easy to obtain, but if the parallel facility volume cannot be obtained or is not available, the prediction of the minor volume can be determined with the model developed without this parameter. If the minor volume to be estimated is either a one-way street or intersects a one-way street, the models developed to estimate volumes by leg can be used. Note that models for three-leg intersections were not specifically developed. The models for estimating volume by leg could be used.

Based on the parameter specifications used in model estimation, the research team recommends that the model be applied within the following ranges:

- Major road AADT < 44,000,
- Parallel road AADT < 18,500,
- Average of approach thru lanes on major road ≤ 3 (for model to estimate total entering volume,
- Average of total approach thru lanes on minor road ≤ 3 , and
- Functional classification of major and minor roads either arterials or collectors.

One acknowledged limitation is that the total entering models assume that the minor entering volumes will be the same from both directions. In addition, the models are calibrated to 2013 traffic volumes. To adjust the volume to current or other years, the year-to-year correction factors will need to be applied as shown in Appendix B.

4.5.1 Sample Application

To illustrate how the estimated model could be applied to predict the AADT for the minor road, a hypothetical problem is presented. Consider a hypothetical intersection with the following parameters:

- Two-way major AADT – 10,000 vpd
- Number of Thru lanes on Major approach 1 – 2
- Number of Thru lanes on Major approach 2 – 2
- Number of Thru lanes on Minor approach 1 – 2
- Number of Thru lanes on Minor approach 2 - 2
- AADT of parallel facility – 6,000 vpd
- Major facility is an arterial
- Minor facility is a collector
- Major facility does not have a TWLTL

Solution:

The intersection is a two-way major and minor facility. For the intersection in this example, the report recommends using the estimated coefficients for the total entering minor volume model listed in Table 4.4. Since both major and minor roads are two-way facilities, the average number of approach thru lanes on the major and minor road is estimated as 2 using the following formula.

*Avg Number of Thru Lanes on Major(Minor) Road =
(Number of thru lanes on major (minor) approach 1 +
Number of thru lanes on major (minor) approach 2)/2*

Thus, the minor road AADT at this intersection can be estimated by substituting the values into the appropriate equation.

$$\begin{aligned}\log(AADT_{Total\ Minor}) &= 0.6837 + 0.686 \log(10,000) \\ &+ 0.1764 \log(6000) - 0.1636(2) + 0.2384(0) - 0.29235(1) \\ \log(AADT_{Total\ Minor}) &= 3.475\end{aligned}$$

Therefore total minor entering AADT = $10^{3.475} = 2,983 \Rightarrow 2,900$ vpd (rounded down).

5.0 SAFETY ANALYSIS FOR SIGNALIZED INTERSECTIONS

The process for the development of signalized intersection SPFs for Oregon included identifying intersection-related (IR) crashes followed by the initial SPF development activity, model validation, and final (enhanced) model refinement. This chapter summarizes these model development activities. At the initial stages of this effort, the research team found that defining IR crashes can prove challenging when modeling the expected number of crashes at signalized intersections. In general, the closer a crash is located and subsequently coded in relation to an intersection the more likely the crash actually is related to some sort of intersection maneuver or activity. Yet, specific features of the intersection, such as left turn pockets, design speed, skew angle, etc. most likely affect IR crash location. The crash could be shown at some unknown distance upstream the intersection when it is actually due to actual intersection activities. The extent of the intersection functional area (IFA), a factor of volume, queue storage, speed, and deceleration, is likely to affect the distance an IR crash is located from an intersection.

Before developing reliable SPFs, therefore, the research team faced the task of correctly identifying related crashes. These IR identification efforts are addressed in Sections 5.1 and 5.2 followed by the SPF development activities presented in Section 5.3 and 5.4.

5.1 MATCHING CRASHES AND INTERSECTIONS

Although it is natural to expect that some given distance from an intersection could be used as an indicator as to whether a crash is related to that intersection, there is no general agreement about a maximum distance for which a crash is too far to be considered when conducting a safety analysis of that intersection. A threshold of 250 feet is a common distance used to indicate that a crash is IR for many state crash databases. In fact, California, Indiana, and Ohio, among other state DOTs, use this threshold to define IR areas at the physical intersection of two roads. In contrast, Utah and Pennsylvania DOTs identify some IR crashes that extend up to 500 feet upstream of the roadway centerline intersection (*Stolof 2008*).

5.1.1 Investigating a Threshold for Distance from Intersection for Crash Classification in Oregon

The research team performed an investigation to classify crashes as IR utilizing a subset of the data collected for this research. The main purpose of this effort was to establish a feasible distance from each intersection to confidently determine IR crashes for the subsequent crash modeling activities using the Oregon data. The study data offers an excellent opportunity to establish this threshold, as this source data consists of a probability sample representative of the state. The additional effort of identifying this IR threshold not only allows accurate crash identification to be used at later stages of this research, but also provides information for how practitioners and future researchers can quickly determine if a crash should be attributed to an intersection.

5.2 METHODOLOGY

The research team determined the IFA for each leg of the 73 intersections available for SPF development. For a leg, the IFA encompasses the area defined by two thresholds: (1) the upstream stopping sight distance (SSD) of the farthest IR geometric feature for that leg (measured in feet), and (2) the downstream SSD. The intersection IFA is the four-legged shaped area that results from simply joining the set of leg IFAs at a given intersection. This shape is similar to the definition provided in the document *A Policy On Geometric Design of Highways and Streets* (commonly referred to as the Green Book) (AASHTO 2011).

The researchers imported the intersection geometric database information and geo-located crash data for years 2010 to 2012 into a GIS commercial software (ESRI 2011). The research team defined circular buffers around each intersection utilizing different radii, including the IFAs previously computed for each intersection (see Figure 5.1). The largest buffer at any given intersection was defined by a radius equal to the largest IFA for that particular intersection, denoted Max IFA.

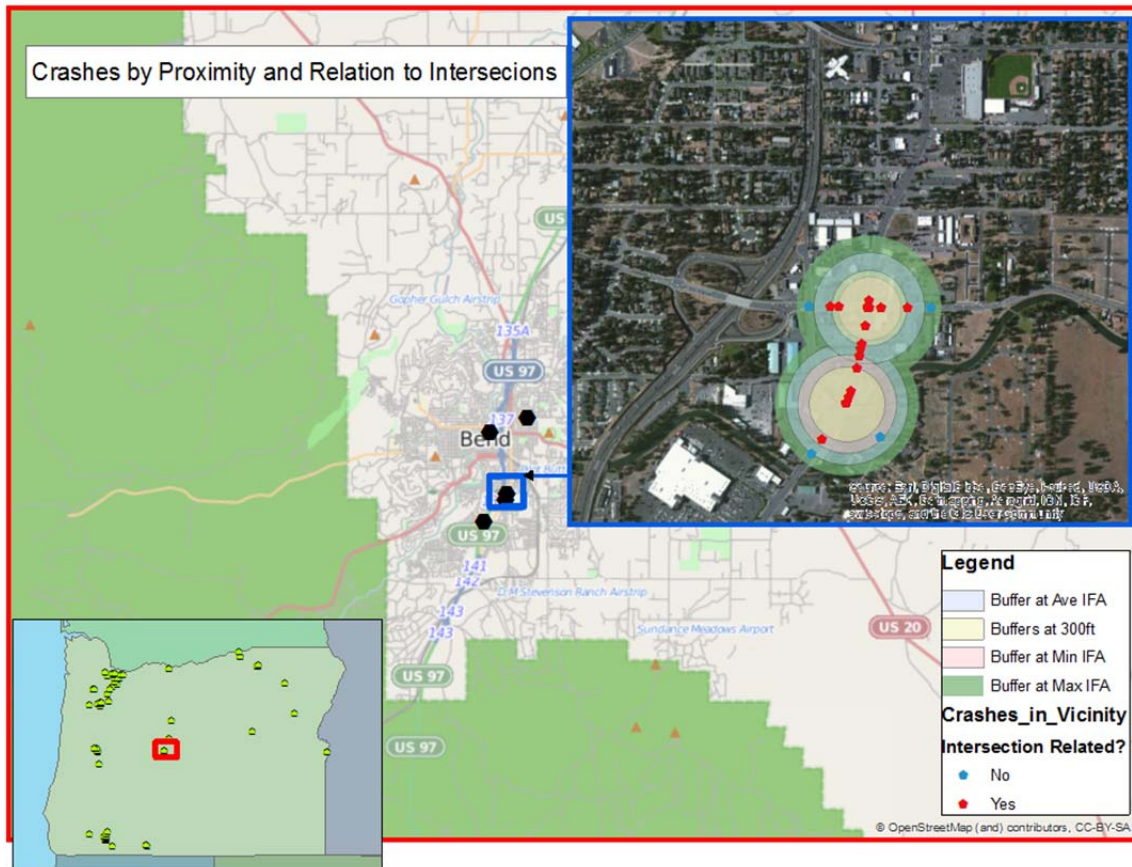


Figure 5.1: Sample Sites with Buffers at Various Radii

The research team examined the differences between buffer radii but did not find any radius that performed significantly better than others. For this reason, the research team decided to perform a systematic evaluation of various classification methods based on the set of crashes within the

Max IFA buffers. The research team considered that a critical step was necessary prior to the statistical analysis: manually classifying the 1944 crashes identified within the max IFA buffers as either IR or not. This effort is summarized in Section 5.2.1.

5.2.1 Manual Classification of Intersection Crashes

To manually classify each crash, the research team drew from the combined data available from the geo-location of crashes, the geometric database, and the various fields in the ODOT crash database.

Naturally, the extent of each buffer radius depends heavily on specific intersection features, as Figure 5.2 shows for three select intersections. In this figure, green circles indicate a crash related to an intersection (IR), and black diamonds indicate non-IR crashes. It is clear from Figure 5.2 that the buffers encircled crashes that corresponded to other streets or intersections in several instances. Figure 5.3 shows an example of non-IR crashes in the buffer that are clearly unrelated to the intersection of interest. After filtering and cleaning the crash database from these types of locations, the research team identified 1535 crashes from the initial pool of 1944 candidate crashes.

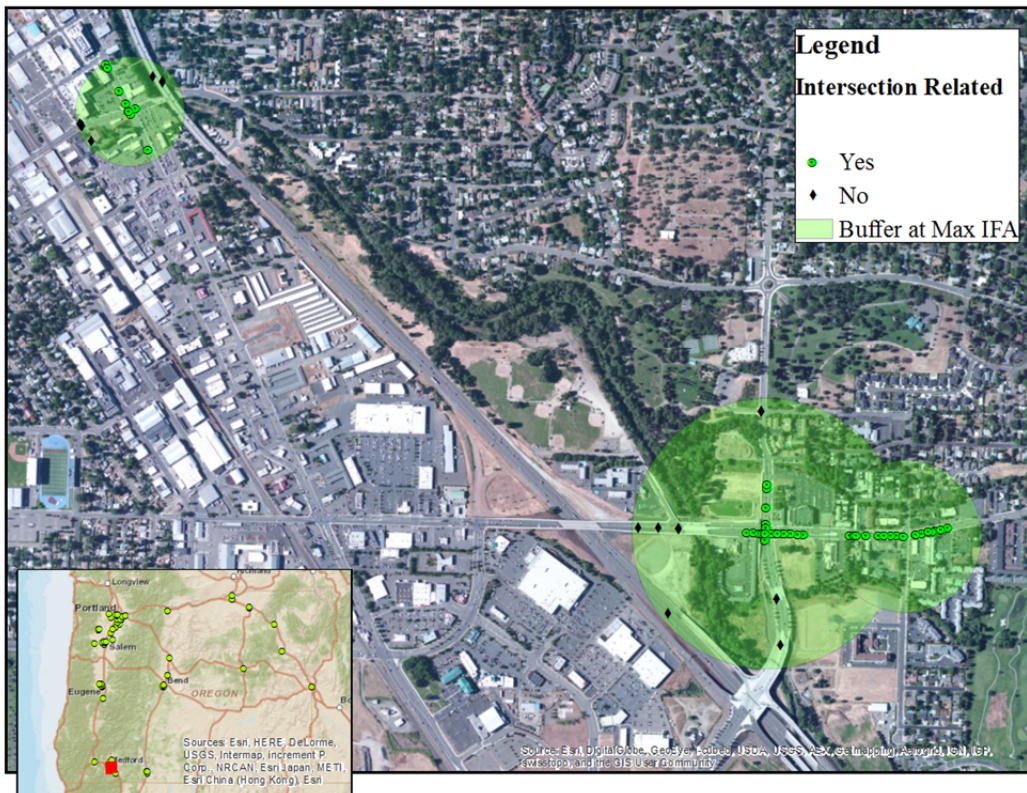


Figure 5.2: Sample Sites of various IFA Radii

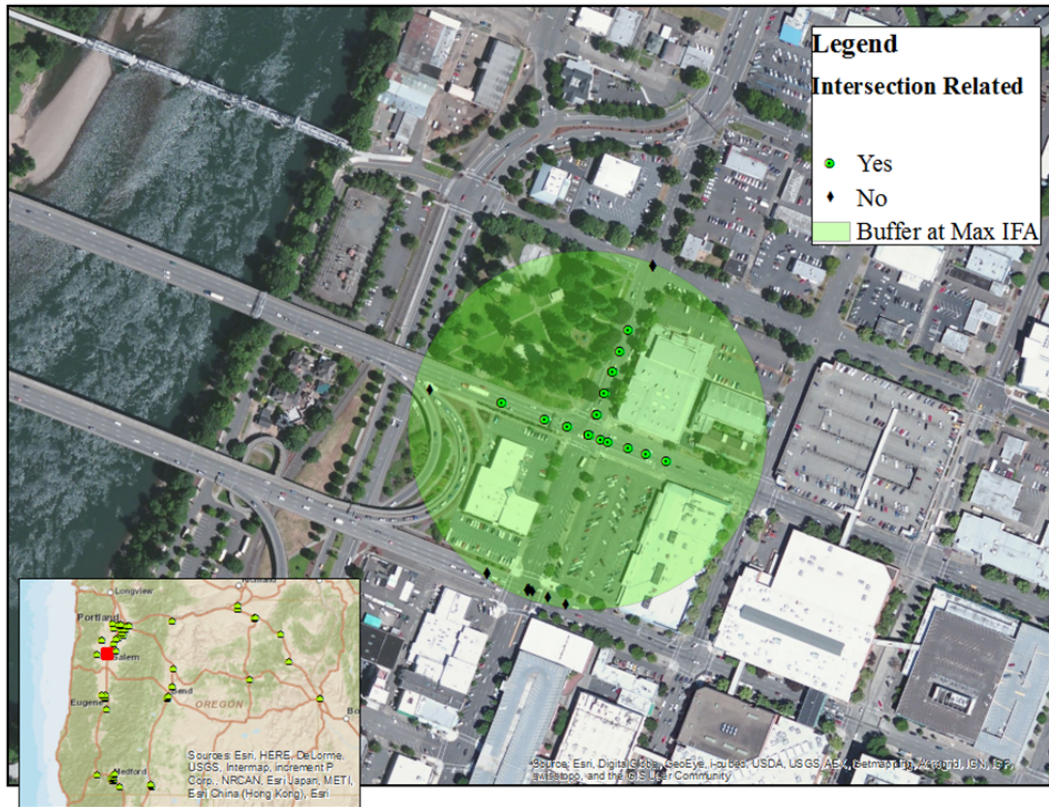


Figure 5.3: Sample Site at Low Speed Limit Urban Area

The research team found that 1330 of the 1535 crashes were geocoded within an IFA in the sample. This preliminary finding indicates that geo-location is a clear indicator of potential IR crashes ($1330/1535=0.866$), in general. However, only 551 of these crashes included crash report codes that indicated a traffic signal might be associated with the crash. This number remained low (673) even after the research team explored alternative IR codes in the Oregon crash database (i.e. ‘Left turn refuge’, ‘Left turn arrow’, ‘right turn prohibited on red’ etc.). There were 65 of the crashes coded as ‘stop sign’ and 96 coded as ‘No Control’ that were geo-located within the IFA of a study site.

5.2.2 Manual Classification of Intersection Related Crashes

The research team proceeded to manually classify the 1535 crashes either as IR or non-IR using the combined information from geo-location, the reported crash descriptions, and their relation with geometric characteristics from each site.

First, the research team inspected all the 205 crashes that did not correspond to any IFA to confirm that the coding in the crash database did not indicate they were IR. Only 105 of these crashes were coded as related to one of the study signalized intersections. Upon consideration of additional crash report code categories that might indirectly indicate a signalized intersection, this count increased to 110 crashes. Given these numbers, the research team estimated that the chances of a crash being coded as signal related are roughly 50 percent (110/205) when that crash does not fall within any IFA.

A subtotal of 1440 IR-candidates crashes resulted from pooling all crashes within IFAs with the 110 crashes outside IFAs that were coded as involving a traffic control device (TCD) related to a traffic signal. This rule alone would exclude only 87 of the 1535 candidate crashes to be classified as non-IR for this analysis. However, 476 out of the 1440 IR candidate crashes were located closer to encroaching non-signalized intersections (456 upstream and 20 downstream of the signalized intersections under study). The research team noted that most of these crashes were not likely to be IR, but would be erroneously classified as IR because they are located within the IFA. After a closer examination of the corresponding crash database records, the research team determined that 306 upstream and 16 downstream of these crashes are clearly associated with an encroaching non-signalized intersection instead of the studied signalized intersection in close proximity. This finding reinforces the notion that geo-location (combined with aerial photography in this case) tends to correctly capture complex situations that may not be observed when only using the information in the crash database.

Finally, for the purposes of this research, the research team established a definitive IR classification as follows:

1. The 110 crashes that were coded as IR in the crash database but not geo-coded as such (via indications of an intersection TCD); and
2. Any crash that was geo-located within an IFA, but that was not closer to an encroaching non-signalized intersection.

In total, 964 crashes were identified as IR and 571 crashes were identified as non-IR.

The creation of a database and manual crash classification is time consuming, thus explaining the appeal of using radius / distance thresholds as previously discussed. Rules that utilize such distance thresholds are popular, even with the prospect of potential shortcomings. By using such rules, a researcher or practitioner places their trust on the reliability of geo-location as a critical piece of information supplementing the codes in the crash database records. For these rules to be useful, therefore, distance from the intersection (as can be obtained from the geo-locations of crash and intersection) should correlate highly with the likelihood of a crash truly being IR. This preliminary examination of the data offers clues that that is likely the case.

Next, the research team performed a formal evaluation of various screening methods, using the dataset readily assembled for that purpose. In Section 5.2.3, two basic types of screening methods are compared:

- Rules that utilize distance thresholds, and
- Rules based on predicting models by utilizing a distance from the intersection as well as other potential predictors.

5.2.3 Statistical Analysis on Distance, Speed Limit and Max IFA for Intersection Crash Classification

To compare models to assess the IR crash selection screening rules –based only on distance thresholds –the research team partitioned the database into two subsets: a training set consisting of three quarters of the dataset (i.e. 55 intersections containing 1149 crashes) selected at random, and a validation subset consisting of 18 intersections containing 386 crashes. The objective of setting aside the validation subset is to later perform comparisons using a subset of sites that is independent to either of the two methods (i.e. distance-based rules vs. rules based on statistical models).

Utilizing the training subset database, the research team developed logistic models to estimate the probability of a crash being IR, given a set of predicting variables. The general form of the models is represented by the following equation:

$$\pi_{IRij} = \text{logistic}(X^T \cdot \beta + \{\alpha_i + \gamma_{ij}\})$$

Where:

π_{IR}	=	Probability of a crash being related to an intersection;
X	=	vector of fixed-effect predictors;
β	=	coefficients corresponding to fixed-effect predictors;
α_i	=	random effect for i^{th} intersection; and
γ_{ij}	=	nested random effect for i^{th} approach in j^{th} intersection.

Utilizing this general model, the research team developed four candidate models that included different predictors. Interestingly, all models incorporated distance from intersection among their independent variables. Table 5.1 summarizes the variables included in each of the four candidate models.

Table 5.1: Predictors included in Probability Models Developed

Model	Distance (ft)	Speed Limit (mph)	IFA (1=inside, 0=otherwise)	Distance to Intersection Upstream (ft)
Distance Model (DS mod)	X			
Speed Limit Model (SL mod)	X	X		
IFA Model 1 (IFA1 mod)	X		X	
IFA Model 2(IFA2 mod)	X		X	X

As an example, Figure 5.4 shows the probability curves resulting from the first two models in Table 5.1. There are two important thresholds represented as dashed lines indicated in this figure. The vertical dashed line indicates a distance of 250 feet from the intersection, a commonly used rule to identify IR crashes. The horizontal line shows a probability of 0.5, which is a natural breaking point for the probability curves.

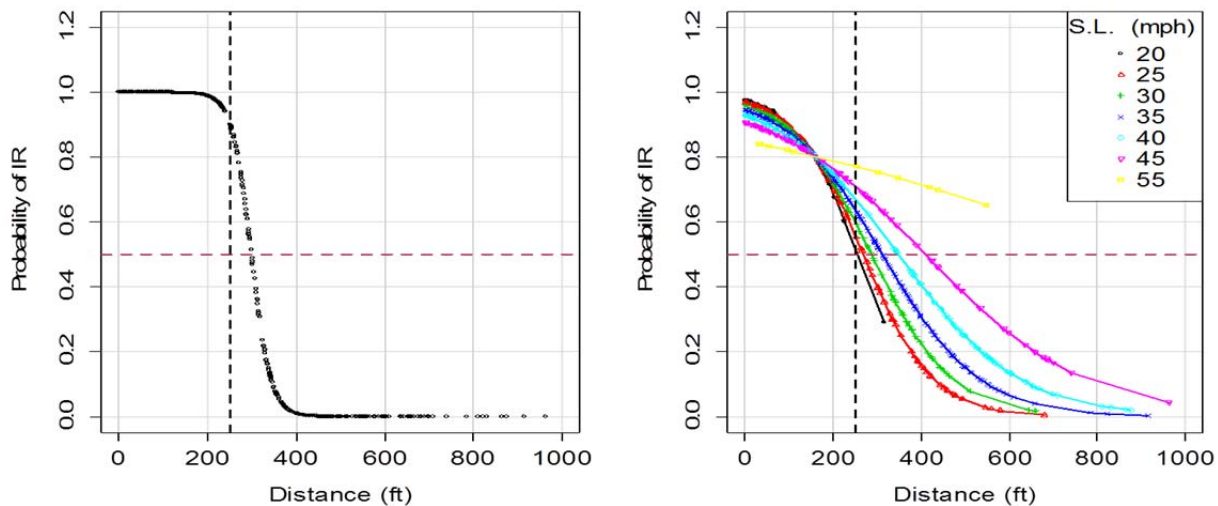


Figure 5.4: Probability curves from DS mod (left) and SL mod (right)

As can be seen for the DS model, the natural IR/non-IR breaking point occurs around 300 feet from the intersection. However, for the SL model, speed limit clearly determines how far from the intersection a curve crosses the 0.5 horizontal line. In general, the higher the speed limit, the more likely that IR crashes are located farther from the intersection.

5.2.3.1 Developing Screening Rules based on Statistical Models

The purpose of developing these models is to estimate the probability that a crash was IR. In order for these models be useful as screening tools, the researchers need to set an adequate probability threshold to use (i.e. How high are the chances that a crash that is IR should be identified as IR?).

Four thresholds were selected: 25, 50, 75 and 90 percent. On the one hand, a threshold of 25 percent implies that there is a probability of 0.25 that an IR crash will be identified as an IR crash. Therefore, the highest number of IR classifications should result when using this threshold. A potential shortcoming is that a significant proportion of crashes are not likely to be associated with the intersection. On the other hand, the lowest number of IR classifications should result from using the strictest threshold: 90 percent, with all or almost all of these crashes being IR in reality. The expected shortcoming in this case is that a considerable number of actual IR crashes will likely be classified as non-IR.

Section 5.2.4 describes the evaluation of various crash screening methods, including the alternative methods that utilized the probability models described in this section.

5.2.4 Evaluation of Crash Screening Methods using the Validation Subset

Using the validation subset, the researchers evaluated different screening criteria based on adequate performance measures.

In addition to applying the screening methods based on the developed models, the research team compared the performance of two rules commonly used by the transportation community to identify IR crashes. The first rule is to classify any crash within a radius of an intersection as IR (commonly a value of 250 feet). The second rule includes the crashes from the previous criterion but it also adds any crash that is coded in its database record as related to an intersection TCD, even when the crash may be located a distance greater than the selected radius from the intersection. The research team developed six specific methods, based on three thresholds for the maximum radius rule:

- The commonly used 250 feet distance;
- A value of 300 feet as clearly suggested in Figure 5.4; and
- A narrower threshold of 200 feet, to try to identify a trend by these rules.

In total, considering the six distance-rule methods and the 12 methods based on statistical models (i.e. the 3 first model specifications x 4 probability thresholds), the research team compared the performance of 18 different screening methods for the validation data.

5.2.4.1 Measures of Effectiveness

In order to evaluate the individual screening methods, the research team classified each crash in the validation data subset using each of the methods selected for evaluation. When all crashes in the validation dataset were classified by all methods, the research team computed the following quantities from the outcomes of each method:

- The cumulative frequencies of the four possible outcomes when classifying IR crashes (True IR, False IR, True non-IR, and False non-IR).
- The percentages of types I and II errors:

- Type-I error= (False non-IRs) / (False non-IRs + True IRs); and
- Type-II error= (False IRs) / (False IRs + True non-IRs).
- The outcome percentages of True IRs and True non-IRs per each method of screening:
 - %True IRs=(True IRs)/ (True IRs+False IRs); and
 - %True non-IRs=(True non-IRs)/ (True non-IRs+False non-IRs)

5.2.4.2 Classic Crash Screening Method Validation Analysis

Table 5.2 shows the results ranked by the absolute difference between false IRs and false non-IR. This difference is of particular interest, since the purpose of this study is to develop an SPF which will ultimately be used to predict crash frequency; therefore, an SPF is expected to yield better predictions if the total absolute amounts of type-I and type-II errors tend to be the same (i.e. tend to ‘cancel out’).

Table 5.2: Performance of Screening Methods on Validation Data

Rank	Method	Freq. True IRs	Freq. False IRs	Freq. True non-IRs	Freq. False non-IRs	Type-I Error (%)	Type-II Error (%)	True IRs (%)	True non-IRs (%)	Abs(False IRs-False non-IRs)
1	D ≤ 300 ft and TCD	227	41	68	50	18	38	85	58	9
2	DSmod at 50% (385 ft)	222	46	63	55	20	42	83	53	9
3	SPmod at 25%	218	71	43	62	22	62	75	41	9
4	IFAMod1 at 25%	232	74	35	45	16	68	76	44	29
5	D ≤ 250 ft and TCD	206	32	77	71	26	29	87	52	39
6	SPmod at 50%	194	47	67	86	31	41	80	44	39
7	DSmod at 25% (510 ft)	250	77	32	27	10	71	76	54	50
8	D ≤ 200 ft and TCD	197	30	79	80	29	28	87	50	50
9	IFAMod1 at 50%	195	20	89	82	30	18	91	52	62
10	SPmod at 75%	181	35	79	99	35	31	84	44	64
11	D ≤ 300 ft	186	16	93	91	33	15	92	51	75
12	SPmod at 90%	161	32	82	119	43	28	83	41	87
13	IFAMod1 at 75%	174	7	102	103	37	6	96	50	96
14	DSmod at 75% (260 ft)	164	9	100	113	41	8	95	47	104
15	D ≤ 250 ft	163	5	104	114	41	5	97	48	109
16	D ≤ 200 ft	153	3	106	124	45	3	98	46	121
17	DSmod at 90% (140 ft)	130	0	109	147	53	0	100	43	147
18	IFAMod1 at 90%	127	3	106	150	54	3	98	41	147

The best ranked threshold-based method, as indicated by shading in Table 5.2, utilizes a 300 feet radius in combination with crash codes that indicate TCDs contributing to the crash event.

5.2.4.3 Leave-One-Out Cross Validation Analysis

To confirm and fine tune these results, the research team performed a Leave-One-Out Cross Validation analysis (LOOCV). Although it is computationally intensive, this procedure maximizes the use of the data at hand giving detailed statistics of the expected performance of the different methods under evaluation. The procedure consists of the following steps:

1. One intersection is set aside;
2. The statistical models under evaluation are then developed for the remaining 72 intersections;
3. All methods under evaluation are applied to screening IR vs. non-IR crashes using the one intersection set aside at the beginning; and
4. The above steps are repeated until every one of the 73 intersections has been set aside and screened for IR crashes.

This process yields 73 performance comparisons where crashes at each intersection are evaluated in fairness, given that the crashes of the intersection evaluated have no bearing over the estimates from the model-based methods (based on the data from the other 72 intersections).

The research team expects that results from the LOOCV analysis should yield better insights regarding the potential benefits of using model-based methods than the classical validation approach for the following three reasons:

- These estimates are based on several coefficient estimations and so incorporate variation due to regression, otherwise overlooked.
- When considering the available data, the models are as refined as they can be for a ‘fair comparison’ with the other methods. Each model is fitted to data from 72 intersections for the LOOCV procedure, in contrast to 55 intersections in the classical validation approach.
- The influence of anomalies in a particular partition of the data in training/validation subsets is removed since results are averaged over all possible 72:1 partitions in the dataset.

Table 5.3 shows the averages obtained from the LOOCV procedure. This result confirms the preliminary finding that using a 300 feet threshold in combination with the TCD indicator codes is the best performing of the distance-threshold rules. Results from this

simple method are comparable with IFAmo1 and SPmod, the only two models that outperformed this simple model based on the LOOCV procedure (see shaded model ranked third in Table 5.3).

Table 5.3: Performance of Screening Methods using LOOCV

Rank	Method	Freq. True IRs	Freq. False IRs	Freq. True non-IRs	Freq. False non-IRs	Type-I Error (%)	Type-II Error (%)	True IRs (%)	True non-IRs (%)	Abs(False IRs-False non-IRs)
1	IFAmo1 at 50%	13.110	2.247	3.301	2.370	9	27	84	64	0.123
2	SPmod at 50%	12.781	2.644	2.740	2.479	10	36	81	47	0.164
3	$D \leq 300$ ft and TCD	12.986	2.205	3.342	2.493	12	26	85	55	0.288
4	DSmod at 50% (385 ft)	13.082	2.849	2.699	2.397	8	45	79	45	0.452
5	IFAmo2 at 25%	13.603	2.479	3.068	1.849	5	37	82	61	0.630
6	IFAmo2 at 50%	13.082	1.479	4.068	2.370	9	20	87	67	0.890
7	$D \leq 250$ ft and TCD	12.329	1.740	3.808	3.151	17	19	86	54	1.411
8	SPmod at 75%	11.973	1.616	3.767	3.288	17	18	85	55	1.671
9	$D \leq 300$ ft	12.151	1.630	3.918	3.329	15	22	87	53	1.699
10	IFAmo1 at 75%	12.123	1.329	4.219	3.356	16	13	88	61	2.027
11	$D \leq 200$ ft and TCD	11.863	1.370	4.178	3.616	19	13	88	55	2.247
12	SPmod at 25%	13.904	3.753	1.630	1.356	5	55	76	37	2.397
13	IFAmo2 at 75%	12.397	0.644	4.904	3.055	14	8	90	66	2.411
14	DSmod at 75% (260 ft)	11.562	1.411	4.137	3.918	19	19	87	51	2.507
15	DSmod at 25% (510 ft)	13.932	4.151	1.397	1.548	4	65	75	27	2.603
16	IFAmo1 at 25%	14.356	4.123	1.425	1.123	3	62	75	36	3.000
17	$D \leq 250$ ft	11.466	1.014	4.534	4.014	19	14	89	53	3.000
18	SPmod at 90%	11.041	0.712	4.671	4.219	21	9	89	53	3.507
19	$D \leq 200$ ft	10.986	0.630	4.918	4.493	22	8	91	54	3.863
20	IFAmo1 at 90%	10.164	0.671	4.877	5.315	33	5	83	50	4.644
21	DSmod at 90% (140 ft)	10.411	0.260	5.288	5.068	25	3	92	54	4.808
22	IFAmo2 at 90%	9.836	0.055	5.493	5.616	36	2	79	55	5.562

Furthermore, comparing the three best performing methods, the research team considers that there is little incremental gain from using any of the two better-performing methods, in terms of input required, statistical tool calibration, etc. In contrast, a simplistic rule of 300 feet + TCD indicators performs similarly and much more straightforward to apply. This observation is also apparent in Figure 5.5.

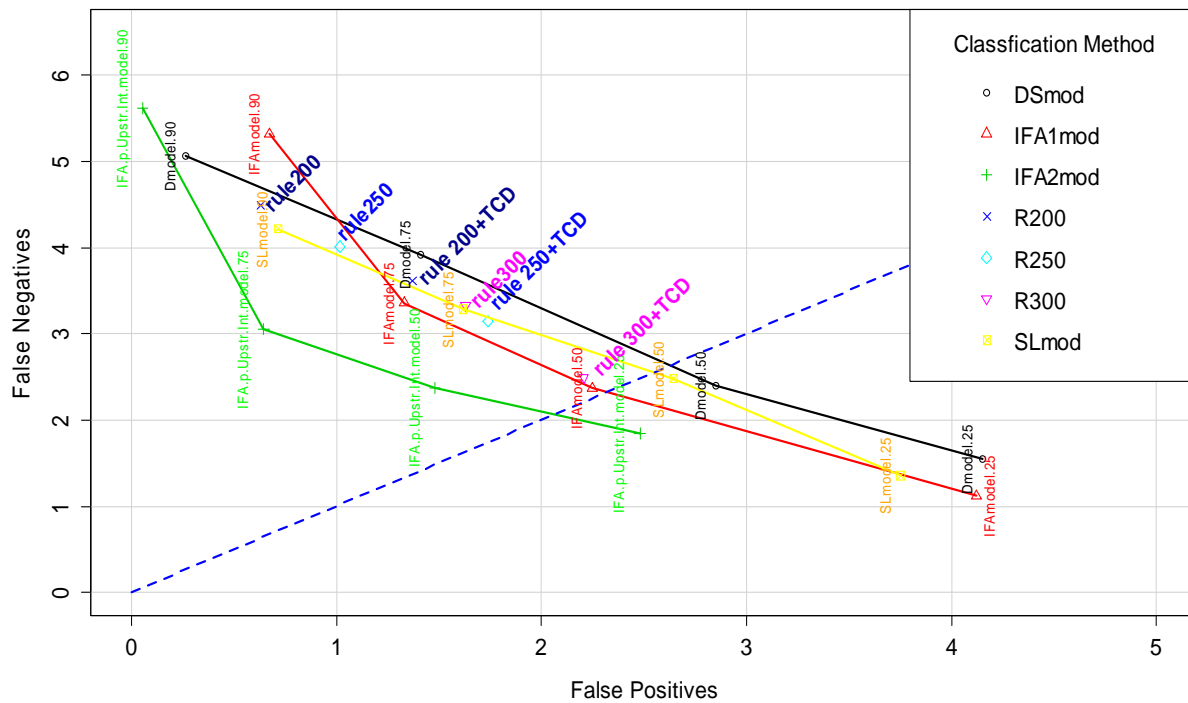


Figure 5.5: Performance Comparison of Screening Methods

The blue dashed line in Figure 5.5 indicates the ideal case of a screening method “cancelling out” exactly the number of false positives and the number of false negatives. The rule of 300 ft + TCD falls very close to this line as do the only two methods that outperformed this rule.

5.2.5 Summary of Evaluation of IR Screening Methods

The research team developed a dataset of intersections for which IR crashes were manually classified. This dataset was then utilized to test the performance of various classification methods. Some of these methods were based on popular rules based on distance from intersection and database codes indicating involvement of intersection-related TCDs. The research team developed additional classification methods based on statistical models fitted to the dataset of manually classified IR crashes.

The research team compared the performance of a total of 22 classification methods utilizing two alternative evaluation techniques: classic validation, which utilizes a subset of sites initially preserved from the development of tools staged; and a Leave-One-Out Cross Validation procedure, which maximizes data utilization at the cost of increased need for computation power. Both evaluations yielded similar results: the recommended screening method identified in this section (i.e. 300 feet + TCD rule) were then be utilized to select the crashes for subsequent years and intersections for the SPF validation effort reviewed in Section 5.3 of this report.

5.3 SPF DEVELOPMENT

To refine IR crash screening procedures, the research team manually reviewed a substantial quantity of crash data (see Section 5.2). Although the purpose of the detailed examination was to screen additional crash data for analysis, the research team determined that the manually screened dataset was sufficiently large so as to facilitate the development of the signalized intersection SPFs, the overall objective of this research effort. The research team reserved data for additional years and for additional intersections for a later validation effort as presented in Appendix D and summarized in Section 5.5. The modeling dataset therefore consists of 964 crashes positively identified as IR corresponding to a total of 73 intersections.

Procuring AADT counts was particularly challenging for minor roads. It was not possible to obtain this count information at all for a few intersections. Similarly, speed limit was not always available for all legs of all intersections. As a result, it was not possible to utilize all 73 intersections for SPF development. Inevitably, some intersections in the dataset had missing information in at least one of the variables critical for this analysis. More details on incomplete data points will be given later in this document.

Given these data shortages, the research team decided to add a longitudinal component to the analysis, instead of treating the data simply as a cross-sectional sample of independent points. This strategy maximizes the amount of useful data, as well as it accounts for year-to-year variability in a more realistic way. Such an approach implies that the unit of analysis is not the sum of crashes that occurred at an intersection during a study period (2010-2012 for the dataset at hand); rather, the unit of analysis is total crashes per intersection for each year in the study period. This analysis unit will be referred to as intersection-year from this point forward in the document.

Section 5.3.1 describes the statistical methodology to be applied to a dataset structured by intersection-year counts rather than counts by intersection.

5.3.1 Statistical Methodology for Initial Model Development

Because more than one time period from each intersection is to be used as an analysis unit, an appropriate methodology should account for the grouping structure that this feature enables: all crashes from a common space unit (i.e. intersection) should be considered a “family” sharing a “baseline” to the crash generation process at that intersection. In other words, the modeling tool should have a way to account for this grouping correlation, even though it is not practical to explicitly consider all the underlying similarities among crashes from a single location. An appropriate way to deal with this need is the use of random effects during the modeling effort. Among other properties of these effects in mixed models, they induce a grouping structure and treat explicitly the resulting correlation from that structure, as is required in this research.

Specifically, the research team elected to perform the analysis using a Poisson-lognormal Generalized Linear Mixed model. The expected crash count at an intersection for a particular year is assumed to follow the Poisson (or random) distribution, whose probability function is represented as:

$$P(N_i = n) = \frac{\lambda_i^n}{n!} \cdot e^{-\lambda_i}$$

Where:

N_i = Number of crashes in a year at i-th intersection;

n = An actual count of yearly crashes, $n \in \{0, \mathbb{Z}^+\}$; and

λ_i = Mean parameter in the Poisson distribution of N_i at the i-th intersection.

It should be noted that in the above definition, the parameter λ_i is defined for a given intersection “i.” The methodology allows a slightly different parameter to be defined for intersection “i+1”, that is, parameter λ_{i+1} . It is then expected then that the distribution of mean parameters in the dataset should influence the resulting SPF. More details will be given later in this report about how this distribution relates to the crash prediction that pertains to this research.

The model estimation describes the relationship between yearly counts at each intersection and the critical factors via a link function, the natural logarithm in this case. For the i-th intersection, the next formula defines the parameter λ_i :

$$\lambda_i = \exp(X^T \cdot \beta + Int_i)$$

Where:

X = Vector of fixed effects (i.e. explanatory variables);

β = Vector of fixed-effects coefficients; and

Int_i = Random effect for i-th intersection.

All other variables as previously defined.

The above definition implies that, in general, different intersections have different crash expectations, even when all predictors in the vector X are the same (say, all the critical variables considered for this analysis: MjAADT, MnAADT, MjSpLm, and MnSpLm).

5.3.1.1 Implications of Selected Statistical Methodology for Crash Prediction

It is of interest to develop predictions about a larger population of intersections thought to be represented by the study dataset. This is a reasonable assumption since the dataset is a random sample of intersections in Oregon. For the purposes of this analysis, the population can be defined as “all signalized intersections with a crash history in the Oregon crash databases.”

Because the estimation of β is performed using a set of given intersections, the crash prediction is inevitably affected by the variability among the intersections. If a more classical approach were feasible to use to fit coefficients for an NB2 regression – such as using Generalized Linear Models (GLM) – then the extra-Poisson variability would be captured by the dispersion parameter. However, for a mixed model proposed in this methodology, this variability is captured by the distribution of the intersection of random

effect. Under the assumption that this effect is normally-distributed in the link scale (an assumption that will be assessed from the model fit) it can be shown that:

$$E(N_{X=x}) = \exp\left(x^T \cdot \beta + \frac{V(Int)}{2}\right)$$

Given that

$$\ln(\lambda_{X=x}) \sim N\left(\mu = (x^T \cdot \beta), \sigma^2 = V(Int)\right)$$

Where:

- $E(N_{IR})$ = Expected yearly crashes for the subpopulation of intersections $X = x$;
- x = A particular value for X , the vector of fixed effects;
- $V(Int)$ = Variance of Intersection random effect, estimated from the intersections in the modeling dataset;
- $N[\cdot, \cdot]$ = The normal distribution;
- μ = Mean parameter for the normal distribution; and
- σ^2 = Variance parameter for the normal distribution.

All other variables are as previously defined.

The next section shows descriptive statistics for the dataset developed for this effort. These characteristics ultimately define the scope and limitations of the developed SPFs.

5.3.1.2 Dataset Characteristics

One advantage of utilizing the approach just described is the potential pool of $73 \times 3 = 219$ intersection-years for analysis, as opposed to just 73 intersections, where the response is the aggregate crash counts for the three years under study. However, this potential pool reduces to 210 useful intersection-years considering that no AADT information at all is available at three intersections for any of the three years in the analysis period. Similarly, speed limit for the major road (MjSpLim) is not available for six intersection-years. In addition, there are 15 intersection-years with missing data about speed limit at the minor approaches (MnSpLim).

For the two primary exposure variables (i.e. AADT variables), there are 36 intersection-years without data for the major road (MjAADT), and 45 intersection-years with data missing for the minor road (MnAADT). Only 162 intersection-years have data available for AADT at both intersection roads. Only 150 intersection-years constitute a complete dataset, having data for both AADTs and both speed limits. These 150 intersection-years represent 50 different intersections as present in Section 3.0. Table 5.4 show the summary statistics for this complete dataset.

As shown in Table 5.4, the yearly average of total crashes per year is 5.74. Most of the observed IR crashes are multivehicle crashes (791 MV_Crashes out of 861 Total Crashes). The range of values of each of the critical variables is an important feature, as it determines the range of validity of the resulting SPF. These minimum and maximum values are shown in the “Min” and “Max” columns in Table 5.4. Consequently, this dataset is representative of intersections with Major AADT ranging from approximately 5,000 to 43,000 vpd; minor AADT from 800 to 23,000 vpd; speed limit for the major street between 20 and 55 mph; and minor street speed limit ranging from 10 to 45 mph.

Table 5.4: Yearly Statistics for Complete Intersection-year Data. Years 2010-2012

Variable Name	Description	Mean	Std.Dev	Min	Max	Total	N
Total Crashes	All crashes	5.74	6.36	0	46	861	150
MV_Crashes	Multiple vehicle crashes	5.27	6.06	0	42	791	150
KAB_Crashes	Fatal and serious injury crashes	0.82	1.30	0	8	123	150
MV_KAB_Crashes	Severe crashes with multiple vehicles	0.57	1.01	0	6	85	150
MjAADT	Major AADT (vpd)	17203.45	8366.87	5007	43160	-	150
MnAADT	Minor AADT (vpd)	7391.48	5184.17	807	23316	-	150
MjSpLimMax	Major Speed Limit (mph)	33.8	7.68	20	55	-	150
MnSpLimMin	Minor Speed Limit (mph)	28.3	6.92	10	45	-	150

The variables have a positive correlation to each other as represented by large solid circles in Figure 5.6. Figure 5.7 shows a direct comparison of the correlation between the individual variables. Sites with higher speed limits, for example, tend to have higher AADTs, which in turn, are subject to more crashes.

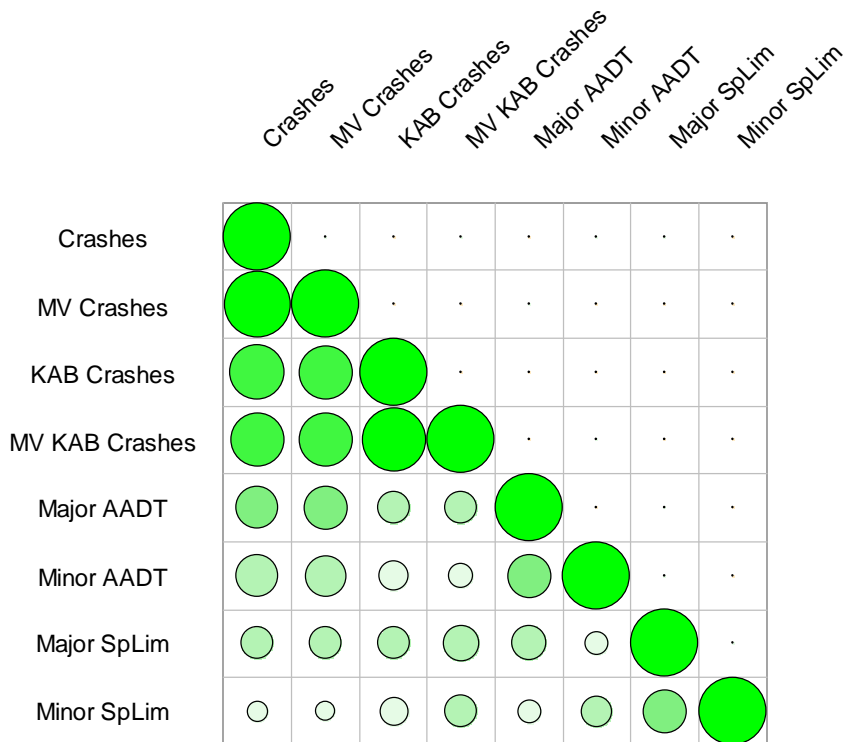


Figure 5.6: Correlations Among Variables in Complete Dataset

MjAADT exhibited the highest correlations with Total and MV crashes. MnSpLim is the variable with the weaker association to the first two types of crashes. Interestingly, the correlations of this variable with KAB and MV KAB crashes are very comparable to the correlations of Major AADT to these crash types.

Unfortunately, the notable correlations between Major and Minor AADTs and between Major and Minor SpLim increase the likelihood of multicollinearity in SPF estimates. In other words, because only so much information is required to produce reasonable crash estimates, some relevant variables may not be part of the final SPF because their contribution ‘overlaps’ with the contributions of other, more influential variables in the prediction, despite there being important links between the less relevant variables and crash occurrence.

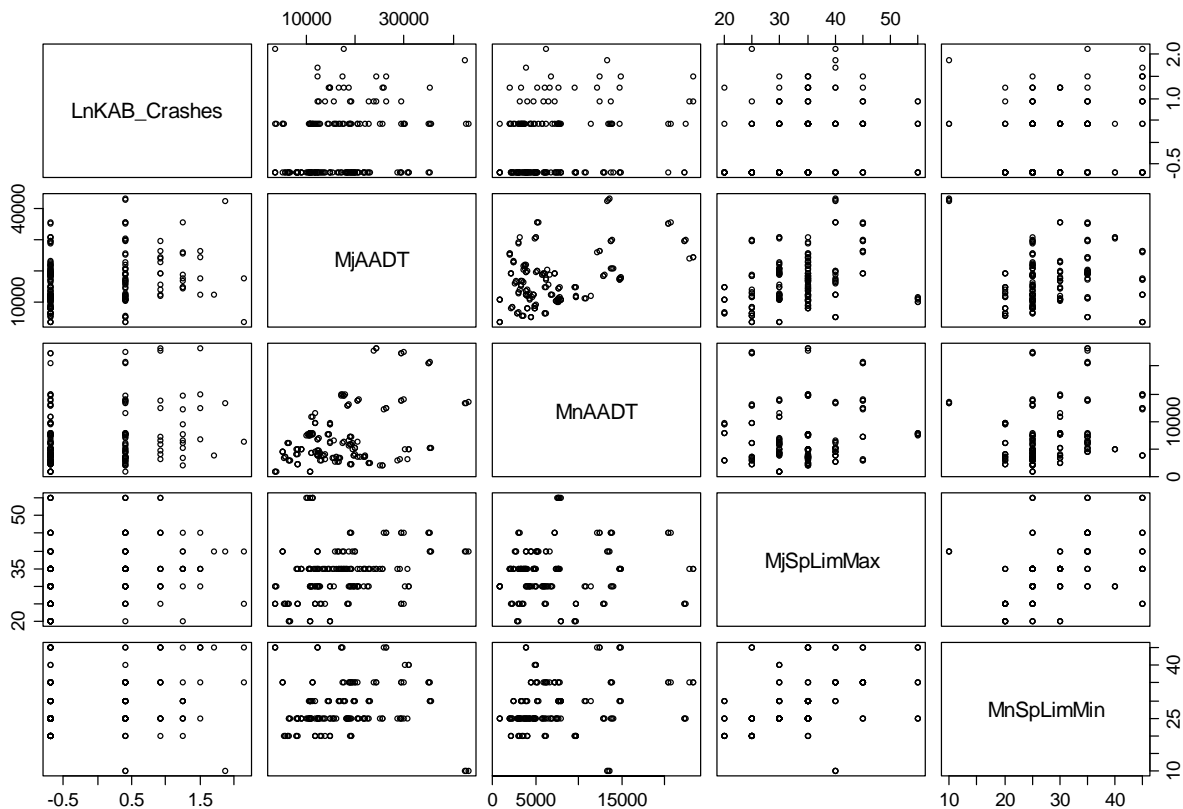


Figure 5.7: Scatter Plot of ln(KAB Crashes) and Critical Variables in the Complete Dataset

Section 5.3.2 describes the model development of an SPF for total crashes at signalized intersections. Similarly, Sections 5.3.3 and 5.4 review the fatal and serious injury SPF development for the signalized intersections.

5.3.2 Initial SPF for Total Crashes

As a first step in the modelling process, the research team developed a full model that included the four critical variables (AADTs and speed limits at both intersecting roads) as well as the number of lanes and median types for both roads. For this full model, only the AADT terms were determined to be statistically significant.

The research team then reduced the model to include a subset of individual variables for different alternative configurations of speed limit, number of lanes and medians, including derived variables such as the difference between speed limits, the module of speed limit, and sites with TWLTL compared to the rest, among others. None of these alternatives were more parsimonious than the simplest of specifications. Only the coefficient for both AADTs proved to be statistically significant. Table 5.5 shows a comparison between the full and reduced models.

Table 5.5: Analysis of Deviance for Full and Reduced Models

Reduced model variables		MjAADT, MnAADT						
Full model variables		MjAADT, MnAADT, MjSpLim, MnSpLim, TWLTL, NoLanesMj, NoLanesMn						
Likelihood Ratio Test								
	Df	AIC	BIC	logLik	deviance	Chisq	Chi Df	Pr(>Chisq)
Reduced	4	758.04	770.08	-375.02	750.04			
Full	9	764.57	791.66	-373.28	746.57	3.4758	5	0.627

Since the Likelihood Ratio test favors the reduced model, the research team recommends this model as the SPF for total crashes at signalized intersections. Model coefficients were then estimated for the recommended SPF including an additional 12 intersection-years (where traffic volume was known) added to the dataset used for a total of 162 intersection-years. These 12 points were incomplete cases for the full model critical variables other than the AADT values. A test on the residuals of the model did not show evidence of over-dispersion (0.5442 p-value from a 155.375 chi-squared statistic on 158 degrees of freedom). The formulation for the resulting total crash model is then:

$$N_{Total} = e^{\beta_0 + \frac{Var(Int)}{2}} \times MjAADT^{\beta_1} \times MnAADT^{\beta_2}$$

Table 5.6 shows the coefficients corresponding to the recommended model.

Table 5.6: Coefficient Estimates for Reduced Model

	Estimate	Std. Error	z value	Pr(> z)	Statistical Significance
β_0	-9.9211	1.7168	-5.779	7.52E-09	***
β_1	0.7079	0.1823	3.882	0.000103	***
β_2	0.5206	0.1303	3.996	6.45E-05	***
Var(Int) = 0.2752					
Significance values are as follows: ° p<0.1; * p < 0.05; ** p < 0.01; and *** p < 0.001					

The resulting SPF for total number of crashes per year, after substituting the coefficients estimates in Table 5.6, is as follows:

$$N_{Total} = (5.63741 \times 10^{-05}) \times MjAADT^{0.7079} \times MnAADT^{0.5206}$$

The research team assessed the fit of the recommended SPF to the modeling dataset using various graphic techniques, in order to assure the appropriateness of the model specification.

There are two components, at a minimum, that should be reviewed when assessing the fit of mixed models intended for prediction: a fit to the modeling data, and (more importantly) a fit considering the assumptions that link the model to an underlying larger population, presumably represented by the modeling data. Therefore, the normality assumption of the intersection random effect should be verified as well.

Figure 5.8 shows the normal Quantile-to-Quantile plot of the random effects of the recommended SPF. There is only one site with an unusually large random effect (i.e. upper right corner), but the research team verified that this outlier does not exert undue influence over the model estimates. Since the normality of the intersection random effect appears reasonable, the research team next assessed the model fits to the sample and the projected fit to the population of signalized intersections in Oregon.

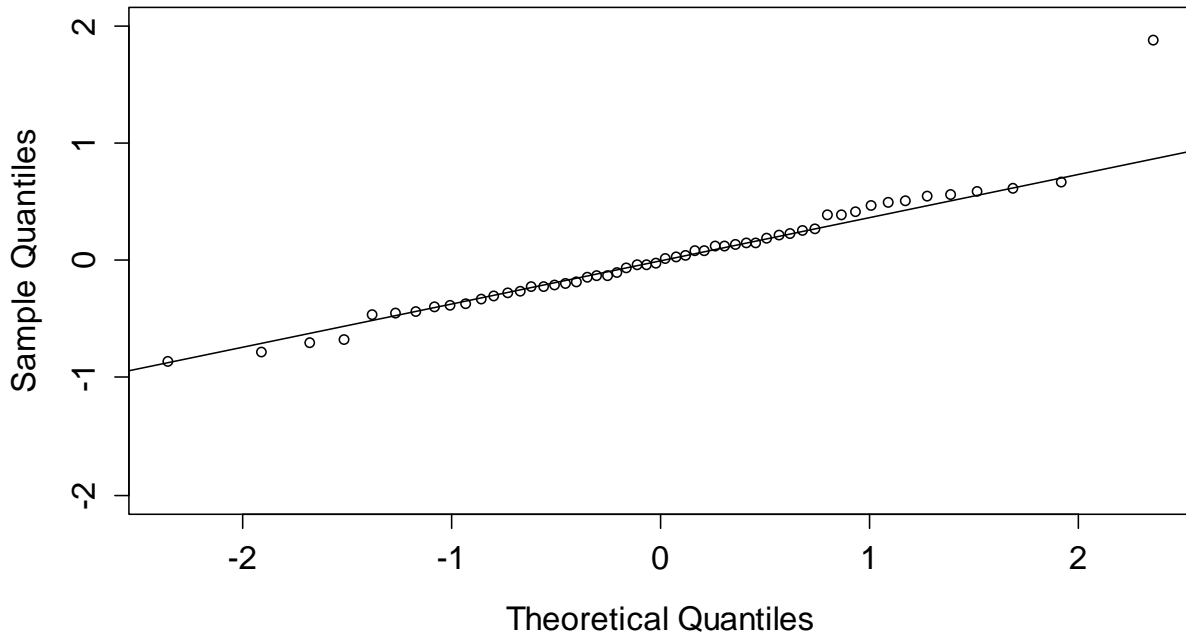


Figure 5.8: Q-Q Plot of Intersection Random Effect

Figure 5.9 demonstrates that the SPF fits adequately the modelling dataset. There are not enough degrees of freedom to statistically assess the fit using a chi-squared Goodness-of-Fit test for this figure. This is because the fit incorporates the 53 random effects specific to each intersection from the modelling dataset.

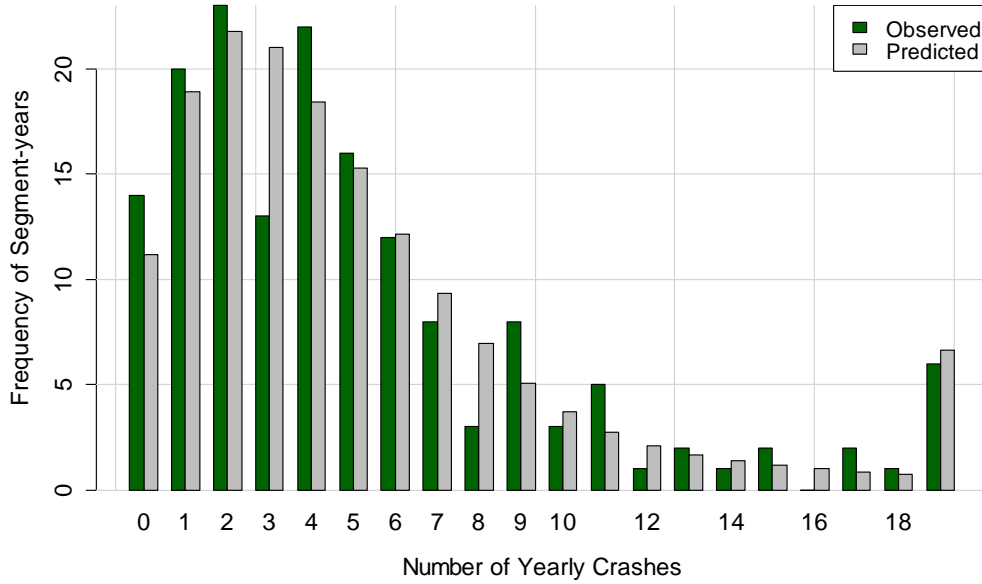


Figure 5.9: Marginal Distribution Fit of Model Parameters Specific to Modeling Data

Similarly, Figure 5.10 shows an adequate fit of the SPF projected for a larger population of sites. This figure relies on the normality of the intersection random effects, as verified in Figure 5.8.

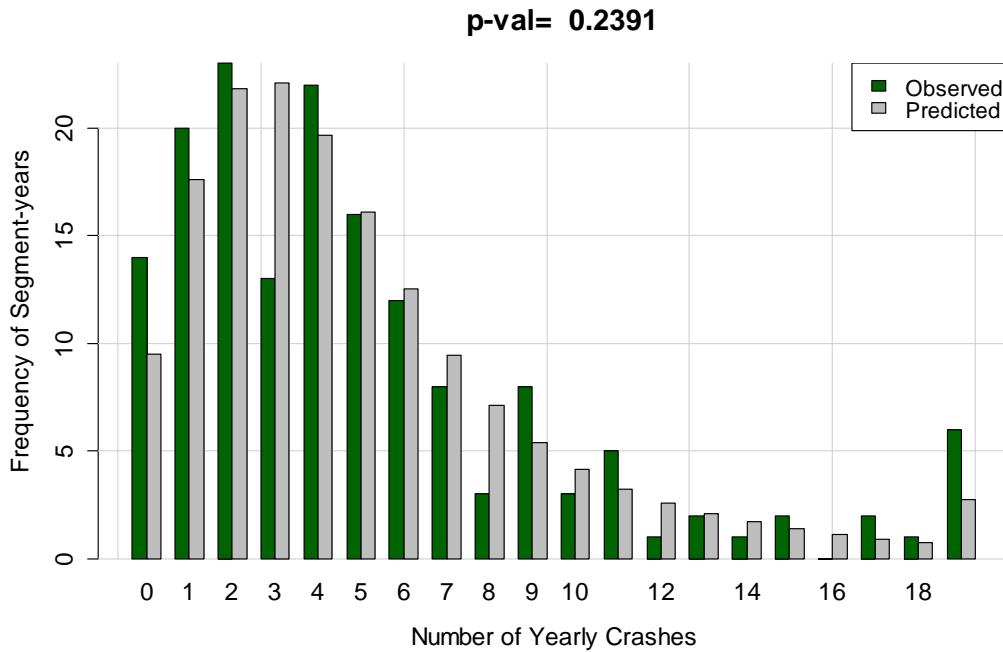


Figure 5.10: Marginal Distribution Fit of Model Parameters Projected to the Population

Figure 5.11 presents the observed frequencies, the model fit to the modeling sample and the population level projection from the model.

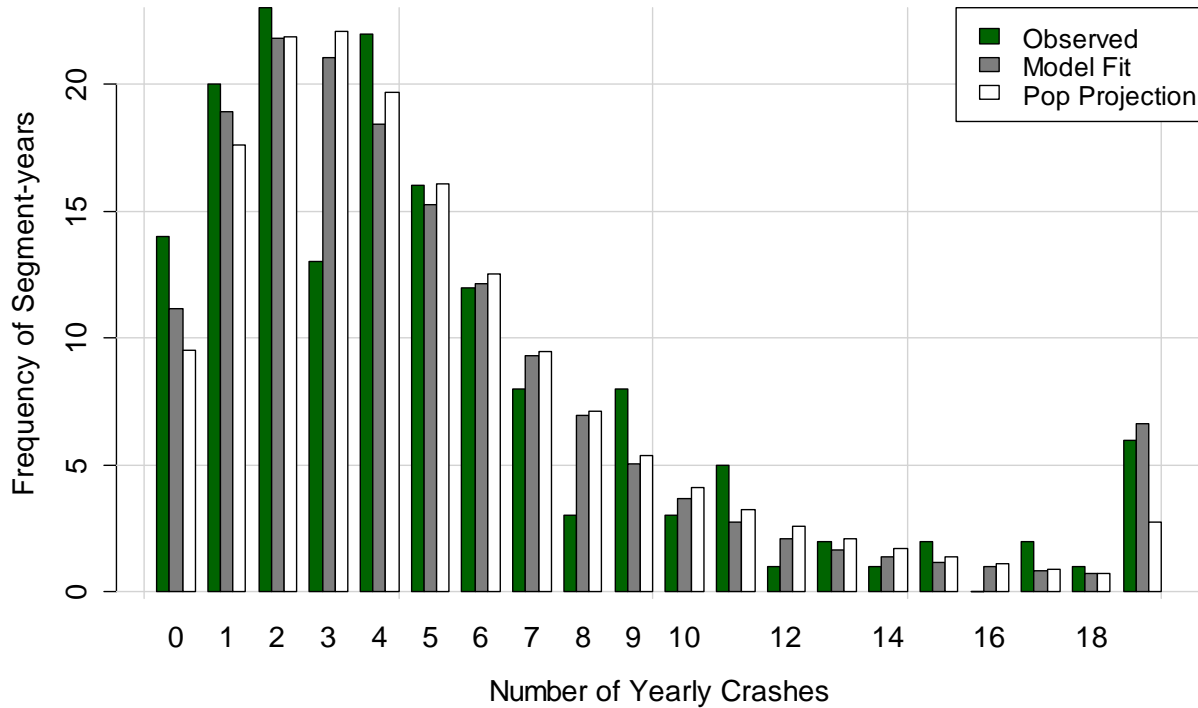


Figure 5.11: Marginal Distribution of Data and the Two Fits of Proposed SPF

An interesting contrast between model projections is that the population projection has a clear shortage in its prediction of nineteen or more crashes, compared to the actual observed frequency. Conversely, the prediction for the sample at hand (i.e. Model fit in Figure 5.11) is better aligned with the observed frequency. Since the population projection draws from the normality assumption on the intersection random effect, the research team expects that the difference between distributions is reflective of the influence of the one outlying site observed in Figure 5.8. Nonetheless, the chi-squared test on the marginal distribution does not warrant removal of this intersection (per Figure 5.10).

Finally, Figure 5.12 shows the CUMulative RESidual (CURE) plots for the two predictors in the SPF. Ideally, the line in a CURE plot should oscillate around the value of zero. The area enclosed by the red dashed lines represents the typical range for the CURE line. As the figure shows, the CURE lines for both variables are within the typical range, which indicates no concerns about significant biases of the SPF within the range of its predictors.

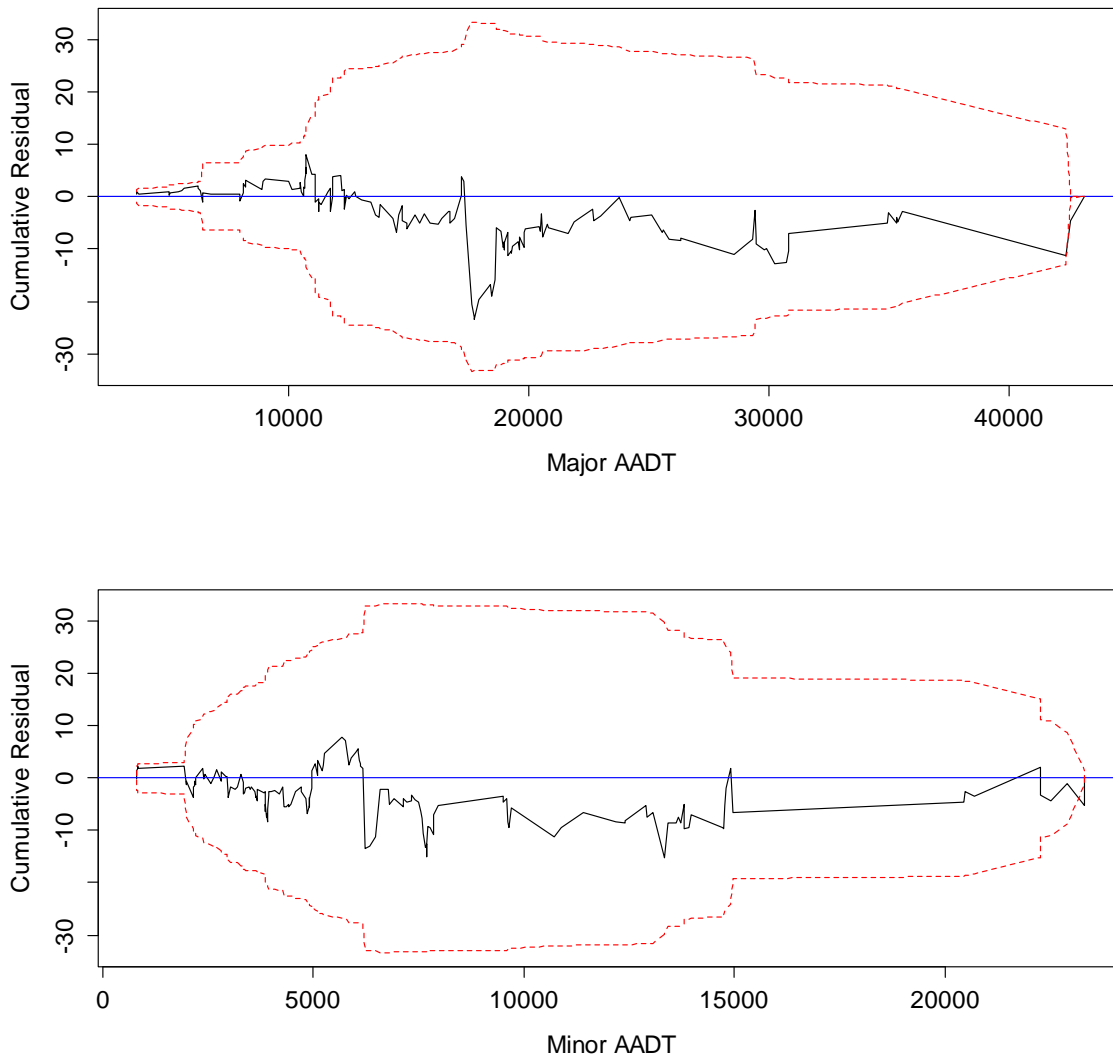


Figure 5.12: CURE Plots for Major and Minor AADTs

5.3.3 Initial SPF for KAB Crashes

The research team conducted a similar analysis for the most severe crash types (i.e. classifications K, A, and B as depicted in the ODOT crash database). Again, the research team started from a full model and then derived from this model the most parsimonious option available from the modeling dataset. The full model included both AADT, major and minor road speed limits, numbers of lanes on major and minor approaches, and median types. The most parsimonious form identified using this approach included only the MjAADT and MjSpLim. Model selection was guided by the Akaike Information Criterion (AIC).

The first stage of model reduction resulted in a model with only four variables: both AADTs and both Speed Limits (Mod1). Only MjAADT proved statistically significant among the four predictors in this model. However, after eliminating the coefficient for MnAADT, there were

two statistically significant coefficients: MjAADT and MjSpLim (Mod2). This is clear evidence of multicollinearity between speed limits. Additionally, the research team suspects that another instance of multicollinearity (between AADTs) explains the coefficient for MnAADT failing to prove statistically different than zero.

After eliminating the coefficient for MnAADT, the research team arrived to Mod3, the most parsimonious model from this model selection procedure. A Likelihood Ratio test clearly favors this model, as shown in Table 5.7.

Table 5.7: Analysis of Deviance for Full and Reduced Models

Analysis of Deviance for Full and Reduced Models								
Mod3	MjAADT, MjSpLim							
Mod2	MjAADT, MnAADT, MjSpLim							
Mod1	MjAADT, MnAADT, MjSpLim, MnSpLim							
Full	MjAADT, MnAADT, MjSpLim, MnSpLim, TWLTL, NoLanesMj, NoLanesMn							
Likelihood Ratio Test								
MODEL	Df	AIC	BIC	logLik	deviance	Chisq	Chi Df	Pr(>Chisq)
Mod3	4	368.94	380.98	-180.47	360.94			
Mod2	5	369.17	384.22	-179.59	359.17	1.7656	1	0.1839
Mod1	6	370.66	388.72	-179.33	358.66	0.5129	1	0.4739
Full	9	376.52	403.62	-179.26	358.52	0.1335	3	0.98757

Because the sign and relative magnitude of the coefficient for MnAADT in Mod2 are similar to the sign and magnitude of this variable in the recommended SPF for total crashes (reduced model from the previous section), the research team suspects that this variable is potentially important, and that its lack of statistical significance is likely explained by the combined effects of magnitude of its contribution to the prediction, multicollinearity between both AADTs, and sample size relative to the reduced variability of the response when considering KAB intersection crashes (as opposed to total intersection crashes). For these reasons, the research team repeated the estimation of Mod3 substituting MjAADT by the Module AADT, defined as:

$$ModAADT = \sqrt{MjAADT^2 + MnAADT^2}$$

This variable can be thought of as the hypotenuse of a right triangle that has both AADTs as legs resulting in a weighted AADT value. A nice property of the module AADT is that its magnitude is mostly determined by the larger AADT, but still reflective of the smaller AADT. As an illustration, when the smaller AADT tends to zero, the module's magnitude simply converges toward the magnitude of the larger AADT.

The research team named the new model utilizing the module AADT Mod4. Table 5.8 shows that Mod4 slightly improves the fit to the data (due to a smaller AIC value), compared to Mod3 (i.e. per deviance criterion).

Table 5.8: AIC, BIC, LogLikelihood and Deviance Comparisons for Mod3 and Mod4

Analysis of Deviance for Full and Reduced Models								
Mod3	MjAADT, MjSpLim							
Mod4	ModAADT, MjSpLim							
MODEL	Df	AIC	BIC	logLik	deviance	Chisq	Chi Df	Pr(>Chisq)
Mod3	4	368.94	380.98	-180.47	360.94	N.A.	N.A.	N.A.
Mod4	4	368.54	380.58	-180.27	360.54	N.A.	N.A.	N.A.

The research team recommends this model be selected as the SPF for KAB crashes for signalized intersections in Oregon, not only because of the improved fit of Mod4, but also because it incorporates a variable suspected to be critical. Similar to the development of the SPF for Total intersection crashes, model coefficients were estimated again including an additional nine intersection-years not included in the model comparisons (for a total of 159 intersection-years). These nine additional points are incomplete cases for the set of four critical variables, but complete cases when only the predictors in the recommended SPF are under consideration. A test of the residuals of the model did not show evidence of over-dispersion (0.695 p-value from a 145.5476 chi-squared statistic on 155 degrees of freedom). The formula for the recommended model is then:

$$N_{KAB} = e^{\beta_0 + \frac{Var(Int)}{2}} \cdot ModAADT^{\beta_1} \cdot e^{\beta_2 \cdot MjSpLim}$$

Table 5.9 shows the coefficients corresponding to the recommended KAB SPF.

Table 5.9: Coefficient Estimates for Recommended KAB SPF

	Estimate	Std. Error	z value	Pr(> z)	Statistical Significance
β_0	-9.32681	3.00549	-3.103	1.91E-03	***
β_1	0.75354	0.31337	2.405	0.01619	*
β_2	0.04149	0.01965	2.111	3.48E-02	*
Var(Int) = 0.4737					
Significance values are as follows: ° p < 0.1; * p < 0.05; ** p < 0.01; and *** p < 0.001					

The resulting equation after substituting the coefficient estimates from Table 5.6 is shown as follows:

$$N_{KAB} = (1.1279 \cdot 10^{-04}) \cdot ModAADT^{0.7535} \cdot e^{0.04149 \cdot MjSpLim}$$

Similar to the SPF for total intersection crashes, the research team assessed the fit of the recommended KAB SPF to the modeling dataset.

First, the research team verified the normality assumption of the intersection random effect. The graphic in Figure 5.13 shows that this is a reasonable assumption as the sample quantiles appear to have a linear configuration when plotted against the theoretical values.

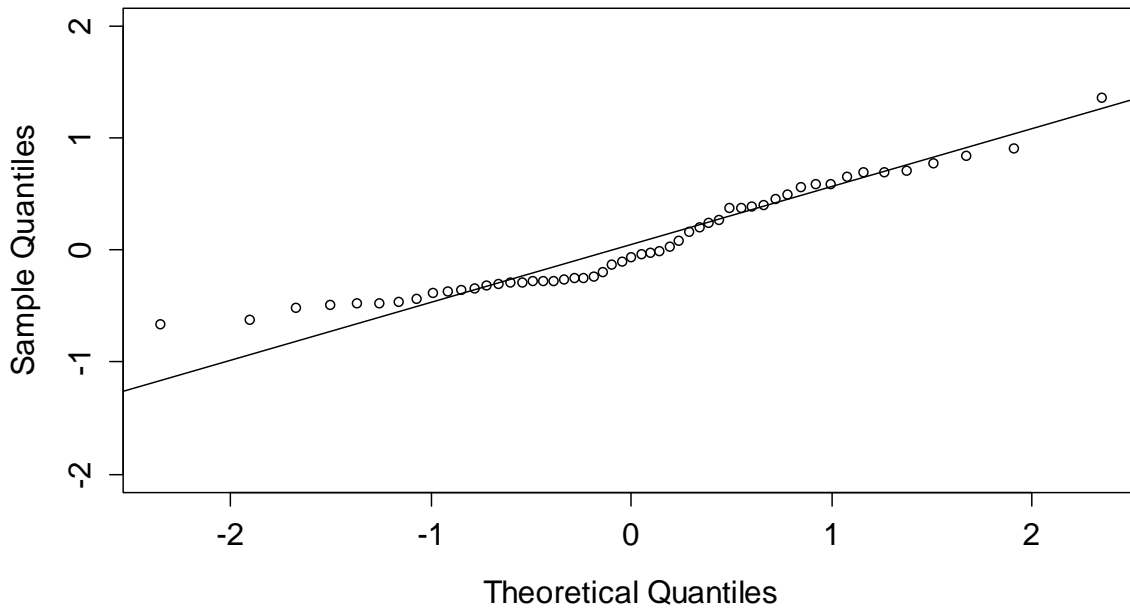


Figure 5.13: Q-Q Plot of Intersection Random Effect in KAB Model

For the KAB model, there is not a site with any unusually large random effects (see Figure 5.13), as opposed to Figure 5.8. Since the normality of the intersection random effect was verified, the research team next assessed the model fits to the study data sample as well as the projected population of signalized intersections in Oregon.

Figure 5.14 shows how the SPF fits both the modeling dataset and a larger population of sites. Although the adequateness of the fit is apparent from this figure, a formal Goodness-of-Fit Chi-Squared Test on the population projection indicates that the data distribution differs from the model-based expected distribution (0.0309 p-value for a 6.957 chi-squared statistic on two degrees of freedom from the population projection fit). The research team considers the model fit satisfactory because of the qualitative evidence represented in Figure 5.14. Additional, there is a potential shortcoming of the result of the statistical test: the limited number of degrees of freedom available when the response is KAB Crashes instead of Total Crashes.



Figure 5.14: Marginal Distribution Fit of KAB SPF to Data and Population Projection

Finally, Figure 5.15 shows the CURE plots for the two predictors in the KAB SPF. This plot indicates that the model tends to over-predict crashes at intersections with major speed limits of 40 mph or more. Additionally, there is a run of negative residuals between approximately 12,000 and 20,000 vpd for ModAADT, even though the plot remains mostly within the confines of the red dashed line.

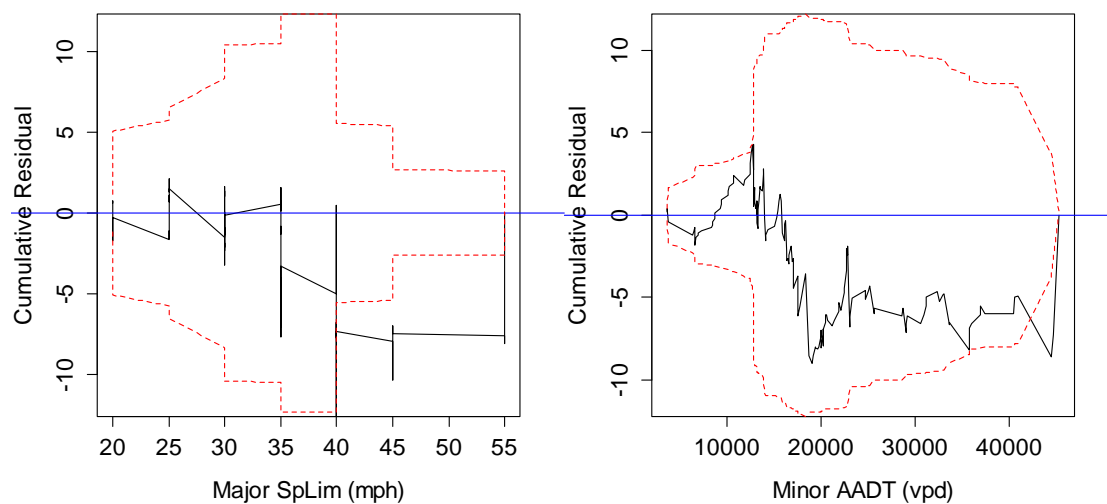


Figure 5.15: CURE Plots for Major SpLim and ModAADT

The research team believes that the limited variability inherent to KAB crashes restricts the predictive power of the SPF developed in this section. Considering these limitations, the research

team elected to fit a severity model in order to take advantage of a richer dataset, comprised by both Total and KAB crashes.

5.4 INITIAL PROBABILITY-BASED SEVERITY MODEL

The research team developed a severity model to be used in conjunction with the Total Crashes SPF as an alternative way to estimate the severity distribution at a signalized intersection, given the limitations found for the KAB SPF developed in the previous section.

The link function in this case is the logit function, also known as the log-odds function. The response variable is the proportion of KAB crashes to Total crashes at a given intersection for a particular year. Various specifications were tested in the composition of the vector of predictors, as in previous analyses. The most parsimonious model obtained had only one predictor: speed limit at the minor street (MnSpLim). However, the researchers expect that speed limit at the major approach also relates with severity in all likelihood, but it was not found significant due to the multicollinearity between the two speed limits (i.e. these are correlated variables). In a manner similar to developing the KAB SPF, the research team tested an alternative model specification that considers both speed limit variables simultaneously. In conjunction with the major speed limit, the speed limit differential was introduced in this model. This new variable is defined as:

$$SpLimDif = MjSpLim - MnSpLim$$

The comparison between these two models is shown in Table 5.10. The Likelihood Ratio test favors the parsimonious model. However, the research team still prefers the extended model because of its interpretability, as will be shown later. The large p-value of the test simply indicates that the slight improvement in log likelihood of the extended model is not substantial enough to warrant an additional parameter in the model. However, the extended model only has four parameters, thus the research team does not believe there is over-fitting involved in this case.

Table 5.10: Analysis of Deviance for Parsimonious and Extended Models

Parsimonious model variables	MnSpLim							
Extended model variables	MjSpLim, SpLimDif							
Likelihood Ratio Test								
	Df	AIC	BIC	logLik	deviance	Chisq	Chi Df	Pr(>Chisq)
Parsimonious	3	396.46	406.18	-195.23	390.46			
Extended	4	397.63	410.6	-194.82	389.63	0.8252	1	0.3637

The research team selected the extended model as a companion function to the SPF for total crashes at signalized intersections. The equation of this model is as follows:

$$P_{KAB} = \frac{e^{\beta_0 + (\beta_1 \times MjSpLim) + (\beta_2 \times SpLimDif) + \frac{Var(Int)}{2}}}{1 + e^{\beta_0 + (\beta_1 \times MjSpLim) + (\beta_2 \times SpLimDif) + \frac{Var(Int)}{2}}}$$

Where:

P_{KAB} = proportion of KAB crashes, out of total crashes at an intersection;

$\beta_0, \beta_1, \text{ and } \beta_2$ = regression coefficient for fixed effects variables;

$Var(Int)$ = variance of intersection random effect, estimated from the intersections in the modeling dataset;

All other variables are as previously defined.

Since no knowledge about AADTs was necessary, there were 189 intersection-years (from 63 intersections) available to fit the severity model. Table 5.11 the corresponding coefficients.

Table 5.11: Coefficient Estimates for Initial Probability-Based Severity Model

	Estimate	Std. Error	z value	Pr(> z)	Statistical Significance
β_0	-2.87248	0.51119	-5.619	1.92E-08	***
β_1	0.03283	0.01468	2.236	0.0253	*
β_2	-0.02087	0.01133	-1.841	0.0656	°
Var(Int) = 0.0714					
Significance values are as follows: ° p<0.1; * p < 0.05; ** p < 0.01; and *** p < 0.001					

It is noticeable that the variance component is quite small. This feature indicates that differences among intersections are minimal and almost inconsequential to the model. The resulting equation, when substituting the coefficient estimates from Table 5.11, is as follows:

$$P_{KAB} = \frac{e^{-2.837 + (0.0328 \times MjSpLim) - (0.0209 \times SpLimDif)}}{1 + e^{-2.837 + (0.0328 \times MjSpLim) - (0.0209 \times SpLimDif)}}$$

A graphical assessment of the severity model is challenging because of the limited range and discrete behavior of the response variable (i.e. proportion of KAB crashes). However, there is evidence of the appropriate fit of the model. A Pearson chi-squared test on the residuals does not indicate over-dispersion (0.6968 p-value for 214.182 chi-squared statistic on 185 degrees of freedom).

Figure 5.16 shows increasing trends for each speed limit depicted, which is consistent with the implication for minor speed limit in the severity model. Finally, Figure 5.17 shows how the severity model varies by speed limit at the major road, and how those curves shift as a function of the speed limit differential.

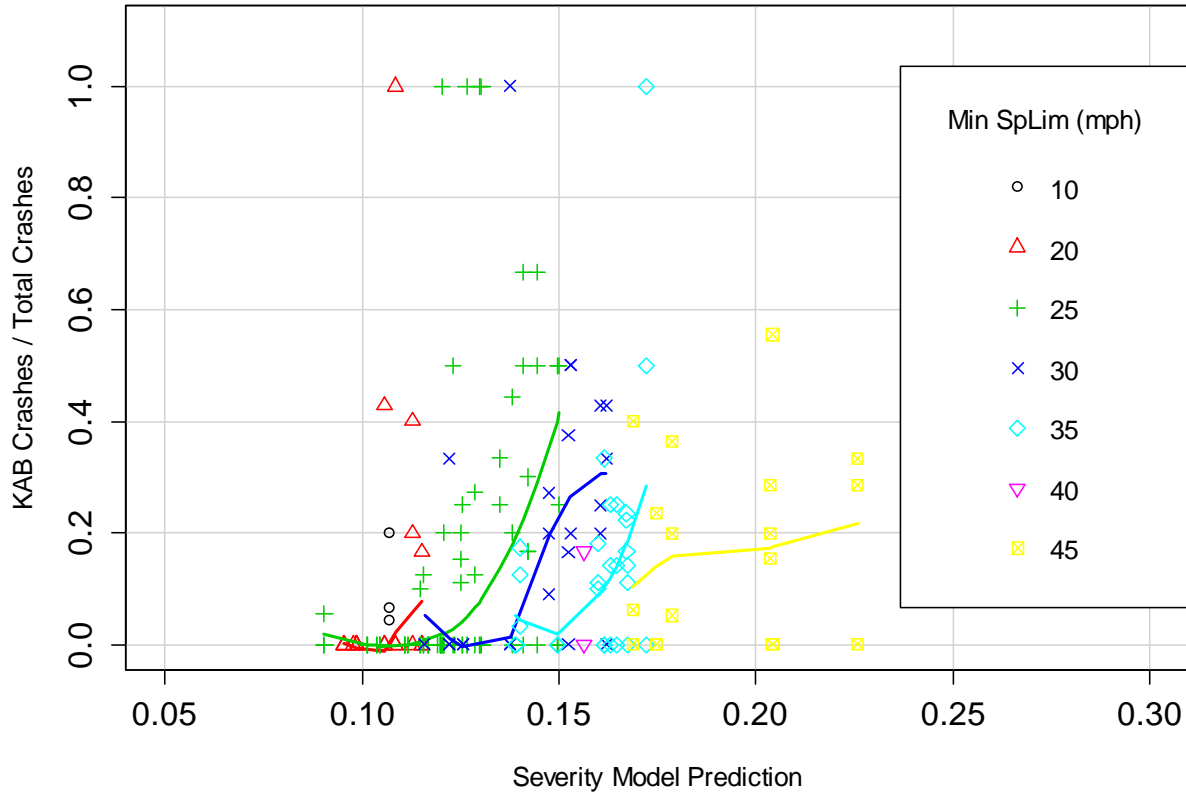


Figure 5.16: KAB Proportion of Crashes vs. Severity Model Prediction by Minor AADT

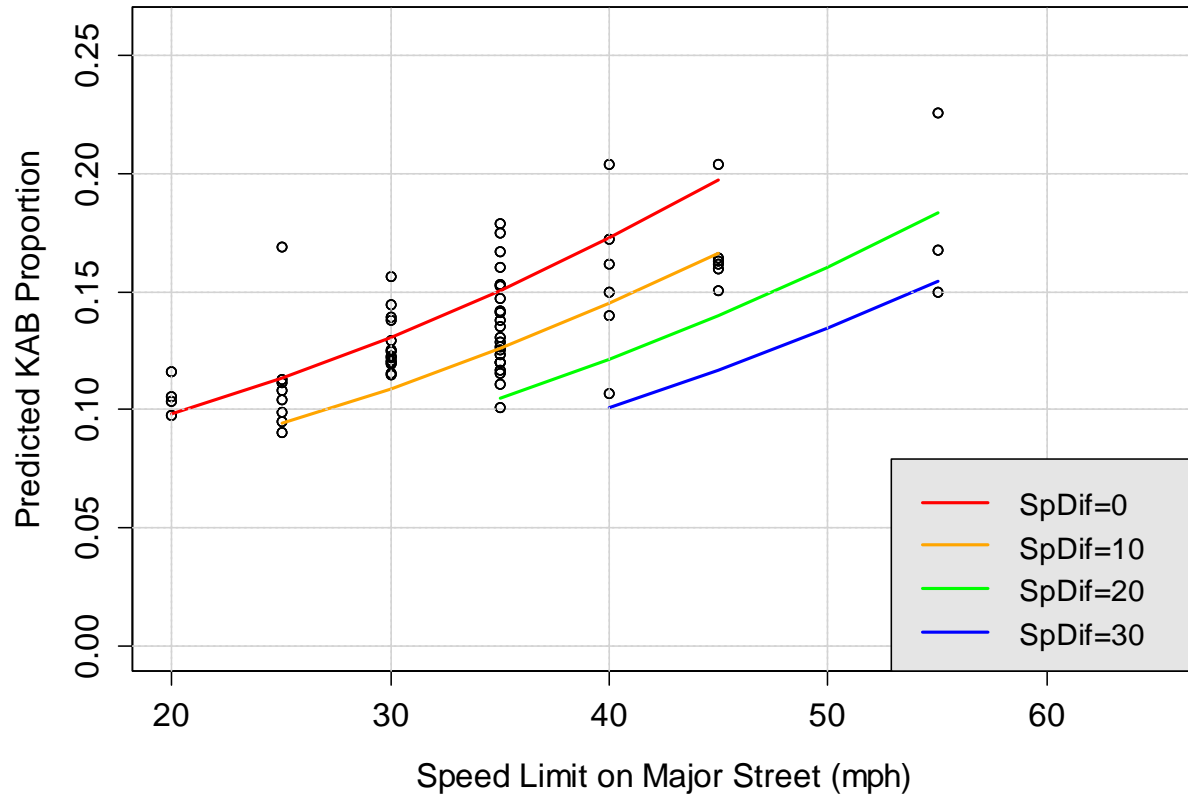


Figure 5.17: Severity Model Prediction vs Major AADT

The most adverse scenario depicted in this figure occurs when the major and the minor speed limits are the same (i.e. SpLimDif=0). Severity decreases as the speed limit at the minor road decreases.

5.5 SPF VALIDATION OVERVIEW

Appendix D provides details about the validation analysis for the SPFs. The research team used the following three validation techniques to assess model suitability:

- Model temporal transferability,
- Model spatial transferability, and
- Model spatial-temporal transferability.

5.5.1 Temporal Transferability

The validation efforts to assess temporal transferability of the initial models provided the following results:

- The temporal transferability for the Total Crashes SPF resulted in a 96 percent fit (indicating the initial model prediction years are statistically similar to the 2013 model prediction year).
- The temporal transferability for the KAB SPF (initial regression model) resulted in a 96 percent fit but appeared to overpredict crashes when the prediction exceeded 1.5 KAB crashes per year.
- The temporal transferability for the probability-based severity model resulted in a 94 percent fit but did not experience the over distribution biases as noted in the KAB SPF regression model assessment.

In summary, the temporal transferability analysis determined that the models are indeed reliable and representative of the Oregon crash conditions over time; however, the probability-based severity model generally represents the overall population better than the associated regression model (with an apparent over representation at higher crash numbers).

5.5.2 Spatial Transferability

The spatial transferability evaluation documented in Appendix D resulted in the following observations:

- The spatial transferability for the Total Crashes SPF resulted in a 98 percent fit indicating similar values between observed total crashes and predicted total crashes at the validation sites.
- The spatial transferability applied to the KAB SPF (regression analysis) demonstrated similar limitations as noted for the KAB SPF for temporal transferability. The model over represented crashes when the number of KAB crashes was greater than 1.6 per year. The validation fit, however, resulted in a 97 percent fit.
- The model spatial transferability for the probability-based severity model resulted in a 92 percent fit, but eliminated the overprediction problem associated with the KAB SPF regression model.

The results indicate that all three models are reliable and representative of Oregon crashes, but once again the probability-based severity model is more precise and better represents the overall injury crash population.

5.5.3 Spatial Temporal Transferability

An evaluation of model transferability over space and time resulted in the following observations:

- Model spatial-temporal transferability for the Total Crashes SPF resulted in a 100 percent fit demonstrating that the predicted total crashes are consistent with the observed crashes over time and space.
- The KAB SPF regression model performed marginally with a 90 percent fit. The overprediction issue noted in the other KAB SPF models, however, was no longer present.
- The probability-based severity model also resulted in a 90 percent fit. Since the predictions tend to be more precise for the probability model, it is logical to use this equivalent model so that it is consistent with the temporal transferability and the spatial transferability.

The spatial-temporal transferability validation results indicate that all three models are reliable and representative of Oregon crashes.

5.6 DEVELOPING ENHANCED SPF MODELS

As summarized in the previous section, the initially developed models fit the validation datasets adequately; however, refining the models with a larger dataset population (original model data plus the validation data) is expected to further strengthen the resulting models. The procedure is similar to that used for the initial model development as demonstrated in the following sections. Since the initial modelling efforts and the subsequent model validation both indicated limitations for the regression based KAB SPF that were not apparent in the probability-based severity models, the enhanced models only include the Total Crashes SPF and the probability-based Severity model.

5.6.1 Characteristics of Assembled Dataset for Model Updates

The assembled dataset included data from 109 intersections, representing 70 intersections from the modelling effort, four additional intersections from the temporal validation effort (i.e. there four additional intersections with data, compared to the modelling effort), and 35 intersections from the spatial validation effort.

The largest dataset containing all the variables in any of the developed functions (both SPFs and the probability-based severity model) consists of 281 site-years from 71 intersections (50 from the initial modelling effort, and one additional intersection from the temporal validation and 20 additional intersections from the spatial validation). Table 5.12 shows the summary statistics for this complete dataset.

As shown in Table 5.12, the range for variables is generally unchanged, suggesting the same for the range of application of the updated SPFs and the Severity Model.

5.6.2 Enhanced SPF for Total Crashes

The original Total Crashes SPF equation format was represented as:

$$N_{Total} = e^{\beta_0 + \frac{V(Int)}{2}} \cdot MjAADT^{\beta_1} \cdot MnAADT^{\beta_2}$$

The enhanced model for total crashes (see Table 5.13) introduced some minor changes when repeating the estimation of the SPF using the dataset described in the previous section.

Table 5.12: Yearly Statistics for Complete 2010-2013 Dataset for Updating the Models

Variable	Description	Mean	Std.Dev	Min	Max	Total	N
Total Crashes	All crashes	5.7	5.57	0	46	1611	281
MV_Crashes	Multiple vehicle crashes	5.3	5.35	0	42	1485	281
KAB_Crashes	Fatal and serious injury crashes	0.8	1.14	0	8	227	281
MV_KAB_Crashes	Severe crashes with multiple vehicles	0.6	0.93	0	6	160	281
MjAADT	Major AADT (vpd)	17,496.6	8309.41	5007	44,464	-	281
MnAADT	Minor AADT (vpd)	6920.9	4605.22	800	23,316	-	281
MjSpLimMax	Major Speed Limit (mph)	33.7	7.96	20	55	-	281
MnSpLimMin	Minor Speed Limit (mph)	28.2	7.13	10	45	-	281

Table 5.13: Updated Coefficient Estimates for Total Crashes SPF

	Estimate	Std. Error	z value	Pr(> z)	Statistical Significance
β_0	-8.6415	1.3575	-6.366	1.94E-10	***
β_1	0.6748	0.1351	4.996	5.86E-07	***
β_2	0.4168	0.1018	4.094	4.24E-05	***
Var(Int) = 0.2399					
Significance values are as follows: ° p<0.1; * p < 0.05; ** p < 0.01; and *** p < 0.001					

The resulting enhanced SPF for total number of crashes per year, when substituting the coefficients estimates in Table 5.13, is as follows:

$$N_{Total} = (1.991 \cdot 10^{-04}) \cdot MjAADT^{0.675} \cdot MnAADT^{0.417}$$

The changes observed in the coefficient estimates reflect a trade-off between an increased constant term (i.e. the first factor in the formula) and slightly smaller exponents for the AADTs.

The enhanced estimates are within two standard errors of the initial model estimates suggesting that both sets of coefficients are statistically equivalent. Figure 5.18 shows the curves corresponding to the original and updated SPF for a minor AADT of 7,000 vpd (i.e. roughly the average in the complete dataset shown in Table 5.12).

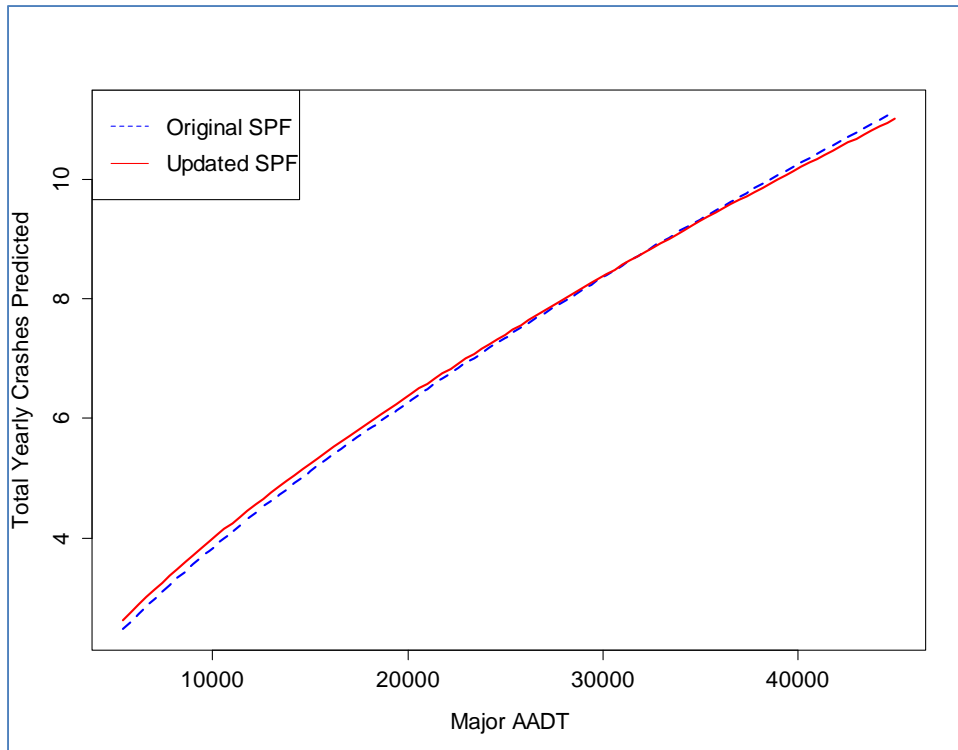


Figure 5.18: Original and Updated SPFs for Minor AADT of 7,000 vpd

As shown in Figure 5.18, the predictions of the two SPFs are very comparable (for the range of variables represented in the figure). The next section evaluates the fit of the enhanced SPF.

5.6.2.1 Fit Assessment

The research team assessed the fit of the updated SPF to the modelling dataset using a variety of techniques. First, a Chi-Squared test on the standardized residuals did not suggest over-dispersion (p-value of 0.4632 for a 303.61 Chi-Squared statistic on 302 degrees of freedom). Next, the research team assessed the normality assumption of the intersection random effect as shown in Figure 5.19.

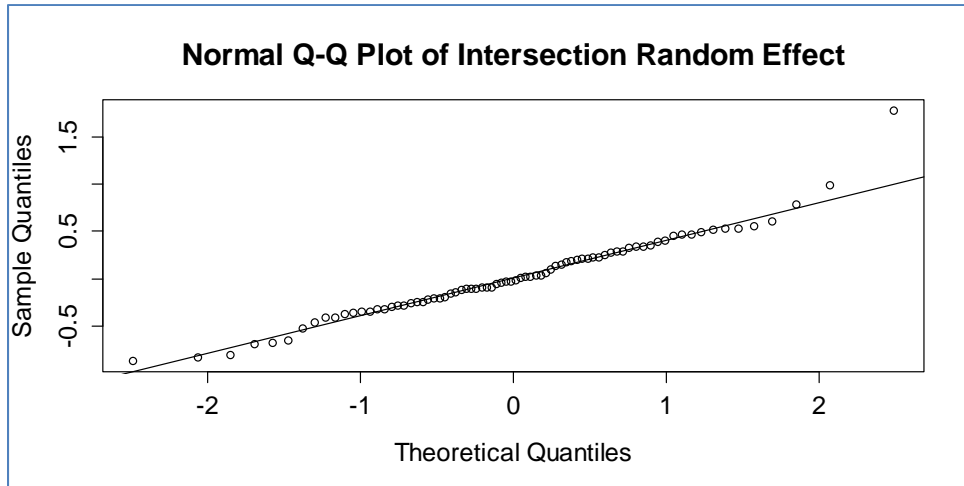


Figure 5.19: Q-Q Plot of Intersection Random Effect in Updated Model

This figure shows the Quantile-to-Quantile plot of the random effects of the enhanced SPF assuming the theoretical normal distribution. The normality of the intersection random effect appears reasonable, with just one random effect appearing as a potential outlier. The research team then evaluated the fit of the marginal distribution of the sites to the marginal distribution emerging from the updated SPF for total crashes (see Figure 5.20).

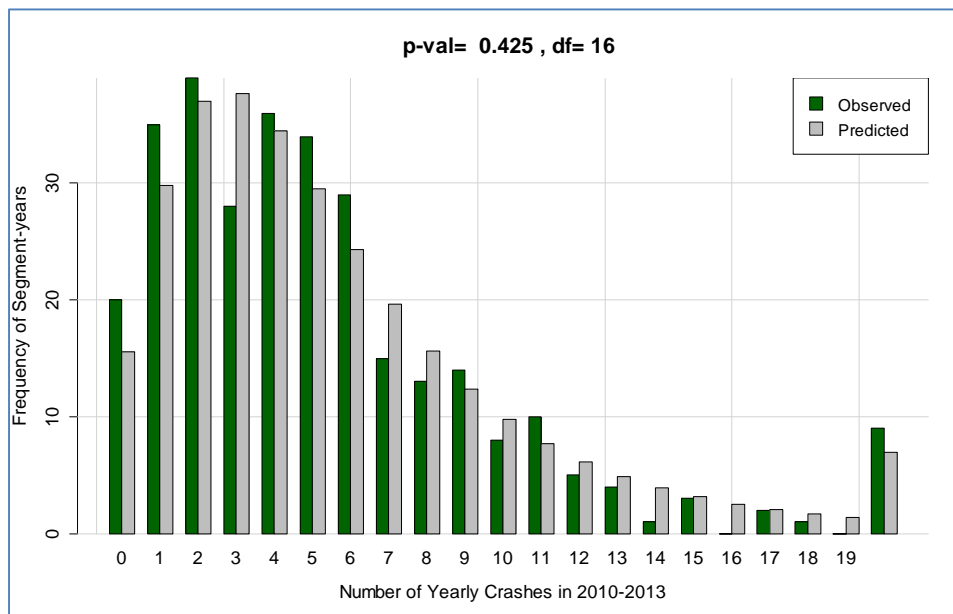


Figure 5.20: Theoretical and Observed Marginal Distributions of Sites by Total Crash Frequencies for Period 2010-2013

Figure 5.20 shows an appropriate fit of the updated SPF to the enhanced dataset. An evaluation of the cumulative residuals (see Figure 5.21) for the enhanced SPF shows oscillation around the zero value as expected.

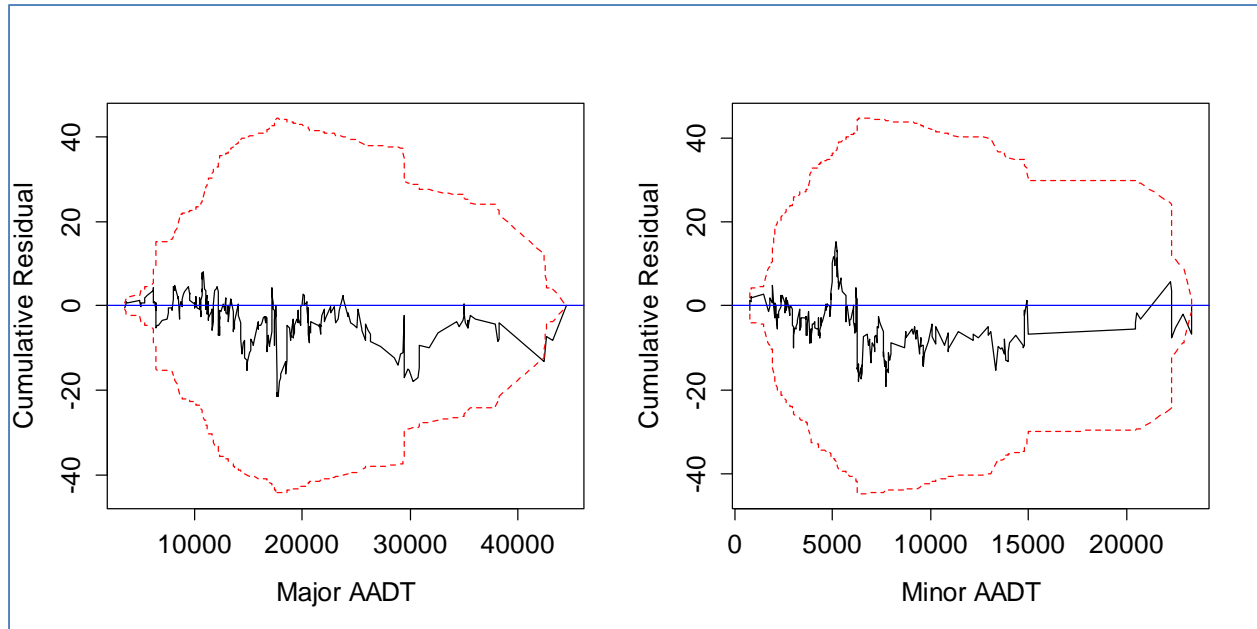


Figure 5.21: CURE Plots for Updated Total Crashes SPF

5.6.3 Enhanced Probability-Based Severity Model

As previously noted, the probability-based severity model produced more precise predictions during model validation than the KAB SPF, so the research team elected to only update the severity model to be used in combination with the Total Crashes SPF. The recommended equation format for the severity model, as indicated in Section 5.4, is represented as:

$$P_{KAB} = \frac{e^{\beta_0 + (\beta_1 \times MjSpLim) + (\beta_2 \times SpLimDif) + \frac{Var(Int)}{2}}}{1 + e^{\beta_0 + (\beta_1 \times MjSpLim) + (\beta_2 \times SpLimDif) + \frac{Var(Int)}{2}}}$$

Table 5.14 shows the new coefficient estimates, derived from 370 intersection-years available from 94 intersections at locations with complete data regarding both major and minor speed limits.

Table 5.14: Coefficient Estimates for Reduced Model

	Estimate	Std. Error	z value	Pr(> z)	Statistical Significance
β_0	-2.69704	0.38166	-7.067	1.59E-12	***
β_1	0.02874	0.01132	2.539	0.0111	*
β_2	-0.02412	0.01054	-2.289	0.0221	*

$$Var(Int) = 0.1282$$

Significance values are as follows: ° p<0.1; * p < 0.05; ** p < 0.01; and *** p < 0.001

The resulting coefficients are very similar to those obtained in the initial analysis. Figure 5.22 shows a comparison of the predicted severities for the entire range of major speed limits when

the minor speed limit is fixed at 30 mph (about the average of this variable in Table 5.12). The largest difference in predictions occurs at a major speed limit of 20 mph. This difference is equivalent to about 12 percent of the KAB crashes based on the initial Severity Model compared to about 14 percent for the enhanced Severity Model.

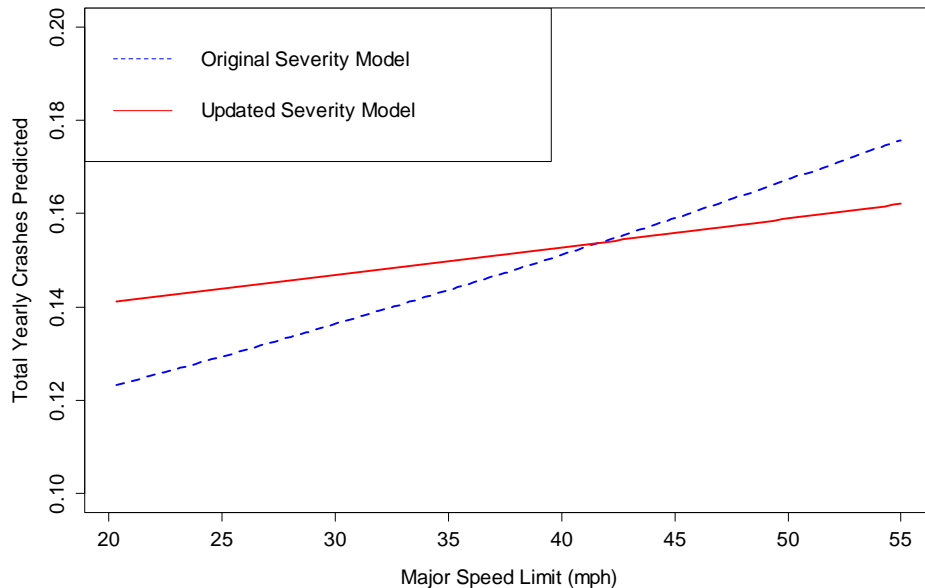


Figure 5.22: Original and Updated Severity Models for Minor Speed Limit of 30 mph

A Pearson chi-squared test for the residuals does not indicate over dispersion (0.87303 p-value for 335.35 chi-squared statistic on 366 degrees of freedom).

5.7 EXAMPLE PROBLEMS APPLYING SPFs

This section demonstrates how to use the methodology outlined in the previous sections. For this demonstration, Section 5.5.1 demonstrates an application of the enhanced total crash model and Section 5.5.2 demonstrates the use of the enhanced probability-based crash severity model.

5.7.1 Example Use of Total Crash Model

A signalized intersection has the traffic volume and speed characteristics shown in Table 5.15. The predicted number of total crashes can then be calculated using the total crash SPF.

Table 5.15: Table of Road Characteristics for an Example Intersection

Signalized Intersection Features	Values
Major Road AADT	22,500 vpd
Minor Road AADT	11,800 vpd
Major Road Speed Limit	45
Minor Road Speed Limit	20

1. Select the Appropriate SPF (for Total Crashes):

$$N_{Total} = (1.991 \times 10^{-4}) \times MjAADT^{0.675} \times MnAADT^{0.417}$$

2. Confirm that the input values are within the minimum and maximum range applicable to the SPF.

✓ Major AADT = 22,500 which is greater than 5007 and less than 44,464 vpd

✓ Minor AADT = 11,800 which is greater than 800 and less than 23,316 vpd

3. Calculate the total number of predicted crashes

$$\begin{aligned} N_{Total} &= (1.991 \times 10^{-4}) \times (22,500)^{0.675} \times (11,800)^{0.417} \\ &= 8.61 \text{ (Say 9 crashes per year)} \end{aligned}$$

Example problem conclusion:

Based on the known exposure, we can predict approximately 9 intersection-related crashes will occur per year.

5.7.2 Example Use of the Crash Severity Model

The calculation of the severe crashes, using the severe crash SPF, can be calculated using the following procedure.

1. Confirm that the speed limit input values are within the minimum and maximum range applicable to the SPF.

✓ Major Road Speed Limit = 45 which is greater than 20 and less than 55 mph

✓ Minor Road Speed Limit = 20 which is greater than 10 and less than 45 mph

2. Calculate the speed limit differential:

$$SpLimDif = MjSpLim - MnSpLim = 45 - 20 = 25 \text{ mph}$$

3. Calculate the KAB proportion of total crashes.

$$P_{KAB} = \frac{e^{-2.697+(0.0287 \times MjSpLim)-(0.02412 \times SpLimDif)+\frac{0.1282}{2}}}{1 + e^{-2.697+(0.0287 \times MjSpLim)-(0.02412 \times SpLimDif)+\frac{0.1282}{2}}}$$

$$P_{KAB} = \frac{e^{-2.697+(0.0287 \times 45)-(0.02412 \times 25)+\frac{0.1282}{2}}}{1 + e^{-2.697+(0.0287 \times 45)-(0.02412 \times 25)+\frac{0.1282}{2}}} = 0.125$$

4. Calculate the number of Total crashes (previously calculated in Section **Error! Reference source not found.**).

$$N_{Total} = 8.61 \text{ crashes per year}$$

5. Calculate the number of predicted severe (KAB) crashes by multiplying the total number of predicted crashes by the KAB proportion.

$$N_{KAB} = 8.61 \times 0.125 = 1.08 \text{ (Say 2 crashes per year)}$$

Example problem conclusion:

Based on the known exposure and speed limits, we can predict approximately 2 KAB intersection-related crashes will occur per year out of 9 Total intersection crashes.

5.8 SUMMARY OF WORK

The objective of this research was to develop SPFs for signalized intersections in Oregon and, where appropriate, explicitly consider the influence of speed limit. For this purpose, the research team used probability sampling to assemble a database of typical sites. As a result, the resulting database resulted in a representative sample for the State of Oregon.

The first issue addressed by the research team was to determine how to identify intersection related (IR) crashes. The research team developed various statistically-based methodologies and compared them against current simpler methodologies (maximum-threshold rules) to screen intersection crashes. This comparative analysis indicates that it is cost-effective to use distance-based rules in combination with crash codes indicative of Traffic Control Devices (TCD) at signalized intersections, despite the flexibility gained by using statistically-based methodologies. The best performing maximum-threshold rule (performance based on the objective of SPF development) is as follows: classify as IR crashes all crashes within three hundred feet of the intersection in addition to other crashes in the vicinity but farther than that distance, as long as they have crash codes indicating their relation to intersection-specific TCDs.

Using the sample of sites already classified as IR, the research team developed three initial predictive models to be considered as SPFs for the state of Oregon: (1) An SPF for Total Crashes, which relies on both major and minor AADTs to predict the expected number of crashes; (2) An SPF for KAB crashes, whose predictions derive from both AADTs (through the defined quantity ModAADT) as well as from the speed limit on the major road; and (3) A severity model to predict the proportion of KAB crashes to be used in combination with the SPF for Total Crashes. The last predicting tool was developed as a way to overcome the limited variability observed in KAB crashes, and the impact on the prediction power of the SPF for KAB crashes alone.

Throughout all the analyses of this research, the speed limit variable significantly improved the quality of the SPFs and severity model, the main products of this work. Following the initial model development, the research team performed a validation analysis on the initial safety prediction models (see Appendix D for an expanded review of this validation effort). Ultimately, the validation effort indicated that the initial models adequately represent Oregon conditions; however, the regression-based KAB models appeared to over predict the number of crashes at higher crash locations. Ultimately, the research team used the combined dataset and developed an enhanced Total Crash SPF and an enhanced probability-based Severity model as the final recommended predictive equations to apply.

6.0 CONCLUSIONS AND RECOMMENDATIONS

This final report reviews the research effort performed for the Oregon signalized intersection SPF project and summarizes the literature review, site selection, data collection, analysis, and findings of statistical analyses required for this effort. In addition to a comprehensive literature review, the research team also developed a technique for estimating minor road traffic volume at signalized intersections, created a procedure for identifying IR crashes, and then performed a statistical analysis and validation effort for SPF development.

The literature review is summarized in Section 2.0. This effort focused on recent research associated with safety performance measurement and assessment as well as AADT estimation techniques. Section 3.0 of this report presents an overview of the site selection process and resulting 50 independent signalized intersections that the research team used for the initial SPF development task and 35 additional independent signalized intersections that the research team ultimately used for validation of the initial models.

Section 4.0 of this report explored the most effective way for estimating a minor road AADT value. While the preference should be to use actual traffic volume information, whenever available, for safety analysis, there are many locations where this exposure information is not available. The evaluation explored ways to estimate minor road AADT for the entire road as well as for a single leg. At locations where a parallel facility existed, the research team used this information to aid with the estimation procedure; however, in locations where parallel traffic information is also not available, an alternative equation has been provided. These equations are depicted, along with the variable definitions and boundary conditions, in Table 6.1. An example calculation is also included in Section 4.0.

Section 5.0 included two key components: (1) a fresh look at how to best identify IR crashes for the purposes of subsequent safety evaluations, and (2) SPFs for signalized intersections with the speed limit explicitly considered as a candidate variable. For the IR crash location, the research team determined that the best option is to use crash data that is geo-located within 300 feet of the centerline intersection at signalized locations plus crashes where the crash report indicates that they were associated with a traffic control device (i.e. traffic signal). The subsequent statistical analysis to develop SPFs focused on predicting total crashes and severe injury crashes (coded as KAB). One common Goodness-of-Fit assessment is a CURE plot. For the KAB regression equation, the residuals did not oscillate about the zero value as expected and were beyond the recommended thresholds; therefore, the research team developed a second technique for estimating the severe crashes that used a probability function applied to the total crashes. The research team then performed a validation effort based on additional sites and an additional year of data. The models all performed well during the validation; however, the research team then developed two enhanced models to improve model reliability based on the larger dataset. The resulting variable definitions, boundary conditions, and associated enhanced SPF equations are presented in Table 6.2. In addition, the Section 5.7 content concludes with an example calculation that demonstrates the procedures.

The Report Appendix B reviews the AADT conversion methodology and Appendix C presents the AADT Model validation review. Similarly, Appendix D reviews the SPF validation effort. Finally, the site summaries for the initial model development are included in Appendix E and the validation site summaries are reviewed in Appendix F.

Table 6.1: Equations to Estimate the Minor Road Volume

Variable Definitions
$AADT_{Major}$ = Major road two-directional daily volume (vpd)
$Parallel_{AADT}$ = Parallel corridor two-directional daily volume (vpd)
LN_{Major} = Average number of approach thru lanes on the major road
LN_{Minor} = Average number of approach thru lanes on the minor road
FC_{Major} = Value of 1 if major road is a collector, otherwise a value of 0
FC_{Minor} = Value of 1 if minor road is a collector, otherwise a value of 0
$TWLTL_{Major}$ = Value of 1 if TWLTL present on major approach, otherwise value of 0
Boundary Conditions for Minor Road Estimation Equations
$AADT_{Major} \leq 44,000$
$Parallel_{AADT} \leq 18,500$
$1 \leq LN_{Major} \leq 3$
$1 \leq LN_{Minor} \leq 3$
Estimating AADT for the Minor Road
<u>Preferred Option -- Parallel Facility Traffic Volume Known:</u>
$\begin{aligned} \log(AADT_{Total\ Minor}) &= 0.6837 + 0.686 \log(AADT_{Major}) \\ &+ 0.1764 \log(Parallel\ AADT) - 0.1636(LN_{Major}) + 0.2384(FC_{Major}) \\ &- 0.29235(FC_{Minor}) \end{aligned}$
<u>Alternative Option -- Parallel Facility AADT is not available:</u>
$\begin{aligned} \log(AADT_{Total\ Minor}) &= 1.05631 + 0.7698 \log(AADT_{Major}) - 0.1915(LN_{Major}) + 0.2343(FC_{Major}) \\ &- 0.32851(FC_{Minor}) \end{aligned}$
Estimating AADT for the Individual Minor Road Leg
<u>Preferred Option -- Parallel Facility Traffic Volume Known:</u>
$\begin{aligned} \log(AADT_{Minor\ by\ Leg}) &= 0.9815 + 0.2318 \log(AADT_{Major}) \\ &+ 0.3019 \log(Parallel\ AADT) + 0.321(LN_{Major}) - 0.2511(FC_{Minor}) \\ &- 0.1299(TWLTL_{Major}) \end{aligned}$
<u>Alternative Option -- Parallel Facility AADT is not available:</u>
$\begin{aligned} \log(AADT_{Minor\ by\ Leg}) &= 1.8516 + 0.2945 \log(AADT_{Major}) + 0.3393(LN_{Minor}) - 0.2892(FC_{Minor}) \\ &- 0.1382(TWLTL_{Major}) \end{aligned}$

Table 6.2: Enhanced SPFs to Estimate Crashes at Signalized Intersections in Oregon

Variable Definitions
$AADT_{Major}$ = Major road two-directional daily volume (vpd)
$AADT_{Minor}$ = Minor road two-directional daily volume (vpd)
$MjSpLim$ = Major road posted speed limit (mph)
$MnSpLim$ = Minor road posted speed limit (mph)
$SpLimDif$ = Major speed limit minus minor speed limit (mph)
P_{KAB} = Proportion of KAB crashes out of total crashes at an intersection
Boundary Conditions for SPFs
$5007 \text{ vpd} \leq \text{Major AADT} \leq 44,464 \text{ vpd}$
$800 \text{ vpd} \leq \text{Minor AADT} \leq 23,316 \text{ vpd}$
$20 \text{ mph} \leq \text{Major Speed Limit} \leq 55 \text{ mph}$
$10 \text{ mph} \leq \text{Minor Speed Limit} \leq 45 \text{ mph}$
Enhanced SPF Equations for Signalized Intersections
<u>Regression Model to Predict Total Crashes:</u>
$N_{Total} = (1.991 \times 10^{-4}) \times MjAADT^{0.675} \times MnAADT^{0.417}$
<u>Probability-Based Model to Predict Severe (KAB) Crashes:</u>
$P_{KAB} = \frac{e^{-2.697+(0.0287 \times MjSpLim)-(0.02412 \times SpLimDif)+\frac{0.1282}{2}}}{1 + e^{-2.697+(0.0287 \times MjSpLim)-(0.02412 \times SpLimDif)+\frac{0.1282}{2}}}$
$N_{KAB} = P_{KAB} \times N_{Total}$

The SPFs that resulted from this effort demonstrated an interesting and somewhat intuitive observation: speed limit (a surrogate value that represents general speeds) is not significant for total crash estimation; however, the speed is significant for injury crash estimation. Currently the AASHTO HSM does not directly consider speed or speed limit in speed prediction equations, yet the Oregon sites are likely to be representative of signalized intersections in other jurisdictions. This research effort focused on signalized intersections, but the findings would suggest that future research efforts should similarly evaluate the influence of speed at unsignalized intersection locations.

7.0 REFERENCES

- Abdel-Aty, M., and K. Haleem. Analyzing Angle Crashes at Unsignalized Intersections using Machine Learning Techniques. *Accident Analysis and Prevention*, Vol. 43, No. 1, 2011, pp. 461-470.
- American Association of State Highway and Transportation Officials (AASHTO). *Highway Safety Manual*. AASHTO, Washington D.C., 2010.
- American Association of State Highway and Transportation Officials (AASHTO). *A Policy on Geometric Design of Highways and Streets*. AAHSTO, Washington, D.C., 2011.
- Anastasopoulos, P., and F. Mannering. An Empirical Assessment of Fixed and Random Parameter Logit Models Using Crash- and Non-Crash-Specific Injury Data. *Accident Analysis and Prevention*, Vol. 43, No. 3, 2011, pp. 1140-1147.
- Appiah, J., N. Bhaven, R. Wojtal, and L. Rilett. Safety Effectiveness of Actuated Advance Warning Systems. *Transportation Research Record: Journal of the Transportation Research Board*, No. 2250, Transportation Research Board of the National Academies, Washington, D.C., 2011, pp. 19-24.
- Bullough, J., E. Donnell, and M. Rea. To Illuminate or Not to Illuminate: Roadway Lighting as It Affects Traffic Safety. *Accident Analysis and Prevention*, Vol. 53, No. 4, 2013, pp. 65-77.
- Castro, M., R. Paleti, and C. Bhat. A Latent Variable Representation of Count Data Models to Accommodate Spatial and Temporal Dependence: Application to Predicting Crash Frequency at Intersections. *Transportation Research Part B: Methodological*, Vol. 46, No. 1, 2012, pp.253-272.
- Chen, H., L. Cao, and D. Logan. Analysis of Risk Factors Affecting the Severity of Intersection Crashes by Logistic Regression. *Traffic Injury Prevention*, Vol. 13, No. 3, 2012, pp.300-307.
- Chen, L., C. Chen, and R. Ewing. Left-Turn Phase: Permissive, Protected, or Both? Presented at 91st Annual Meeting of the Transportation Research Board, Washington, D.C., 2012.
- Chiou, Y.-C., C.-C. Hwang, C.-C. Chang, and C. Fu. Modeling Two-Vehicle Crash Severity by a Bivariate Generalized Ordered Probit Approach. *Accident Analysis and Prevention*, Vol. 51, 2013, pp.175-184.
- Das, A., A. Pande, and M. Abdel-Aty. Characteristics of Urban Arterial Crashes Relative to Proximity to Intersections and Injury Severity. *Transportation Research Record: Journal of the Transportation Research Board*, No. 2083, Transportation Research Board of the National Academies, Washington, D.C., 2008, pp. 137–144.
- Datta, T., K. Schattler, and S. Datta. Red Light Violations and Crashes at Urban Intersections. *Transportation Research Record: Journal of the Transportation Research Board*, No. 1734, Transportation Research Board of the National Academies, Washington, D.C., 2000, pp. 52-58.

Davis, G., and N. Aul. *Safety Effects of Left-turn Phasing Schemes at High-Speed Intersections*. Report MN/RC-2007-03. Minnesota Department of Transportation, Minneapolis, MN. 2007.

Dixon, K., C. Monsere, X. Fei, and K. Gladhill. *Calibrating the Highway Safety Manual Predictive Methods for Oregon Highways*. Final Report SPR-684; Report OTREC-RR-12-02. Oregon Transportation Research and Education Consortium, 2012.

El-Shawarby, I., A. Amer, A. Abdel-Salam, and R. Hesham. Empirical Study of Yellow and Red Light Running Behavior on High-Speed Signalized Intersection Approaches. Presented at 90th Annual Meeting of the Transportation Research Board, Washington D.C., 2011.

Environmental Protection Agency. *Smart Location Database*. 2013. Located at <http://www.epa.gov/smartgrowth/smartlocationdatabase.htm#SLD>. Accessed November 2014.

Environmental Systems Research Institute. *ArcGIS Desktop: Release 10*. [Software], Redlands, CA, ESRI, 2011.

Federal Highway Administration (FHWA). *Traffic Monitoring Guide*. FHWA, United States Department of Transportation, Washington, D.C., May 2001.

Federal Highway Administration (FHWA). *Traffic Monitoring Guide*. 2013. FHWA, United States Department of Transportation, Washington, D.C. Located at: <http://www.fhwa.dot.gov/policyinformation/tmguide/>. Accessed November 2014.

Fox, J., and S. Sanford. *An {R} Companion to Applied Regression*, 2nd Edition. Thousand Oaks, CA: Sage, 2011.

Garber, N., P. Haas, and C. Gosse. Safety Performance Functions for Two-Lane Roads in Virginia. Presented at 89th Annual Meeting of the Transportation Research Board, Washington, D.C., 2010.

Garber, N.J., and L.A. Hoel. *Traffic and Highway Engineering*, 4th Edition, Cengage Learning, Toronto, ON, 2009.

Google Inc. Google Earth v7.1. *Mountain View, CA*. Google Inc., 2014.

Huang, H., H. Chin, and M. Haque. Bayesian Hierarchical Analysis of Crash Prediction Models. Presented at 87th Annual Meeting of the Transportation Research Board Washington, D.C., 2008.

Jonsson, T., J. Ivan, and C. Zhang. Crash Prediction Models for Intersections on Rural Multilane Highways: Differences by Collision Type. *Transportation Research Record: Journal of the Transportation Research Board*, No. 2019, Transportation Research Board of the National Academies, Washington D.C., 2007, pp. 91-98.

Kim, D., Y. Lee, S. Washington, and K. Choi. Modeling Crash Outcome Probabilities at Rural Intersections: Application of Hierarchical Binomial Logistic Models. *Accident Analysis and Prevention*, Vol. 39, No. 1, 2007, pp. 125-134.

Kim, D., and S. Washington. The Significance of Endogeneity Problems in Crash Models: An Examination of Left-Turn Lanes in Intersection Crash Models. *Accident Analysis and Prevention*, Vol. 38, No. 6, 2006, pp. 1094-1100.

Kweon, Y. Disaggregate Safety Evaluation for Signalized Intersections and an Evaluation Tool. Presented at 90th Annual Meeting of the Transportation Research Board Washington, D.C., 2011.

Li, W., and A. Tarko. Effect of Arterial Signal Coordination on Safety. *Transportation Research Record: Journal of the Transportation Research Board*, No. 2237, Transportation Research Board of the National Academies, Washington, D.C., 2011, pp.51-59.

Li, Z., and Y. Lee. *Geographically-Weighted Regression Models for Improved Predictability of Urban Intersection Vehicle Crashes*. Transportation and Development Institute Congress, 2011, pp. 1315-1329.

Lord, D., and P. Park. Investigating the Effects of the Fixed and Varying Dispersion Parameters of Poisson-Gamma Models on Empirical Bayes Estimates. *Accident Analysis and Prevention*, Vol. 40, No. 4, 2008, pp. 1441-1457.

Ma, M., X. Yan, M. Abdel-Aty, H. Huang, and X. Wang. Safety Analysis of Urban Arterials Under Mixed-Traffic Patterns in Beijing. *Transportation Research Record: Journal of the Transportation Research Board*, No. 2193, Transportation Research Board of the National Academies, Washington D.C., 2010, pp. 105-115.

Miller, J. Geographic Information Systems. Unique Analytic Capabilities for the Traffic Safety Community. *Transportation Research Record: Journal of the Transportation Research Board*, No. 1734, Transportation Research Board of the National Academies, Washington, D.C., 2000, pp. 21-28.

Miller, J., N. Garber, and S. Korukonda. Understanding Causality of Intersection Crashes: Case study of Virginia. *Transportation Research Record: Journal of the Transportation Research Board*, No. 2236, Transportation Research Board of the National Academies, Washington, D.C., 2011, pp.110-119.

Mitra, S., and S. Washington. On the significance of omitted variables in intersection crash modeling. *Accident Analysis and Prevention*, Vol. 49, 2012, pp.439-448.

Mohamad, D., K. Sinha, T. Kuczek, and C. Scholer. Annual Average Daily Traffic Prediction Model for County Roads. *Transportation Research Record: Journal of the Transportation Research Board*, No. 1617, Transportation Research Board of the National Academies, Washington D.C., 1998, pp. 69-77.

Monsere, C., T. Johnson, K. Dixon, J. Zheng, and I. van Schalkwyk. *An Assessment of Statewide Intersection Safety*, Final Report, Oregon Department of Transportation SPR Project No. 667, 2011.

Oregon Department of Transportation (ODOT). *Oregon State Highway Video Log*. Oregon.gov [Online] <http://www.oregon.gov/ODOT/TD/TDATA/pages/rics/videolog.aspx>. Accessed November 2014.

Oregon Department of Transportation (ODOT). *TransGIS*. Accessed at <https://gis.odot.state.or.us/transgis/>. Accessed November 2014.

Pinheiro, J., and D.M. Bates. *Mixed-Effects Models in S and S-PLUS*. New York: Springer, 2000. ISBN 0-387-98857-9.

Potts, I., D. Harwood, and K. Richard. Relationship of Lane Width to Safety on Urban and Suburban Arterials. *Transportation Research Record: Journal of the Transportation Research Board*, No. 2023, Transportation Research Board of the National Academies, Washington, D.C., 2007, pp.63-82.

Potts, I., K. Bauer, D. Torbic, and J. Ringert. Safety of Channelized Right-Turn Lanes for Motor Vehicles and Pedestrians. Presented at 92nd Annual Meeting of the Transportation Research Board. Washington, D.C., 2013.

Pulugurtha, S., and P. Kusam. Modeling Annual Average Daily Traffic with Integrated Spatial Data from Multiple Network Buffer Bandwidths. *Transportation Research Record: Journal of the Transportation Research Board*, No. 2291, Transportation Research Board of the National Academies, Washington, D.C., 2012, pp. 53-60.

Qi, Y., M. Azimi, and L. Yu. Safety Impacts of Increasing Lengths of Left-Turn Lanes. Presented at 92nd Annual Meeting of the Transportation Research Board, Washington, D.C., 2013.

The R Development Core Team. *R: A language and Environment for Statistical Computing*. [Online] R Foundation for Statistical Computing, Vienna, Austria, 2013. Version 2.10.1 (2009-12-14). <http://www.R-project.org>. ISBN 3-900051-0700. Accessed November 2014.

Savolainen, P., F. Mannering, D. Lord, and M. Quddus. The Statistical Analysis of Highway Crash-Injury Severities: A Review and Assessment of Methodological Alternatives. *Accident Analysis and Prevention*, Vol. 43, No. 5, 2011, pp. 1666-1676.

Sayed, T., M. El-Esawaey, and J. Pump. Evaluating Impact on Safety of Improved Signal Visibility at Urban Signalized Intersections. *Transportation Research Record: Journal of the Transportation Research Board*, No. 2019, Transportation Research Board of the National Academies, Washington, D.C., 2008, pp. 51-56.

Seaver, W., A. Chatterjee, and M. Seaver. Estimation of Traffic Volume on Rural Local Roads. *Transportation Research Record: Journal of the Transportation Research Board*, No. 1719, Transportation Research Board of the National Academies, Washington, D.C., 2000, pp. 121-128.

Selby, B., and K. Kockelman. Spatial Prediction of AADT in Unmeasured Locations by Universal Kriging. Paper 11-1665. Presented at 90th Annual Meeting of the Transportation Research Board, Washington D.C., 2011.

Shankar, V., E. Donnell, R. Porter, F. Gross, W. Hu, M. Gemar, and J. Oh. Estimating the Safety Effects of Roadway Lighting at Intersections: Cross-sectional Study Approach. Presented at 90th Annual Meeting of the Transportation Research Board, Washington, D.C., 2011.

Sharma, A., L. Rilett, Z. Wu, and S. Wang. *Speed Limit Recommendation in Vicinity of Signalized, High-Speed Intersection*. Report SPR-P1(11) M307. University of Nebraska-Lincoln, Lincoln, Nebraska, 2012.

Souleyrette, R., T. McDonald, and M. O'Brien. Safety Effectiveness of All-Red Clearance Intervals at Urban Low-Speed Intersections. Presented at 86th Annual Meeting of the Transportation Research Board, Washington, D.C., 2007.

Stephan, K., and S. Newstead. Towards Safer Urban Roads and Roadsides: Factors Affecting Crash Risk in Complex Urban Environments. Australasian Road Safety Research Policing Education Conference, 2012, Wellington, New Zealand, October 2012.

Stollof, E. Intersection and Junction Fatalities in the Context of Access Management. Eighth National Conference on Access Management, Baltimore, MD. Sponsored by the Transportation Research Board, Washington, D.C., July 2008.

United States Census Bureau. *State and County Quick Facts*. Accessed at <http://quickfacts.census.gov/qfd/states/41000.html>. Accessed November 2014.

Venables, W.N., and B.D. Ripley. *Modern Applied Statistics with S*, 4th Edition. New York: Springer, 2002. ISBN 0-387-95457-0.

Wang, T. Improved Annual Average Daily Traffic Estimation for Local Roads using Parcel-Level Travel Demand Modeling. Ph.D. Dissertation, Florida International University, Miami, Florida, 2012.

Wang, X., and M. Abdel-Aty. Temporal and Spatial Analyses of Rear-end Crashes at Signalized Intersections. *Accident Analysis and Prevention*, Vol. 38, No. 6, 2006, pp.1137-1150.

Wang, X., and M. Abdel-Aty. Right-Angle Crash Occurrence at Signalized Intersections. *Transportation Research Record: Journal of the Transportation Research Board*, No. 2019, Transportation Research Board of the National Academies, Washington, D.C., 2007, pp. 156–168.

Wang, X., and M. Abdel-Aty. Modeling Left-turn Crash Occurrence at Signalized Intersections by Conflicting Patterns. *Accident Analysis and Prevention*, Vol. 40, No. 1, 2008, pp. 76-88.

Wang, X., M. Abdel-Aty, A. Nevarez, and J. Santos. Investigation of Safety Influence Area for Four-Legged Intersections: Nationwide Survey and Empirical Inquiry. *Transportation Research Record: Journal of the Transportation Research Board*, No. 2083, Transportation Research Board of the National Academies, Washington, D.C., 2008, pp. 86-95.

Wang, X., and K. Kockelman. Forecasting Network Data: Spatial Interpolation of Traffic Counts from Texas Data. *Transportation Research Record: Journal of the Transportation Research Board*, No. 2105, Transportation Research Board of the National Academies, Washington, D.C., 2009, pp. 100-108.

Wu, Z., A. Sharma, F. Mannering, and S. Wang. Safety Impacts of Signal-Warning Flashers and Speed Control at High-Speed Signalized Intersections. *Accident Analysis and Prevention*, Vol. 54, 2013, pp.90-98.

Xia, Q., F. Zhao, Z. Chen, L.D. Shen, and D. Ospina. Estimation of Annual Daily Traffic for Nonstate Roads in a Florida County. *Transportation Research Record: Journal of the Transportation Research Board*, No. 1660. Transportation Research Board of the National Academies, Washington, D.C., 1999, pp. 32-40.

Xie, F., K. Gladhill, K. Dixon, and C.M. Monsere. Calibration of Highway Safety Manual Predictive Models for Oregon State Highways. *Transportation Research Record: Journal of the Transportation Research Board*, No. 2241, Transportation Research Board of the National Academies, Washington, D.C., 2011, pp. 19–28.

Xie, K., X. Wang, X. Chen, and H. Huang. Corridor-Level Signalized Intersection Safety Analysis in Shanghai, China using Bayesian Hierarchical Models. Presented at 91st Annual Meeting of the Transportation Research Board, Washington D.C., 2012.

Xie, Y., and Y. Zhang. Crash Frequency Analysis with Generalized Additive Models. *Transportation Research Record: Journal of the Transportation Research Board*, No. 2061, Transportation Research Board of the National Academies, Washington, D.C., 2008, pp.86-95.

Yan, X., and E. Radwan. Characteristics of Unprotected Left-Turn Accidents at Signalized Intersections. *International Journal of Injury Control and Safety Promotion*, Vol. 15, No. 1, 2008, pp.45-48.

Yan, X., E. Radwan, and M. Abdel-Aty. Characteristics of Rear-End Accidents at Signalized Intersections using Multiple Logistic Regression Model. *Accident Analysis and Prevention*, Vol. 37, No. 6, 2005, pp. 983-995.

Ye, L., and D. Lord. Investigation of Effects of Underreporting Crash Data on Three Commonly Used Traffic Crash Severity Models: Multinomial Logit, Ordered Probit, and Mixed Logit. *Transportation Research Record: Journal of the Transportation Research Board*, No. 2241, Transportation Research Board of the National Academies, Washington, D.C., 2011. pp.51-58.

Young, J., and P. Park. Comparing the Highway Safety Manual's Safety Performance Functions with Jurisdiction-Specific Functions for Intersections in Regina. Implementation of Safety Prediction Methods in the Processes and Procedures of a Transportation Agency Session of the 2012 Annual Conference of the Transportation Association of Canada. 2012.

Zhao, F., and N. Park. Using Geographically Weighted Regression Models to Estimate Annual Average Daily Traffic. *Transportation Research Record: Journal of the Transportation Research Board*, No. 1879, Transportation Research Board of the National Academies, Washington, D.C., 2004, pp. 99-107.

Zhao, F., and S. Chung. Contributing Factors of Annual Average Daily Traffic in a Florida County: Exploration with Geographic Information System and Regression Models. *Transportation Research Record: Journal of the Transportation Research Board*, No. 1769, Transportation Research Board of the National Academies, Washington, D.C., 2001, pp. 113-122.

Zhong, M. and B. Hanson. GIS-Based Travel Demand Modeling for Estimating Traffic on Low-Class Roads. *Transportation Planning and Technology*, Vol. 32, No. 5, 2009, pp. 423-439.

APPENDIX A

**SUPPLEMENTAL TABLES AND EXAMPLE DATA COLLECTION
FORM**

LIST OF APPENDIX A TABLES

Table A.1: Abbreviations and Acronym Definitions	A-1
Table A.2: Data Collection Form Key	A-3

APPENDIX A

This appendix contains supplemental tables as well as an example data collection form.

SUPPLEMENTAL TABLES

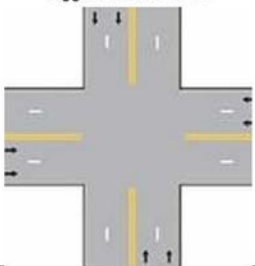

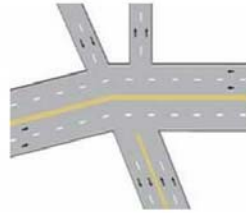
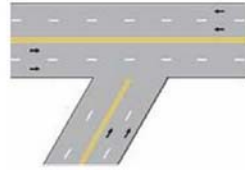
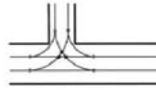

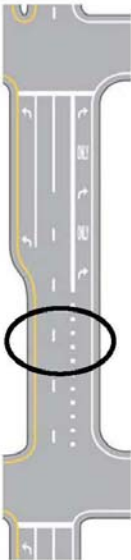
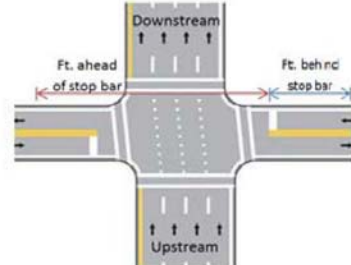










Table A.1: Abbreviations and Acronym Definitions

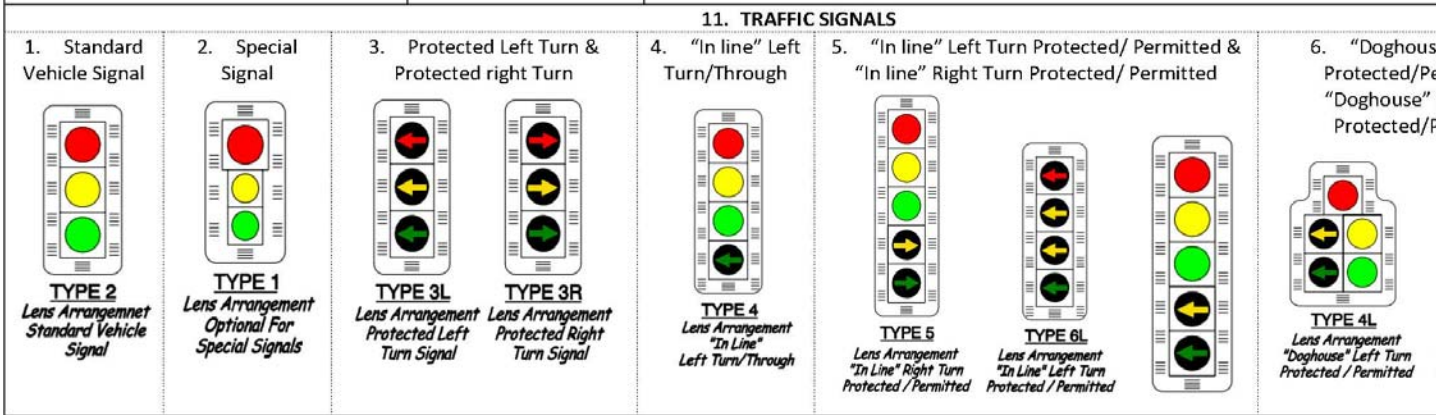
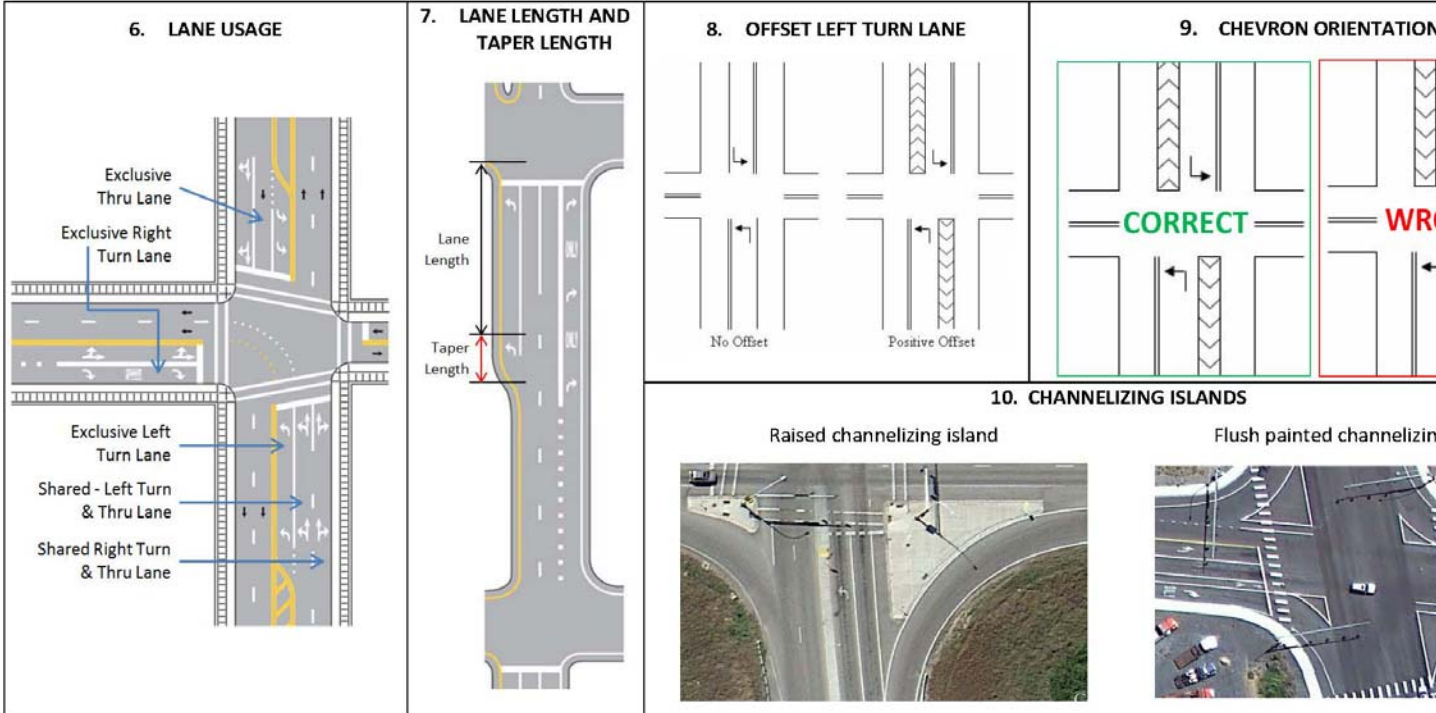
Acronym	Definition
AASHTO	American Association of State Highway and Transportation Officials
AADT	Average Annual Daily Traffic
ADT	Average Daily Traffic
AIC	Akaike Information Criterion
ATR	Automatic Traffic Recorders
BGOP	Bivariate Generalized Ordered Probit
BOP	Bivariate Ordered Probit
CMF	Crash Modification Factor (or Function)
CURE	Cumulative Residual Plot
DOT	Department of Transportation
EB	Empirical Bayes
EPA	Environmental Protection Agency
GAM	Generalized Additive Model
GEE	Generalized Estimating Equations
GIS	Geographic Information Systems
GLM	Generalized Linear Model
GWR	Geographically Weighted Regression
HSM	Highway Safety Manual
IFA	Intersection Functional Area
IR	Intersection-Related (crashes)
ITE	Institution of Transportation Engineers
KAB	Fatal and serious injury crashes
KPH	Kilometers per Hour
LOOCV	Leave-One-Out Cross Validation analysis
MAPE	Mean Absolute Percent Error
MARS	Multinomial Adaptive Regression Splines
MjAADT	Major Road AADT
MjSpLm	Major Road Speed Limit
ML	Mixed Logit
MnAADT	Minor Road AADT
MNL	Multinomial Logit
MnSpLm	Minor Road Speed Limit
MPH	Miles per Hour
ODOT	Oregon Department of Transportation

Acronym	Definition
OLS	Ordinary Least Squares (Regression)
OP	Ordered Probit Model
PDO	Property Damage Only
R4SG2	Rural Two-lane Four-leg Signalized Intersection
R4SG4	Rural Four-lane Four-leg Signalized Intersection
SPF	Safety Performance Function
SSD	Stopping Sight Distance
TCD	Traffic Control Device
TWLTL	Two-Way Left-Turn Lane
U3SG	Urban/Suburban Three-leg Signalized Intersection
U4SG	Urban/Suburban Four-leg Signalized Intersection
vpd	Vehicles per Day
vph	Vehicles per Hour

Table A.2: Data Collection Form Key

DATA COLLECTION FORM KEY			
INTERSECTION TYPE 1 - 4-Way Intersection 2 - T-Intersection 3 - Multi-leg Intersection 4 - Y-Intersection 5 - 4-Legged Staggered Intersection 6 - Other	TRAFFIC CONTROL DEVICE 1 - Traffic Signal - Suspended Cantilever 2 - Traffic Signal - Suspended Span Wire 3 - Traffic Signal - Corner Signals 4 - Flashing Beacon - Red 5 - Flashing Beacon - Amber 6 - School Crossing Sign or Special Signal 7 - Wigwag or Flashing Lights w/o Drop-Arm Gate 8 - Special Pedestrian Signal 9 - Flashing Lights with Drop Arm-Gate 10 - Supplemental Overhead Signal (RR xing only) 11 - Right Turn at All Times Sign 12 - Traffic Signal - Cantilever and Corner Signals 13 - Traffic Signal - Span Wire and Corner Signals 14 - Other	SHARED / EXCLUSIVE TRHU LANE SIGNALIZATION 1 - Standard Vehicle Signal 2 - Special Signal 3 - Protected Right Turn 4 - "In-line" Left Turn / Through	32 - Right Turn Yield to Pedestrians and Bikes 33 - Stop 34 - Combination Signal Ahead and Photo Enforced Sign 35 - Right Lane Bikes Only 36 - Two Way Left Turn Only Signal 37 - Grade Crossing (Crossbuck) 38 - Grade Crossing Advanced Warning - Pavement Markings 39 - Pedestrian Crossing - Diamond Sign 40 - Bike Lane Merges with Vehicle Lane 41 - Right Lane Must Turn Right Except Bikes 42 - Right Lane Must Turn Right Except Bus and Bikes 43 - Bike Lane Ends 44 - Truck Route
DOTTED LINE MARKINGS TO EXTEND LANE LINE MARKINGS INTO INTERSECTION 1 - Yes 2 - No	SIGNS ON TRAFFIC LIGHT POLE/SPAN WIRE 1 - Left Turn Only 2 - Right Turn Only 3 - Through Lane Only 4 - Optional Movement Lane Control 5 - Left Turn Yield to Oncoming Traffic 6 - Left Turn Yield on Green 7 - No U-turn 8 - No Right Turn 9 - Crosswalk Closed 10 - No Pedestrian Crossing 11 - Right Turn Yield to Pedestrians on Green 12 - No Left Turn 13 - One Way 14 - Left Turn Signal 15 - School Crossing Sign 16 - Bikes OK	RIGHT TURN LANE SIGNALIZATION 1 - Standard Vehicle Signal 2 - Special Signal 3 - Protected Right Turn 4 - "In-line" Right Turn/Through 5 - "In-line" Right Turn Protected/Permitted 6 - "Doghouse" Right Turn Protected/Permitted	45 - Center Lane Two Way Left Turn Only 46 - End School Zone 47 - Right Turn Yield to Pedestrians 48 - School Crossing Sign 49 - Seat Belts Must be Worn 50 - School Crossing Ahead 51 - School Zone Sign 52 - Bike Route 53 - Combined Right Lane/Bike Lane 54 - Truck Route to the Right 55 - Right Turn Only 56 - Caution: Vehicle Exit Alley 57 - School Zone: Speed 20 when Children are Present 58 - Stop Here for Pedestrians 59 - Bicycle Crossing 60 - Traffic Laws Photo Enforced 61 - Animal Crossing 62 - Bike Lane - No Parking 63 - Post Mounted Flashing-light Signals w/ Crossbuck 64 - Flashing-light Signals w/ Crossbuck and Drop-arm 65 - 40ft. between tracks and Highway 66 - Vehicular Traffic Warning - Bicycle 67 - Right Turn Yield to Bikes 68 - Drop-arm Gate (RR Crossing Only) 69 - No Skating Boarding or Biking on Sidewalk 70 - Tow Away No Parking in this Block (3AM to 6AM) 71 - One Way - Do Not Enter 72 - School Speed Limit 20 - School Day 7AM - 5PM 73 - Intersection Warning 74 - School Bus Stop Ahead 75 - Cantilevered Amber Flashing Beacon - School Speed when Flashing 76 - Do Not Block Intersection 77 - Handicapped Parking 78 - No Turn on Red 79 - Do Not Pass 80 - Pedestrian Crossing Ahead 81 - Reduced Speed Ahead 82 - Bicycle and Pedestrian Crossing Ahead
DRIVEWAY LOCATION 1 - Right Side of the Road 2 - Left Side of the Road	DRIVEWAY TYPE 1 - Residential 2 - Commercial 3 - Industrial 4 - Institutional 5 - Other 6 - Driveway for Non-motorized Vehicles	ADVISORY SIGN LOCATION 1 - Right Side 2 - Left Side 3 - Median 4 - Both Sides 5 - Across Intersection 6 - Channelizing Island	
MEDIAN TYPE 1 - Painted 2 - TW/LTL 3 - Grass 4 - Raised 5 - Concrete Barrier 6 - None 7 - Raised Pavement Markers	ON-STREET PARKING 1 - Left Side 2 - Right Side 3 - Both Sides 4 - No	ADVISORY SIGNS 1 - Bikes Merge 2 - Snow Zone 3 - Do Not Enter 4 - Left Lane Must Turn Left Plaque 5 - Two Way Traffic 6 - No Parking Symbol with Arrow 7 - No Parking Symbol w/ Double Headed Arrow 8 - One Way Plaque 9 - Parking with Time Restrictions 10 - No Right Turn 11 - No Motorized Vehicles 12 - No Left Turn 13 - Begin Right Turn Lane Yield to Bikes 14 - Advanced Intersection Lane Control 15 - Crosswalk Closed 16 - No Pedestrian Crossing 17 - Keep Right 18 - Right Lane Must Turn Right 19 - Yield 20 - Signal Ahead 21 - Added Lane Sign 22 - Wrong Way 23 - Cantilevered Flashing-light Signals w/ Crossbuck 24 - Do Not Stop on Tracks 25 - Grade Crossing Advanced Warning 26 - Signal Ahead Sign w/ Yellow Flashing Beacon 27 - Divided Highway Begins 28 - Horizontal Alignment and Advisory Speed 29 - No Left Turn 30 - Shared Lane Marking 31 - Bicycle Lane Ahead	
BIKE LANE 1 - Left Side 2 - Right Side 3 - Both Sides 4 - No 5 - Sharrow Lane / Shared Lane	CHANNELIZATION 1 - Raised Channelizing Island 2 - Flush Painted Channelizing Island 3 - None		
BUS STOP NEAR INTERSECTION 1 - Right Side of the Road 2 - Left Side of the Road 3 - None	LEFT TURN LANE SIGNALIZATION 1 - Standard Vehicle Signal 2 - Special Signal 3 - Protected Left Turn 4 - "In-line" Left Turn/Through 5 - "In-line" Left Turn Protected/Permitted 6 - "Doghouse" Left Turn Protected/Permitted		
PEDESTRIAN CROSSING LIGHT 1 - Yes 2 - No			
OFFSET LEFT TURN LANE 1 - Yes 2 - No 3 - N/A			
ARE CHEVRONS PROPERLY ORIENTED? 1 - Yes 2 - No 3 - N/A			

Data Collection Form Key									
1. 4 Way Intersection: Any 4-legged intersection 		2. T-intersection: Any 3-legged intersection in which one roadway ends at a section of another roadway 		3. Multi-Leg Intersection: Intersection that has five or more intersecting roads 		4. Y-intersection: Any 3-legged intersection other than a 'T' 		5. 4-Leg Staggered 	
						6. Other: An intersection not mentioned			
2. TOTAL NO. OF ROAD LANES Write in parentheses lanes per direction and TWLTL if there is one Count number of lanes here (i.e. total number of lanes: 3)		3. FACE-TO-FACE MEASUREMENT 		5. TRAFFIC CONTROL DEVICES - EXAMPLES					
		4. UPSTREAM & DOWNSTREAM DEFINITION 		1. Suspended Cantilever 		2. Suspended Span Wire 		3. Corner 	
				4. Flashing Beacon - Red (stop) 		5. Flashing Beacon - Amber (slow) 		6. School crossing sign or special signal 	
				7. Special 		8. Wigwag or flashing lights w/o drop-arm gate 		9. Flashing lights with drop arm gate 	
				10. Supplemental signal (RR x) 					



APPENDIX B

AADT CONVERSION METHODOLOGY

LIST OF APPENDIX B TABLES

Table B.1: List of Automatic Traffic Recorders used in the Analysis.....	B-2
Table B.2: Monthly Factor (Weekday Averages) for Automatic Traffic Recorders used in the Analysis	B-3
Table B.3: Annual AADT Estimates for Automatic Traffic Recorders used in the Analysis.....	B-4
Table B.4: ATR 03-017 Year-Year Factors.....	B-5
Table B.5: Year-Year Factors for ATR 17-005	B-5

APPENDIX B: AADT CONVERSION METHODOLOGY

The AADT data for the major or minor road for each year were not available for many of intersections. If available, the research team obtained short-term traffic counts from local agencies or ODOT. Some of these counts were available in Transportation System Plans or other documents. For the sites without any available traffic data, the team attempted to contact private vendors for historical counts. All of the short-term counts were then converted to AADT using a similar methodology. Next, all sites were factored to year over year volumes using the trends established from the nearest automatic traffic recorders (ATR).

B.1 METHODOLOGY

For each site, the research team selected the nearest and most compatible ATR station. A list of the ATR stations is shown in Table B.1. The Traffic Monitoring Guide (*FHWA 2001*) provides the following formula to convert 24-hour axle counts to AADT:

$$AADT_{hi} = VOL_{hi} \times M_h \times D_h \times A_i \times G_h$$

where

$AADT_{hi}$ = the annual average daily travel at location i of factor group h (vpd);

VOL_{hi} = the 24-hour axle volume at location i of factor group h;

M_h = the applicable seasonal (monthly) factor for factor group h;

D_h = the applicable day-of-week factor for factor group h (if needed);

A_i = the applicable axle-correction factor for location i (if needed); and

G_h = the applicable growth factor for factor group h (if needed).

For this effort, however, the counts available to the project team are not axle counts, but vehicle counts. Traffic and Highway Engineering (*Garber and Hoel 2009*) presents a modified equation which uses hourly, daily, and monthly expansion factors to convert counts of durations shorter than 24 hours. In general, a two-hour traffic volume count is converted to AADT with the following formula:

$$AADT_{hi} = VOL_{hij} \times H_{ij} \times M_h \times D_h$$

where

$AADT_{hi}$ = the annual average daily travel at location i of factor group h (vpd);

VOL_{hij} = the two-hour peak volume during time period j at location i of factor group h;

H_{ij} = the applicable hourly factor during time period j at location I;

M_h = the applicable seasonal (monthly) factor for factor group h; and

D_h = the applicable day-of-week factor for factor group h.

Table B.1: List of Automatic Traffic Recorders used in the Analysis

ATR Station	Highway Number	Mile Post	Highway Name	ATR Nearby Cross
03-017	OR 8	14.84	Tualatin Valley Highway No. 29	0.28 mile west of NW 334th Ave.
03-018	OR 212 / OR 224	6.8	Clackamas Highway No. 171	0.14 mile west of SE 130th Ave
09-009	OR 224	3.6	Clackamas Highway No. 171	0.13 mile west of Johnson Road
15-017	US 97	137.36	The Dalles-California Highway No. 4	0.23 mile south of Revere Ave.
17-005	OR 62	1.11	Crater Lake Highway No. 22	0.64 mil east of Pacific Highway
18-018	US 199	4.68	Redwood Highway no. 25	0.50 mile east of Redwood Ave.
24-001	OR 39 / US 97	4.08	Klamath Falls-Malin Highway no. 50	0.46 mile south of Main St.
26-003	OR 99 E	34.03	Pacific Highway East No. 81	1.16 mile south of Hillsboro Silverton (214)
27-002	US 26	14.36	Mt. Hood Highway No. 26	0.18 mile southeast of SE Powell Valle
30-019	OR 221	18.6	Salem-Dayton Highway No. 150	0.09 mile north of Brush College Rd N
30-021	US 395	8.7	Umatilla Stanfield Highway No. 54	0.12 mile northwest of Feedville Road
34-009	OR 11	34.46	Oregon-Washington Highway No. 8	0.86 mile south of Oregon-Washingto

Table B.2: Monthly Factor (Weekday Averages) for Automatic Traffic Recorders used in the Analysis

ATR Station	2012												Average
	Jan	Feb	Mar	Apr	May	Jun	Jul	Aug	Sep	Oct	Nov	Dec	
03-017	1.087	1.038	1.038	1.006	0.999	0.964	0.945	0.933	0.941	0.989	1.037	1.048	1
03-018	1.048	0.997	1.013	0.969	0.993	0.966	1.006	0.979	0.978	0.982	1.022	1.057	1
09-009	1.153	1.090	1.085	1.010	0.979	0.921	0.903	0.885	0.947	0.983	1.042	1.080	1
15-017	1.067	1.009	1.019	0.977	0.973	0.940	0.949	0.963	1.012	1.021	1.041	1.046	1
17-005	1.159	1.081	1.089	1.046	0.981	0.923	0.847	0.855	0.924	0.996	1.062	1.169	1
18-018	1.028	1.001	1.044	0.950	0.953	0.960	1.011	0.990	0.981	0.951	1.017	1.146	1
24-001	1.129	1.054	1.072	1.015	0.972	0.954	0.904	0.888	0.928	0.954	1.051	1.161	1
26-003	1.072	1.016	1.033	1.006	1.006	0.965	0.945	0.921	0.966	1.011	1.066	1.017	1
27-002	1.094	1.023	1.062	0.998	0.967	0.913	0.951	0.946	0.996	0.993	1.041	1.047	1
30-019	1.145	1.007	1.031	0.990	0.962	0.963	0.945	0.935	0.952	0.982	1.036	1.095	1
30-021	1.172	1.065	1.038	0.979	0.954	0.935	0.930	0.934	0.958	0.971	1.046	1.077	1
34-009	1.041	1.001	1.002	0.964	0.983	0.973	0.988	0.995	0.998	1.009	1.027	1.026	1

Table B.3: Annual AADT Estimates for Automatic Traffic Recorders used in the Analysis

ATR Station	Yearly (vpd)										
	2003	2004	2005	2006	2007	2008	2009	2010	2011	2012	2013
03-017					35,655	32,177	32,093	32,404	32,240	32,857	33,849
03-018					35,285	35,285	35,434	35,149	35,163	35,368	34,995
09-009	37,125	38,565	39657	42,163	42,825	39,229	38,140	38,467	38,506	39,052	41,556
15-017	37,946	38,516	38483	38,400	44,222	42,382	41,914	42,370	42,399	41,620	41,686
17-005	11,737	11,860	11725	11,561	11,422	10,553	10,927	10,954	10,453	10,310	10,468
18-018	23,385	23,432	24085	23,202	24,757	23,409	22,965	22,496	21,520	21,163	21,224
24-001	10,676	10,810	10301	10,748	10,954	10,254	10,263	10,224	10,147	10,050	10,573
26-003	39,138	37,657	33743	33,471	33,225	31,776	32,252	32,273	30,530	29,978	30,315
27-002				12,273	12,578	11,802	12,022	12,229	12,096	12,084	12,114
30-019				7,743	7,727	7,469	7,618	7,706	7,567	7,347	7,384
30-021	14,323	14,360	14819	14,882	14,863	14,310	14,718	14,739	14,521	14,333	14,201
34-009					33,620	33,838	33,042	33,237	33,248	33,333	33,000

B.2 SAMPLE APPLICATIONS

Example 1: Site with AADT from local agencies or ODOT

Site Description

The major road is SE. Sunnyside Road in Clackamas County, OR intersecting with SE. Stevens Road. SE. Stevens Road had an AADT of 13,350 vpd in 2011. Since AADT is already available, there is no need to apply time of day, month of year, or day of week factors. However, yearly factors have to be applied to the AADT from 2011, to estimate AADT for other years. The year-year factors are taken from ATR 03-017 and depicted in Table B.4. Also shown are the AADT for the different years, which are computed using the formula:

$$AADT_{hi} = Y_{hi} * AADT$$

where

$AADTh_i$ = the annual average daily travel at location i of factor group h (vpd);
 Y_{hi} = the applicable year factor for location i of factor group h ; and
 $AADT$ = the available AADT for a particular year (vpd).

Table B.4: ATR 03-017 Year-Year Factors

	2003	2004	2005	2006	2007	2008	2009	2010	2011	2012	2013
Factor	-	-	-	-	1.106	0.998	0.995	1.005	1.000	1.019	1.050
AADT	-	-	-	-	14,764	13,324	13,289	13,418	133,50	13,605	14,106

Example 2: Site with four-hour counts for the minor road and obtained from local agencies

Site Description

The major road is E. Pine St, which is located in Central Point, OR. It intersects with N 4th St. The counts on each leg of the minor facility were 431 and 617, with an average count of 524. They were collected between 2-6 p.m. on 9/29/2010.

Step 1: Convert peak hour traffic count to daily traffic volume

The research team converted the peak hour traffic count to daily traffic volume using a time of day factor of 0.31.

$$\text{Daily traffic volume} = \frac{\text{Peak hour count}}{\text{Time of Day factor}} = 1690 \text{ vpd}$$

Step 2: Calculate AADT

The ATR for this site occurs at station 17-005. Since the count was collected in September, the associated monthly factor is 0.92 and the day of the week factor is 1.0

$$AADT_{hi} = VOL_{hi} \times M_h \times D_h = 1690 \times 0.92 \times 1.0 = 1555 \text{ vpd}$$

Step 3: Calculate AADT for Other Years

The year-year factors are computed using the counts from ATR 17-005 and are listed in Table B.5. The AADT for the various years can then be computed by applying these factors to the AADT previously computed.

Table B.5: Year-Year Factors for ATR 17-005

	2003	2004	2005	2006	2007	2008	2009	2010	2011	2012	2013
Factor	1.071	1.083	1.070	1.055	1.043	0.963	0.998	1.000	0.954	0.941	0.956
AADT	1667	1684	1665	1642	1622	1498	1552	1555	1484	1464	1486

If two-hour peak period counts are available, the same procedure can be followed, except that the time of day factor will be different and will have to be estimated.

APPENDIX C

AADT MODEL VALIDATION

LIST OF APPENDIX C TABLES

Table C.1: Validation Sample Descriptive Statistics	C-1
Table C.2: Summary of Categorical Variables	C-2
Table C.3: List of Intersections used for Model Validation	C-4
Table C.4: Descriptive Statistics for Minor Volume Models	C-5
Table C.5: Model Outputs for Total Entering Volume, Two-way Major and Minor Roads (with Parallel Facility).C-7	
Table C.6: Model Outputs for Total Entering Volume, Two-way Major and Minor Roads (without Parallel Facility)	C-7
Table C.7: Model Outputs for Minor Volume Estimation Model by Leg (without Parallel Facility AADT)	C-10

LIST OF APPENDIX C FIGURES

Figure C.1: Predicted and Observed Minor Road Volumes for Two-way Major and Minor Facilities.....	C-3
Figure C.2: Predicted and Observed Minor Road Volumes Estimated by Leg	C-3
Figure C.3: Summary Diagnostic Plots for Total Minor Entering Volume (with Parallel Facility AADT)	C-8
Figure C.4: Summary Diagnostic Plots for Total Minor Entering Volume (without Parallel Facility AADT)	C-8
Figure C.5: Comparison of Estimated Total Entering Volumes to Observed Volumes for Minor Facility (with Parallel AADT)	C-9
Figure C.6: Comparison of Estimated Total Entering Volumes to Observed Volumes for Minor Road (without Parallel Facility AADT)	C-9
Figure C.7: Summary Diagnostic Plots for Minor Volume Estimation by Leg (without Parallel Facility AADT).C-11	
Figure C. 8: Comparison of Estimated Volumes by Leg and Observed Volumes for Minor Facility	C-12

APPENDIX C: AADT MODEL VALIDATION

To confirm model reliability, this section of the report summarizes the validation activities for the AADT models. The purpose of validation is to assess if the model is able to reproduce the estimated parameters within reasonable limits. For the purpose of validation, twenty-five additional intersections were sampled from across the state. Of these, nine were in Region 1 (36 percent), five in Region 2 (20 percent), five in Region 3 (20 percent), four in Region 4 (16 percent), and two in Region 5 (8 percent). The selection of these intersections was based on available data, including major and minor volumes, and the volume on the parallel facility. Thus, this sample was not a random sample; the list of intersections is included at the end of this section.

C.1 MODEL VALIDATION RESULTS

Table C.1 shows the descriptive statistics for the validation sample. For the sample intersections, the major road AADT varied between 9,865 and 17,562 vpd with a mean of 3,603 vpd. Similarly, the volumes for the facility parallel to the minor road varied between a minimum of 860 vpd to a maximum of 14,409 vpd. The total number of lanes on both the major and minor roads varied between a minimum of one and a maximum of three.

Table C.1: Validation Sample Descriptive Statistics

Parameter		Validation Sample (n = 25)			
		Max	Min	Mean	Std. Dev
Volume	Major Road Volume (2013)	17562	3603	9865	4390.20
	Log (Major Road Volume) (2013)	4.245	3.56	3.95	0.21
	Parallel Facility Volume (2013)	14409	860	4740	3187.67
	Log (Parallel Facility Volume) (2013)	4.159	2.93	3.58	0.31
Geometry	Avg. Number of Approach Thru Lanes of Major Road	3	1	1.96	0.52
	Avg. Number of Approach Thru Lanes of Minor Road	3	1	1.52	0.59

Table C.2 shows the summary of the dummy variables in the validation sample that were used in the final model specifications. In the sample, ten intersections had a two-way left-turn lane on the minor road. The major and minor roads were classified as collectors at nine and 21 intersections respectively.

Table C.2: Summary of Categorical Variables

Parameter	Validation Sample (n = 25)	
	0 = No	1 = Yes
Two way Left Turn Lane on Minor Road	15	10
Functional Class of Major Road: Collector	16	9
Functional Class of Minor Road: Collector	4	21

The research team performed the model validation for both models that were developed in the research summarized in Chapter 4. The first model estimated minor road volumes at intersections where both the major and minor roads were two-way facilities, using parallel facility volumes.

The model was applied to the validation intersection variables and the estimates compared to the actual (observed) volumes. Figure C.1 shows the plot of predicted and observed values for two-way major and minor roads using the model specification that includes the parallel facility volume. The MAPE was calculated as the difference between the observed and predicted values using the following formula.

$$\text{Mean Absolute Percent Error (MAPE)} = \frac{1}{n} \sum_{t=1}^n \frac{\text{Observed}_t - \text{predicted}_t}{\text{Observed}_t} * 100$$

The mean absolute error was obtained as 1951.36 vehicles and MAPE was obtained as 52.4 percent. The second model specification estimated minor road volumes by each leg. Figure C.2 shows the plot of predicted and observed minor road volumes for the model estimates by leg. For majority of the intersections, the predicted volumes are underestimated compared to the observed volumes. For this model, the mean absolute error is 1401.54 vehicles and the MAPE is obtained as 49.1 percent. Figure C.2 demonstrates that the model significantly overestimated minor road AADT for one intersection. The intersection was located at NW 185th Avenue and NW West Union Road in Washington County (intersection at index=11 in the figure). One potential source of error could be related to the factoring process used in estimating volumes for multiple years. For the model estimation process, the intersections in Washington County were factored using data from an automatic traffic recorder (ATR) on OR 8. For this ATR, factors were developed for years 2007 to 2013. However, in the validation sample, the volume at this intersection and other Washington County intersections were originally collected in 2006. Hence, factors obtained from a different ATR located on US 26 were used for estimating major road and parallel facility volumes in 2013, which could have induced some error.

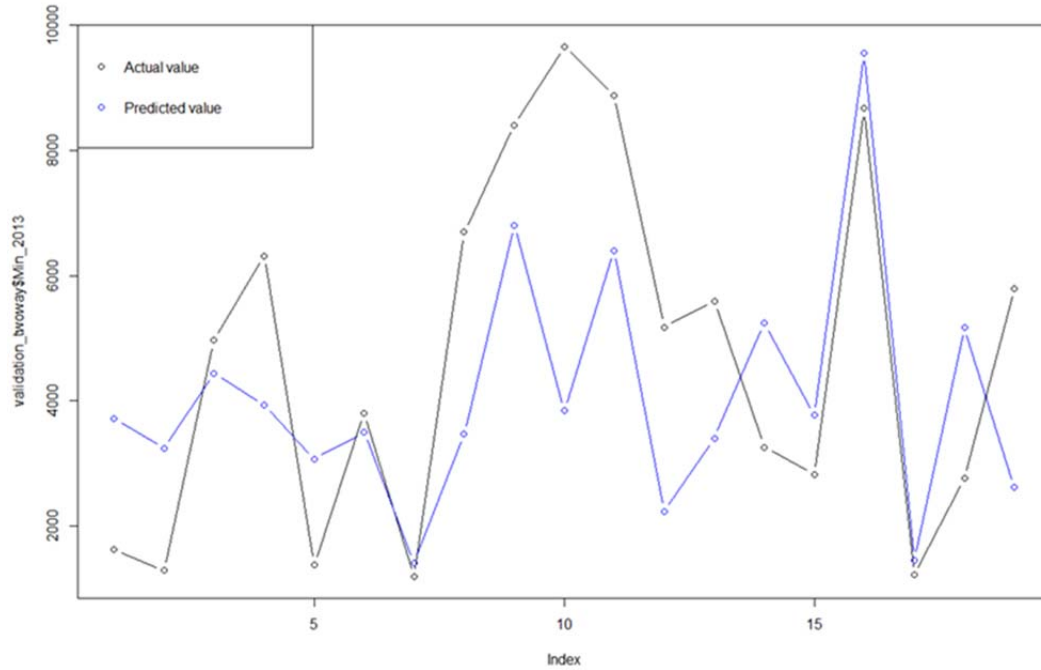


Figure C.1: Predicted and Observed Minor Road Volumes for Two-way Major and Minor Facilities

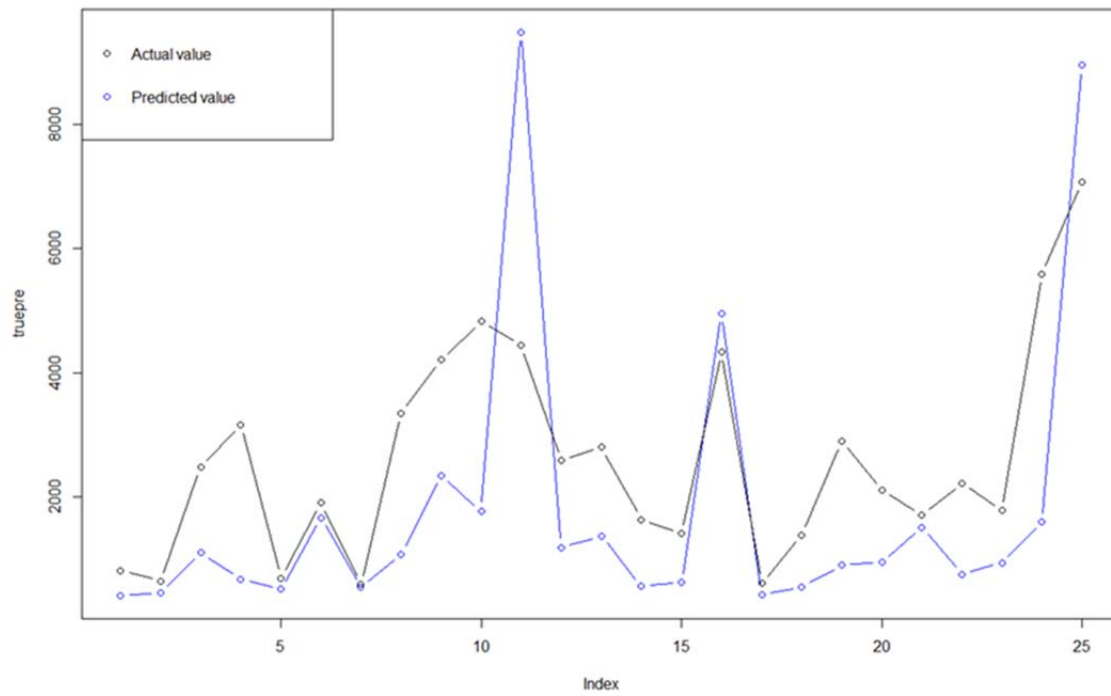


Figure C.2: Predicted and Observed Minor Road Volumes Estimated by Leg

Table C.3: List of Intersections used for Model Validation

Major Street	Minor Street	County	Maj Volume (2013)	Min Volume (2013)	Parallel Road Volume (2013)	Total Lanes Major	Total Lanes Minor	Two-way Left-Turn Lane Major	Function al Class Major	Function al Class Minor	Comments
Roberts Rd	Keene Way Dr	Jackson	6689	1625	1529	3	2	1	Collector	Collector	
4th Street	Front Street	Jackson	6355	1290	860	3	2	0	Collector	Collector	
E Jackson St	Sunrise Ave	Jackson	6546	4969	4587	3	3	0	Collector	Collector	
Seneca Rd	5th Ave	Lane	11,696	6317	5429	3	2	1	Arterial	Collector	
Donald St	46th Ave	Lane	3603	1382	1974	2	2	0	Collector	Collector	
Broadway St	Main St	Baker	5650	3800	3000	4	3	0	Arterial	Arterial	
10th St	Broadway St	Baker	4800	1191	1520	4	3	1	Arterial	Collector	
3rd St	Wilson Ave	Deschutes	16,647	6699	5688	5	3	1	Arterial	Collector	
Olney Ave	Portland Ave	Deschutes	13,235	8410	9665	4	4	0	Collector	Collector	
3rd St	Revere Ave	Deschutes	17,562	9665	8204	5	4	1	Arterial	Collector	
185th Ave	West Union Rd	Washington	17,221	8885	10,302	6	6	0	Arterial	Arterial	
Thompson Rd	Saltzman Rd	Washington	6637	5178	5797	4	3	0	Arterial	Collector	
Cornell Rd	113 Ave	Washington	13,153	5597	4376	4	4	1	Arterial	Collector	
198th Ave	Johnson St	Washington	8926	3262	3495	3	2	1	Collector	Collector	
185th Ave	Rosa Rd	Washington	11,794	2821	4098	3	2	1	Arterial	Collector	
Farmington Road	185th Ave	Washington	16,356	8674	14,409	4	4	0	Arterial	Arterial	
Beef Bend Rd	Barrows Rd	Washington	4332	1219	915	3	2	0	Arterial	Collector	
198th Ave	Alexander St	Washington	8926	2760	3262	3	2	1	Collector	Collector	
West Union Rd	Kaiser Rd	Washington	8608	5797	5178	4	3	1	Arterial	Collector	
8th Street	Oakdale Ave	Jackson	5065	4205	2007	4	3	0	Arterial	Collector	Maj One way
11th Ave	Olive St	Lane	13,523	3405	4343	6	3	0	Arterial	Collector	Maj One way
8th Ave	Willamette St	Lane	5379	4442	3060	4	2	0	Collector	Collector	Maj One way
Pearl St	Broadway Ave	Lane	12,289	3553	3307	4	2	0	Arterial	Collector	Maj One way
NW Franklin Blvd	NW Bond St	Deschutes	8916	5589	5191	4	4	0	Collector	Collector	Minor One way
Central Ave	Main Street	Jackson	12,710	7072	6307	6	6	0	Arterial	Arterial	Maj, Min One way

C.2 MODEL RE-ESTIMATION

Multiple linear regression models to estimate minor AADT were re-estimated using all the combined intersections from training as well as the validation sample set. This was done to test if any significant differences were found in the models estimated from a larger sample. The combined sample consisted of a total of 91 intersections (66 – training set, 25 – validation). The variable descriptive statistics for the combined data used in model estimation are shown in Table C.4 .

Table C.4: Descriptive Statistics for Minor Volume Models

Parameter		Min	Max	Mean	St. Dev
AADT	Major Road Volume (2013)	3,603	44,464	15589	8396.74
	Log (Major Road Volume) (2013)	3.56	4.65	4.13	0.24
	Parallel Facility Volume (2013)	733	18,497	5714	3829.41
	Log (Parallel Facility Volume) (2013)	2.87	4.27	3.88	0.30
Roadway	Avg. Number of Approach Thru Lanes on Major Road	1	3	1.97	0.60
	Avg. Number of Approach Thru Lanes on Minor Road	1	3	1.42	0.58

Within the combined sample, the major road AADT for 2013 varied between 3,603 to 44,464 vehicles per day (vpd), with a mean of 15,589 vpd. The parallel facility volume varied between a minimum of 733 to a maximum of 18,497 vpd. The average number of approach thru lanes on the major road varied between one and four, whereas on the minor road they varied between one and three.

Previously, a total of four models were estimated to predict AADT for the minor road, either by leg (for 1-way roads) or two-way with or without parallel facility volumes. However, using the combined data, only three models were estimated, one by leg and two for two-way facilities. The model estimating minor AADT by leg did not incorporate the parallel facility volume, as the inclusion of this variable rendered the major road AADT as insignificant predictor of minor road AADT. The research team determined that the major road AADT variable was of higher priority than the parallel facility volume, which may not be always available. However, two model specifications (with and without parallel facility volume) were estimated for two way facilities that predicted total entering volume for the minor facility

C.3 MODEL TO RE-ESTIMATE TOTAL MINOR ENTERING VOLUME (AADT)

Two regression models were estimated to predict minor AADT when both the major and minor roads were two way facilities. Table C.5 shows the significant variables for the model that estimates minor volume AADT, along with model fit parameters and goodness of fit parameters using the parallel facility volume. The R-squared of the model is 0.63 and the standard error of the residuals is 0.19. Table C.6 shows the significant variables for the model estimated without the parallel volume variable. The R-squared of the model is 0.54 and the standard error of the residuals is 0.21.

As shown in both tables, major road volume has a positive relationship with minor road AADT, implying that as major road volume increases, minor road AADT also increases. The other variable that showed a positive relationship with minor road AADT was the nearest parallel road volume. Variables that exhibited a negative relationship with log (AADT) for the minor road were the average number of approach thru lanes on the major road and functional class of the minor road (1= collector, 0 = arterial).

Further diagnostics of these model are shown in Figure C.3 and Figure C.4 . To better understand the model outputs, the predicted and observed volumes are transformed back to volumes (rather than log model inputs). In the figures, the plot in the upper left shows the predicted minor volumes on the y-axis with the observed minor volumes on the x-axis. The solid line represents the equal line (where the modeled volume would equal observed volumes). In these plots for both models, it is clear that modeled and observed volumes are in reasonable agreement. To explore any issues with bias by major road volumes, the plot in the upper right shows the residuals on the y-axis with the observed major AADT on the x-axis. The two lower histograms show two other diagnostics that explain the predictive quality of the models. In the lower left, the histogram shows the absolute percent predicted error as well as the mean absolute percent error (MAPE). Finally, in the lower right the histogram shows the error expressed in vehicles per day as well as the mean error.

Inspection of the goodness of fit parameters presented in the tables and plots in Figure C.3 and Figure C.4 indicate that the models do a reasonable job of estimating the minor road AADT. The mean absolute error for the models with and without parallel facility AADT are about 38 percent and 41 percent respectively, with the majority of the estimates having less than 50 percent error and only a small number of locations have high percent error. The mean error (the difference in the predicted minor volume and actual minor volume) varies between 1,800 - 2,000 vpd. The errors (residuals) do not show any trends over the range of major AADT included in the model (3,300 to 44,000 vpd). Given that the models will be used to estimate minor volumes that will be then be applied in SPF for crash prediction, the level of error is acceptable.

Figure C.5 and Figure C.6 show comparison plots between estimated volumes predicted using training data, combined data (training and validation) with the observed volumes for two-way facilities with and without parallel facility AADT. Both the models perform reasonably well in estimating minor road volumes. There is no apparent estimation bias with either model.

Table C.5: Model Outputs for Total Entering Volume, Two-way Major and Minor Roads (with Parallel Facility)

Parameter	Estimate	Std. Error	t value	Pr(> t)
(Intercept)	0.5404	0.4313	1.25	0.2148
log(Major AADT)	0.5528	0.1149	4.81	9.27×10 ⁻⁶ ***
Log(Parallel AADT)	0.3384	0.0857	3.95	0.0002***
Avg. Number of Approach Thru Lanes on Major	-0.1099	0.0480	-2.29	0.0252**
Func. Class Minor (Arterial=0, Collector=1)	-0.2379	0.0573	-4.16	9.70×10 ⁻⁵ ***
Residual standard error	0.1927 on 65 degrees of freedom			
R-squared	Multiple R-squared: 0.6267, Adjusted R-squared: 0.6037			
F-statistic	27.84 on 4 and 65 DF, p-value: 2.638×10 ⁻¹³			
* Significant at 90% confidence				
** Significant at 95% confidence				
***Significant at 99% confidence				

Table C.6: Model Outputs for Total Entering Volume, Two-way Major and Minor Roads (without Parallel Facility)

Parameter	Estimate	Std. Error	t value	Pr(> t)
(Intercept)	1.116	0.449	2.49	0.0154**
log(Major AADT)	0.742	0.115	6.43	1.67×10 ⁻⁸ ***
Avg. Number of Approach Thru Lanes on Major	-0.144	0.052	-2.76	0.007***
Func. Class Minor (Arterial=0, Collector=1)	-0.319	0.059	-5.41	9.33×10 ⁻⁷ ***
Residual standard error	0.213 on 66 degrees of freedom			
R-squared	Multiple R-squared: 0.5371, Adjusted R-squared: 0.5161			
F-statistic	25.53 on 3 and 66 DF, p-value: 4.441×10 ⁻¹¹			
* Significant at 90% confidence level				
** Significant at 95% confidence level				
***Significant at 99% confidence level				

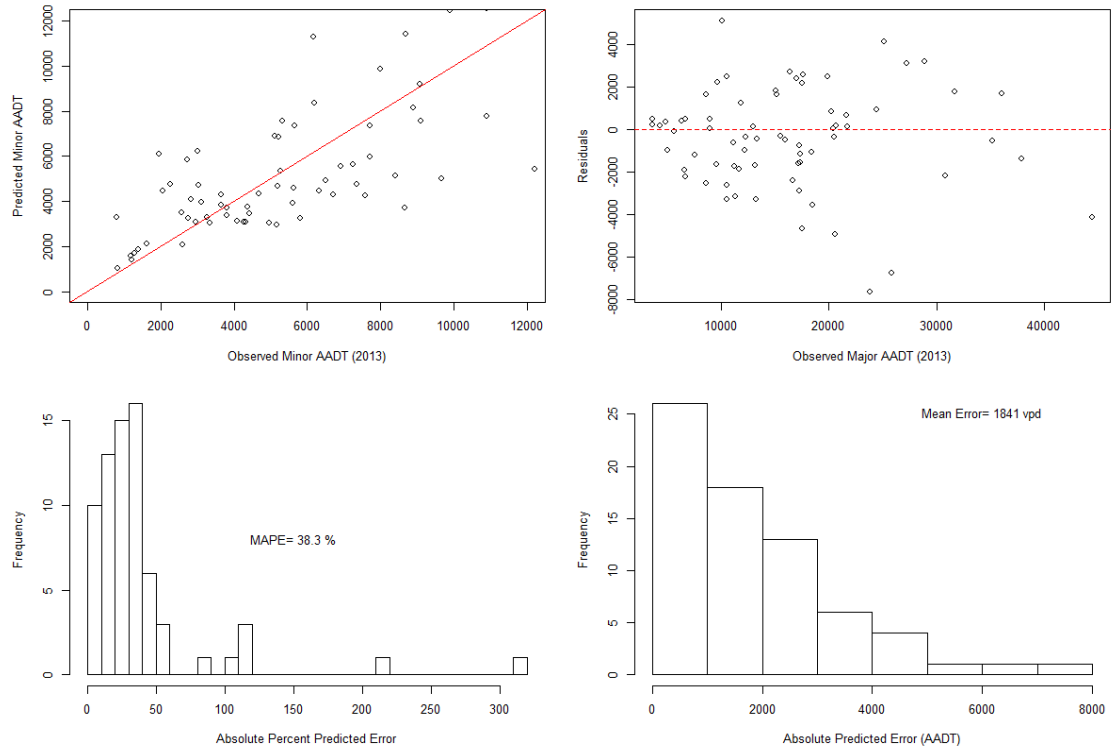


Figure C.3: Summary Diagnostic Plots for Total Minor Entering Volume (with Parallel Facility AADT)

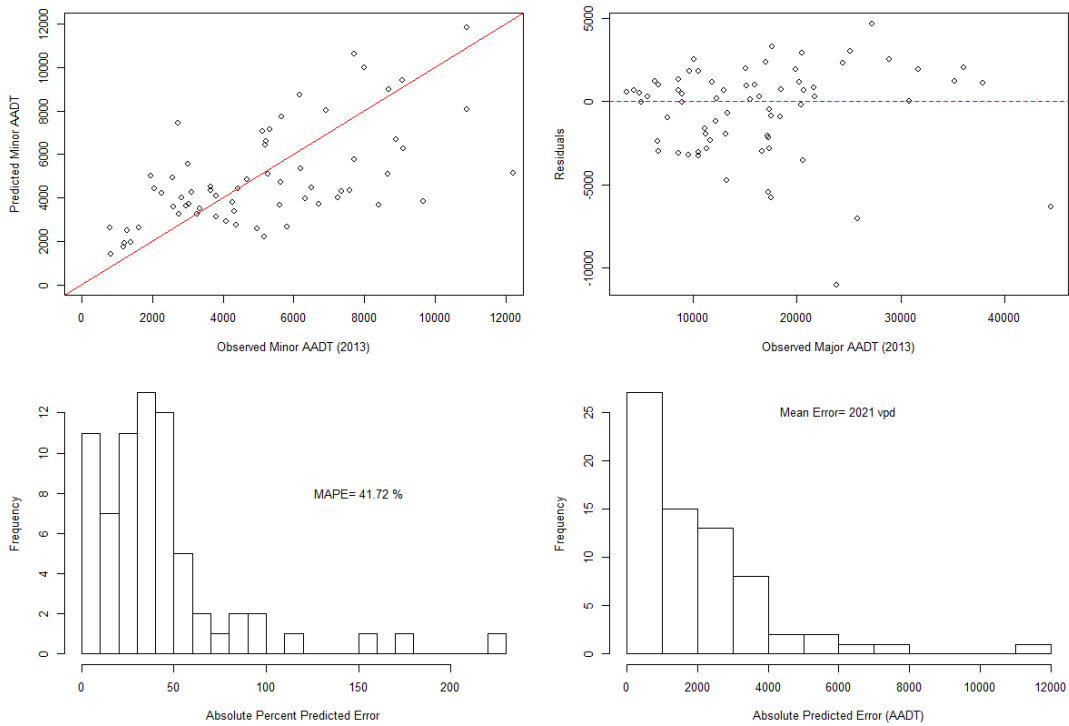


Figure C.4: Summary Diagnostic Plots for Total Minor Entering Volume (without Parallel Facility AADT)

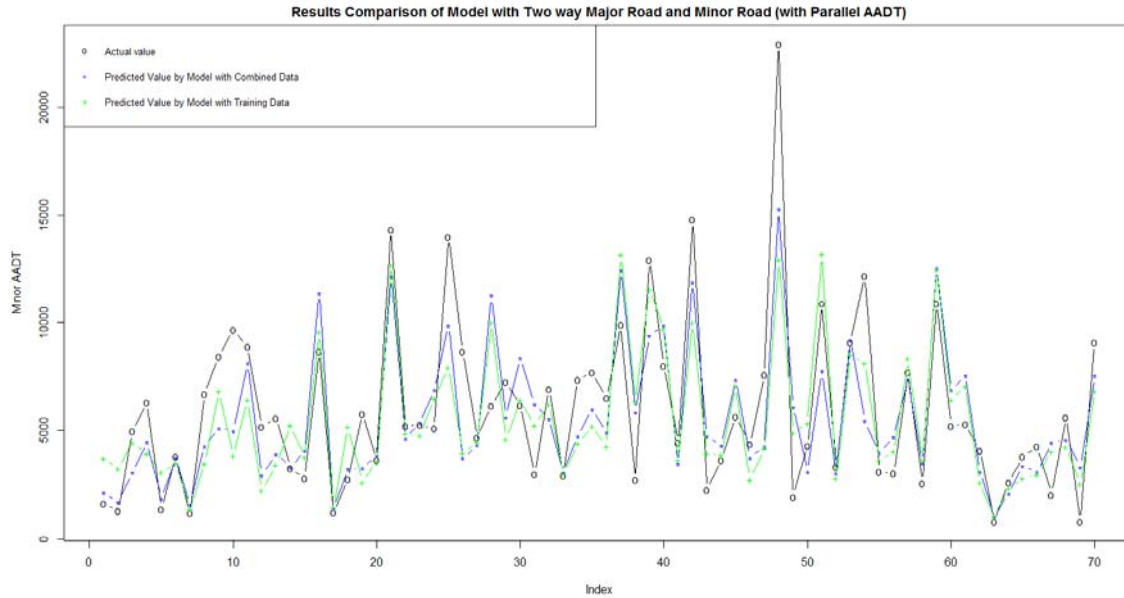


Figure C.5: Comparison of Estimated Total Entering Volumes to Observed Volumes for Minor Facility (with Parallel AADT)

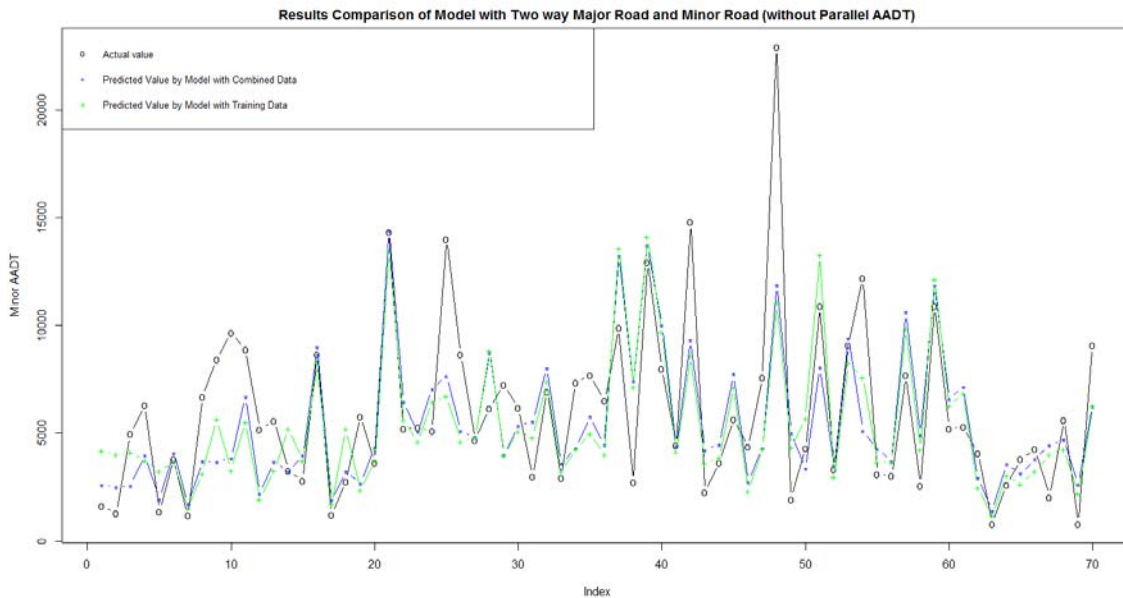


Figure C.6: Comparison of Estimated Total Entering Volumes to Observed Volumes for Minor Road (without Parallel Facility AADT)

C.4 MODELS TO ESTIMATE MINOR VOLUME BY LEG

A regression model was also estimated to predict minor volume by leg. This model could be used to predict minor road AADT for one way facilities. A total of 91 intersections were used in the combined model. As outlined previously, parallel facility volume was not used as a parameter to estimate minor AADT. Table C.7 shows the significant variables along with the

associated model fit parameters and goodness of fit parameters. The R-squared of the model is 0.60 and the standard error of the residuals is 0.25. As shown, three variables were significant predictors of the minor AADT. These included log transformed major road volume, average number of approach through lanes on minor facility and functional class of minor road. Except for functional class variable on the minor facility, the other two variables showed a positive relationship with minor facility AADT.

Table C.7: Model Outputs for Minor Volume Estimation Model by Leg (without Parallel Facility AADT)

Parameter	Estimate	Std. Error	t value	Pr(> t)
(Intercept)	2.1489	0.4007	5.36	6.7×10^{-7} ***
log(Major AADT)	0.1781	0.1035	1.72	0.0888*
Avg. Number of Approach Thru Lanes on Minor	0.3922	0.0507	7.74	1.66×10^{-11} ***
Func. Class Minor (Arterial=0, Collector=1)	-0.1959	0.0633	-3.10	0.0026***
Residual standard error	0.2452 on 87 degrees of freedom			
R-squared	Multiple R-squared: 0.6033, Adjusted R-squared: 0.5897			
F-statistic	44.11 on 3 and 87 DF, p-value: $< 2.2 \times 10^{-16}$			
* Significant at 90% confidence level				
** Significant at 95% confidence level				
***Significant at 99% confidence level				

Additional diagnostics of the model are shown in Figure C.7. Overall, the goodness of fit parameters presented in the tables and inspection of the figures reveal that the model does a reasonable job of estimating the minor road volume by leg. The mean absolute error is about 45 percent. Still, the majority of the estimates have less than 50 percent error and only a small number of locations have a high percent error. The mean error (the difference in the predicted minor volume and actual minor volume) is around 1,000 vpd. This corresponds to the error in the total entering volume since the analysis primarily modelled 50 percent of the AADT for the two-way legs. As shown in the histogram, the majority of these errors are less than 1000. The errors (residuals) do not show any trends over the range of major AADT included in the model.

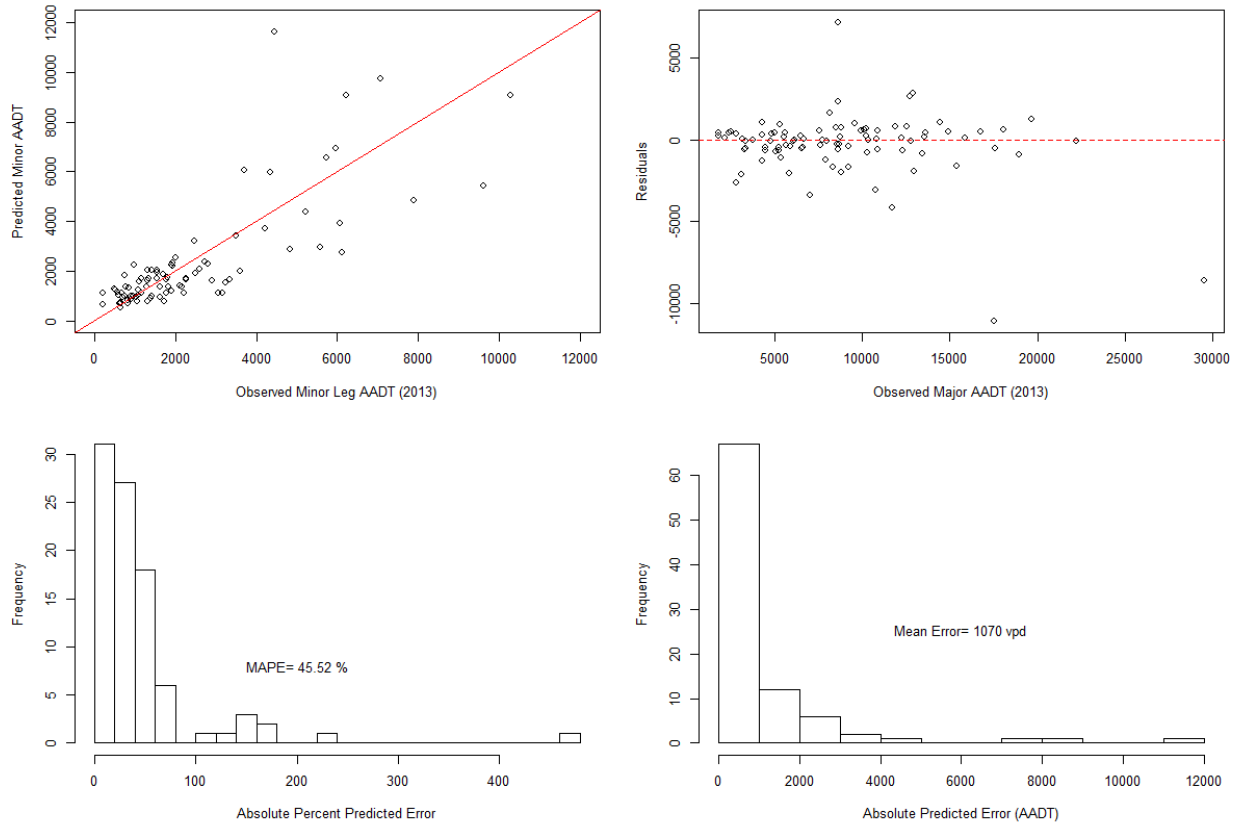


Figure C.7: Summary Diagnostic Plots for Minor Volume Estimation by Leg (without Parallel Facility AADT)

Figure C.8 shows the comparison between estimated volumes by leg and observed volumes for the minor facility with the training as well as combined data. Both the models perform reasonably well when estimating minor facility volume by leg.

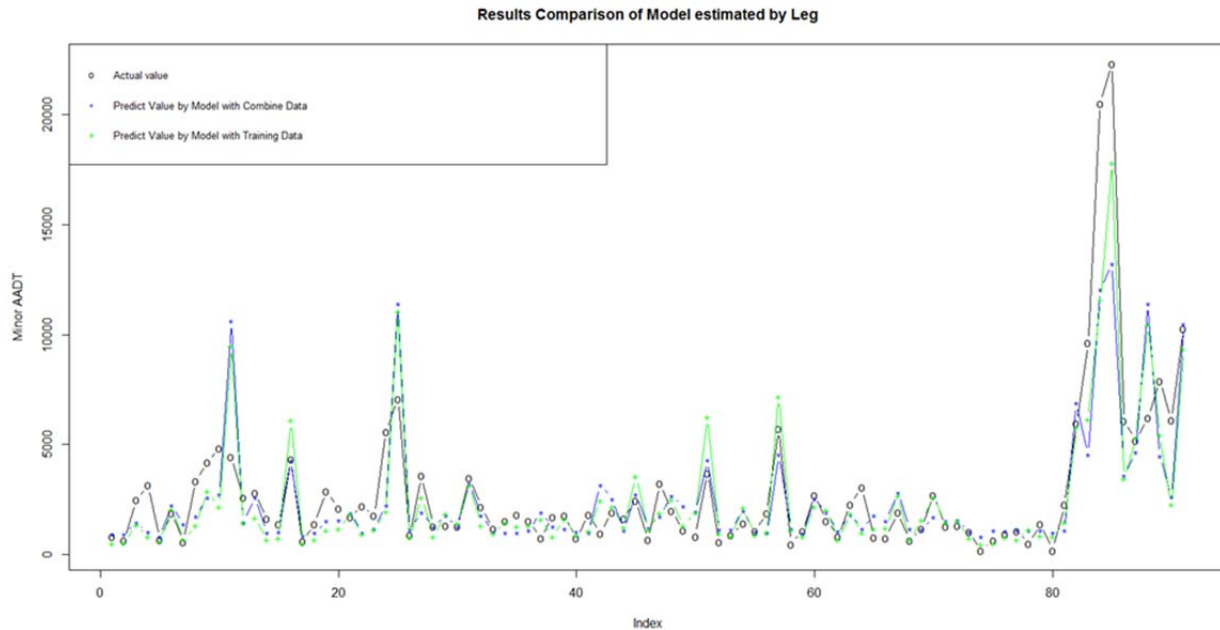


Figure C. 8: Comparison of Estimated Volumes by Leg and Observed Volumes for Minor Facility

C.5 SUMMARY

In this section, model validation was performed using twenty five intersections. Overall, the models estimated the minor facility AADT reasonably well. In addition, the regression models to predict minor facility AADT were also re-estimated using a larger set of intersections drawing from both the training and the validation set. A total of 91 intersections were used for re-estimation. Two sets of models were estimated for total entering volume and by leg without using parallel facility volume as a predictor. The goodness of fit parameters revealed that these models performed reasonably well in predicting minor road AADT and were similar to the models estimated using training data only. However, as the validation intersections were not chosen randomly, the research team recommends the use of models estimated using the training data only as outlined in Chapter 4.0 for estimating minor facility AADT.

APPENDIX D

PREDICTIVE METHOD VALIDATION

LIST OF APPENDIX D TABLES

Table D.1: Yearly Statistics for Complete 2013 Dataset for Temporal Validation	D-2
Table D.2: Yearly Statistics for Complete 2010-2013 Dataset for Spatial and Spatial-Temporal Validations	D-10

LIST OF APPENDIX D FIGURES

Figure D.1: Correlations Among Variables in Complete 2013 Dataset.....	D-3
Figure D.2: Marginal Distribution of Crashes compared to Site-Specific SPF Predictions	D-4
Figure D.3: Marginal Distribution of Crashes compared to Population SPF Predictions.....	D-5
Figure D.4: Observed vs. Predicted Crash Frequencies by Site for 2013.....	D-6
Figure D.5: Marginal Distribution of KAB Crashes Compared to the KAB SPF Predictions	D-7
Figure D.6: Observed vs. Predicted KAB Crash Frequencies by Site for 2013	D-7
Figure D.7: Comparison of KAB Predictions Using Alternative SPFs	D-8
Figure D.8: Correlations Between Variables in Complete 2013 Dataset.....	D-11
Figure D.9: Theoretical and Observed Marginal Distributions of Sites by Total Crash Frequencies: Spatial Validation Sample for 2010-2012	D-12
Figure D.10: Observed vs. Predicted Yearly Crash Frequencies for 2010-2012 at Spatial-Validation Sample	D-13
Figure D.11: Theoretical and Observed Marginal Distributions of Sites by KAB Crash Frequencies: Spatial Validation Sample for 2010-2012	D-14
Figure D.12: Observed KAB Crash Frequencies vs. KAB SPF Predicted Frequencies for 2010-2012	D-15
Figure D.13: Comparison of KAB Predictions Using KAB SPF and the Probability-Based Severity Model.....	D-16
Figure D.14: Theoretical and Observed Marginal Distributions of Sites by Total Crash Frequencies: Spatial- Temporal Validation Sample 2013	D-17
Figure D.15: Observed vs. Predicted Yearly Crash Frequencies for 2013 at Spatial-Temporal-Validation Sample	D-18
Figure D.16: Theoretical and Observed Marginal Distributions of Sites by KAB Crash Frequencies: Spatial- Temporal-Validation Sample for 2013	D-19
Figure D.17: Observed KAB Crash Frequencies vs. KAB SPF Predicted Frequencies for 2013	D-20
Figure D.18: Comparison of KAB Predictions Using KAB SPF and Severity Model on Spatial-Temporal-Validation Sample.....	D-20

APPENDIX D: PREDICTIVE METHOD VALIDATION

To confirm model reliability, this section of the report summarizes the validation activities for the signalized intersection SPFs for the state of Oregon. The focus of this validation analysis was to verify the predicting power of the previously developed (referred to as initial) signalized-intersection SPFs. The research team performed this verification using three approaches:

- Model temporal transferability: reviews the validity of model results for the same sites in the original analysis but for a new period of time (2013);
- Model spatial transferability: reviews the validity of model results for the same years in the original analysis (2010 through 2012) but at a new set of sites; and
- Model spatial-temporal transferability: verifies the predicting power of the model for a different time period (2013) at the new set of sites.

The basic validation approach is to directly compare the model crash predictions to a new independent sample of crashes. The transferability of the model is then satisfactorily validated if the differences between the observed and predicted crashes do not exceed the theoretical thresholds imposed by the model (i.e. differences are not statistically significant).

Prior to developing the SPFs, the research team determined the appropriateness of using a maximum threshold rule to match crashes to intersections. Accordingly, the research team used a threshold of 300 ft in combination with crash codes indicating the involvement of traffic control devices (TCDs) specific to signalized intersections.

D.1 TEMPORAL TRANSFERABILITY

To verify the temporal transferability of the models, the research team acquired crash data for an additional year (2013) at the same locations utilized in the SPF development phase.

D.1.1 Available Data for Temporal-Transferability Assessment

A total of 624 crashes that occurred in 2013 were identified in the vicinity of the 73 intersections comprising the modelling dataset. The definition of “vicinity” is, for the purpose of this analysis, the same as for the modelling dataset: a distance equal to or shorter than the maximum IFA in each intersection. Out of the 624 crashes, 423 were located within a radius of 300 ft, leaving 201 crashes to be examined for TCD indicators.

After querying the 201 crashes for TCD indicators, only 68 crashes had codes indicating signalized-intersection TCDs (i.e. Advanced Flashing Beacons, Left or Right turn Signal Phase, or Traffic Signal). However, most of the 68 crashes were related to other signalized intersections/driveways. The research team could identify only six out of the 68 crashes that were related to the study sites but beyond the 300 ft buffers.

In total, there were 429 crashes from 2013 available for the temporal transferability validation. The research team obtained AADTs using the same techniques used when developing the SPFs. Ultimately data from only 64 sites could be used for the validation effort since the research team could not identify AADT data for the nine excluded sites. A total of 370 crashes occurred in the vicinity of the 64 available sites. Even though there are 64 crashes with AADT data, there were sites with at least one speed limit value missing (a key focus of the SPF development). Consequently, the research team evaluated data from 54 of the initial model sites for the temporal validation analysis.

D.1.2 Characteristics of Filtered Dataset for Temporal-Transferability Assessment

The data the research team collected for the validation effort was filtered using the same approach utilized for the development of the SPFs. Data for the year 2013 was collected for the 54 sites noted in the previous section. This was the same dataset available to evaluate the validity of using the Total Crash Model and the Severity Model. In the case of the KAB SPF, an additional intersection was available with values for all the variables from the models. This additional intersection resulted in a complete dataset of 55 intersections for validating the KAB Model.

The largest dataset that contained all of the variables that were determined to be significant for all of the developed safety functions included 50 out of the 73 intersections. Table D.1 shows the summary statistics for this complete dataset.

Table D.1: Yearly Statistics for Complete 2013 Dataset for Temporal Validation

Variable Name	Description	Mean	Std.Dev	Min	Max	Total	N
Total Crashes	All crashes	6.4	5.99	0	31	320	50
MV_Crashes	Multiple vehicle crashes	5.98	5.91	0	30	299	50
KAB_Crashes	Fatal and serious injury crashes	0.96	1.11	0	5	48	50
MV_KAB_Crashes	Severe crashes with multiple vehicles	0.76	0.94	0	4	38	50
MjAADT	Major AADT (vpd)	17,353.78	8575.37	5019	44,464	867,689	50
MnAADT	Minor AADT (vpd)	7442.38	5221.59	800	22,924	372,119	50
MjSpLimMax	Major Speed Limit (mph)	33.8	7.73	20	55	1690	50
MnSpLimMin	Minor Speed Limit (mph)	28.3	6.97	10	45	1415	50

As shown in Table D.1, the average of total crashes for the year 2013 was 6.4, similar to the 5.74 crashes per year value in the complete dataset for the initial models. This value is also very close to the proportion of multiple vehicle (MV) crashes observed in the initial model dataset, which includes most of the crashes in the temporal validation set (299 MV crashes out of 320 total

crashes). Not surprisingly, the correlations between the explanatory variables and crashes in the dataset are also similar to the correlations in the initial model dataset as shown in Figure D.1.

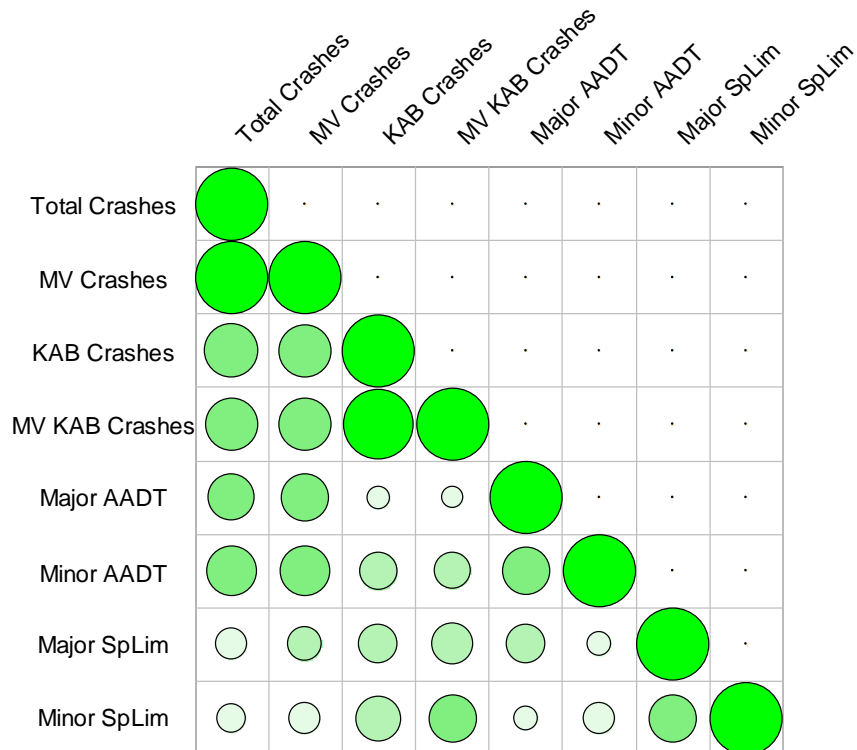


Figure D.1: Correlations Among Variables in Complete 2013 Dataset

The next section describes the evaluations of the predictive powers of the initial SPFs and companion Severity Model for the new 2013 dataset.

D.1.3 Temporal Transferability of Total Crashes SPF

The research team calculated the SPF predictions for 2013 at each site in the database utilized to develop the SPFs. Using these predictions, the research team estimated the expected marginal distribution of crashes. The first evaluation presented in this section compares this predicted marginal distribution to the actual marginal distribution of 2013 crashes, as shown in Figure D.2 and Figure D.3.

Figure D.2 shows the fit of the model using site-specific predictions, as obtained from the random terms originally obtained for each site. Because users will not know the specific random terms for sites other than those in the SPF development dataset, this comparison does not reflect the conditions that users of the SPF will face. In any case, there is some value to this comparison as a baseline to begin this analysis. However, no p-value can be computed for this fit because there are 54 site-specific random terms, which leaves a defect of 40 degrees of freedom, compared to the 15 classes available from the plot.

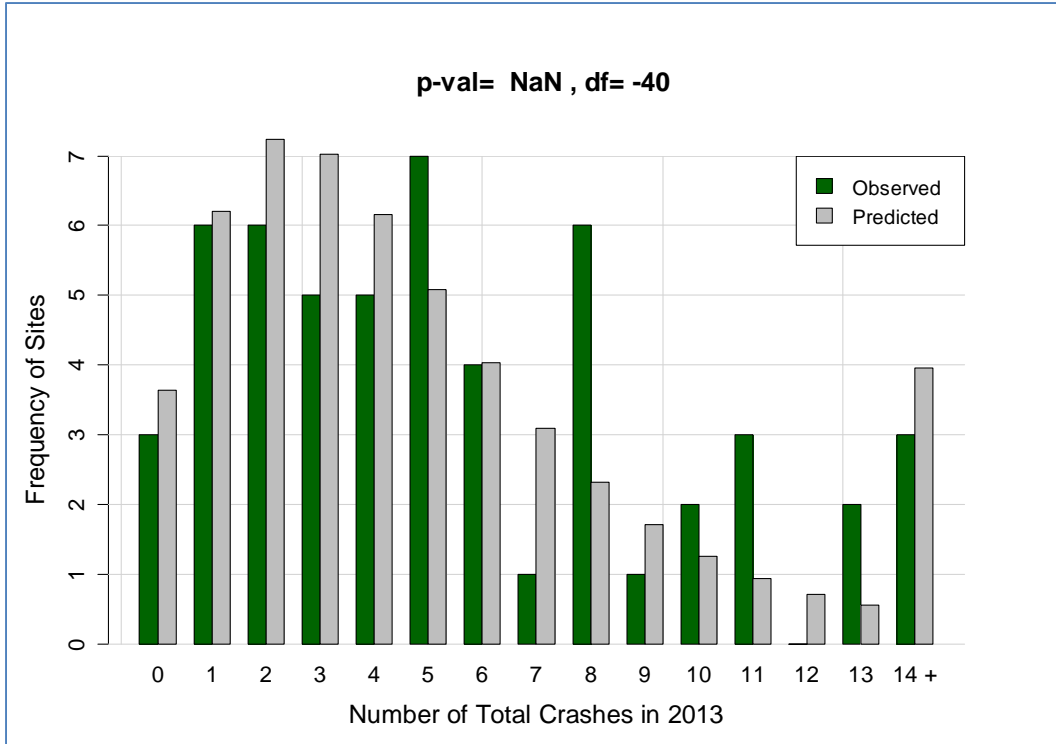


Figure D.2: Marginal Distribution of Crashes compared to Site-Specific SPF Predictions

Figure D.3, in contrast, shows a more realistic scenario: the marginal distribution fit of the SPF population-level predictions instead of the aggregate from site-specific predictions. It is notable how similar Figure D.2 is to Figure D.3; this similarity suggests that the explicit Poisson overdispersion included in the computation of the predictions is well-represented by the variation of the random effects, as defined for the Poisson log-normal mixed model (utilized in the predictions in Figure D.3).

It is possible to compute a Chi-Squared Goodness-of-Fit test for Figure D.3 since there are enough degrees of freedom for that purpose. The p-value represents the probability that the average of the relative squared differences between the two distributions is at least as extreme as observed in the plot, under the assumption that the predicted distribution is correct. This test indicates that the distribution of sites by their crash frequencies for 2013 corresponds very well to what would be expected from the developed SPF for total crashes, at a 0.05 significance level.

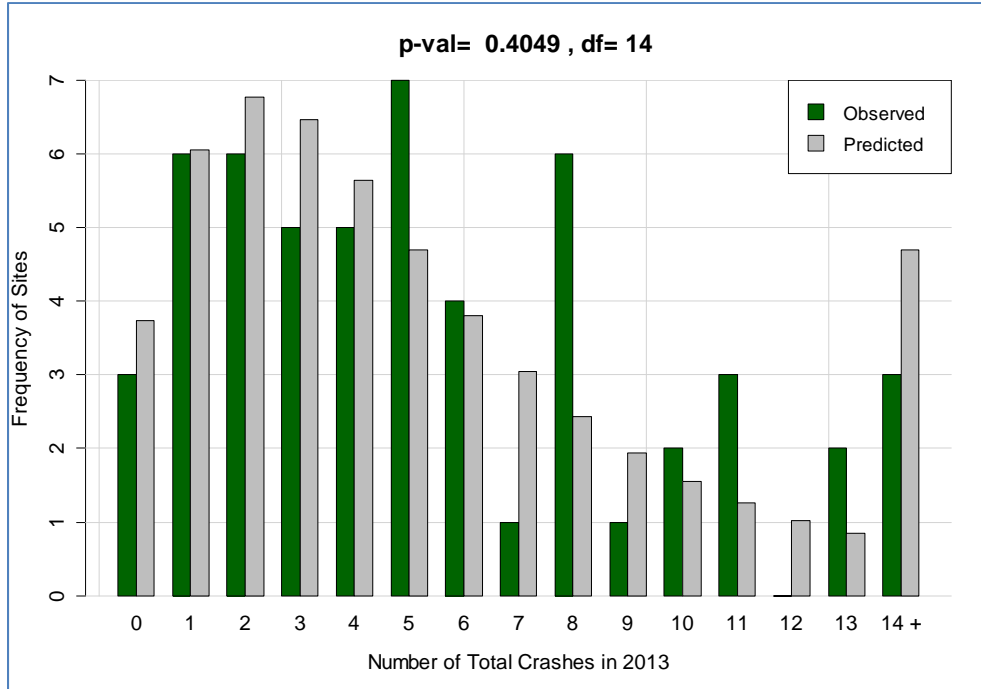


Figure D.3: Marginal Distribution of Crashes compared to Population SPF Predictions

The biggest absolute difference between distributions occurs for a frequency of eight crashes. There should be 2.431 sites with eight crashes according to the joint predictions from the Total SPF, but instead there were six sites with eight crashes in the dataset for 2013. However, this mismatch is offset by the better match between distributions for other crash frequencies: for example, the predicted frequency of sites with frequency of zero crashes is 3.738 sites whereas actually there are three sites with exactly zero crashes in the temporal validation dataset.

The next step in the temporal validation was an examination of the difference between the model prediction and the corresponding crash frequency site by site. Figure D.4 demonstrates this comparison graphically.

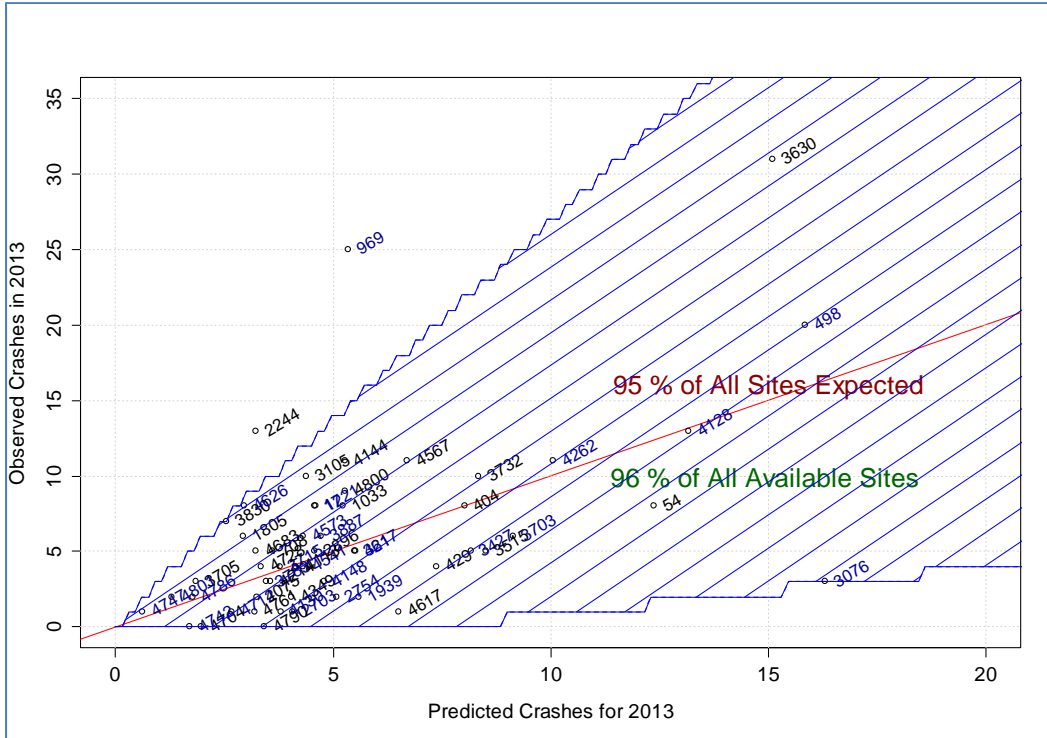


Figure D.4: Observed vs. Predicted Crash Frequencies by Site for 2013

The shaded zone corresponds to a region where 95 percent of all sites are expected to have their observed crash frequencies. Figure D.4 shows that 52 out of 54 sites have crash frequencies within this blue shaded zone, corresponding to 96 percent of all sites. This result indicates that the Total Crash SPF adequately predicts the crash frequencies observed in 2013.

D.1.4 Temporal Transferability of KAB Crashes SPF

The first comparison the research team performed was between the actual marginal distribution of KAB crashes in 2013 and the distribution of site frequencies predicted from the KAB SPF. Figure D.5 shows this comparison.

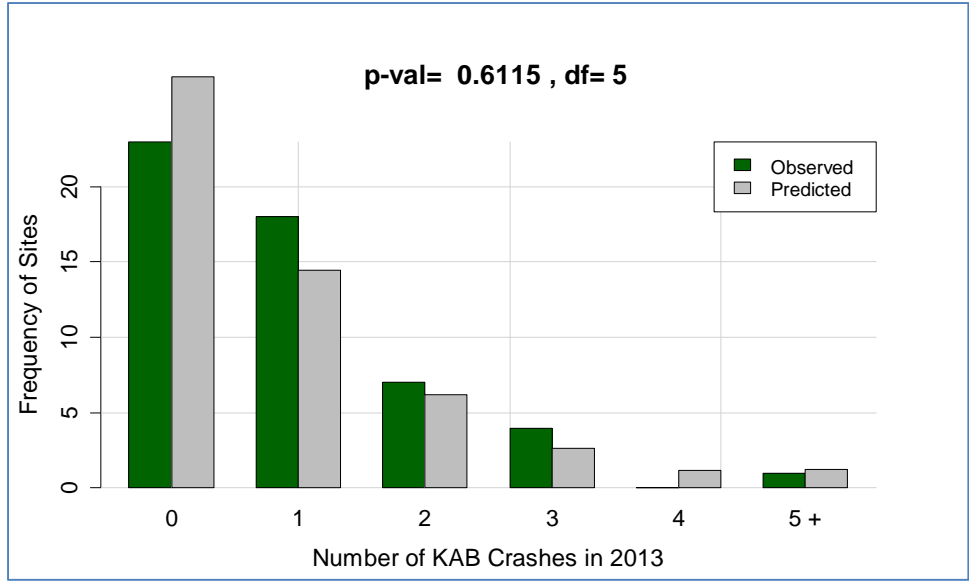


Figure D.5: Marginal Distribution of KAB Crashes Compared to the KAB SPF Predictions

The research team concluded that the data collected for 2013 is adequately described as a whole by the KAB SPF predictions for 2013, since Figure D.3 shows an approximate fit. Next, the research team examined the difference between the individual model predictions and the corresponding crash frequencies, similar to the comparisons for Total Crashes. Figure D.6 shows this result.

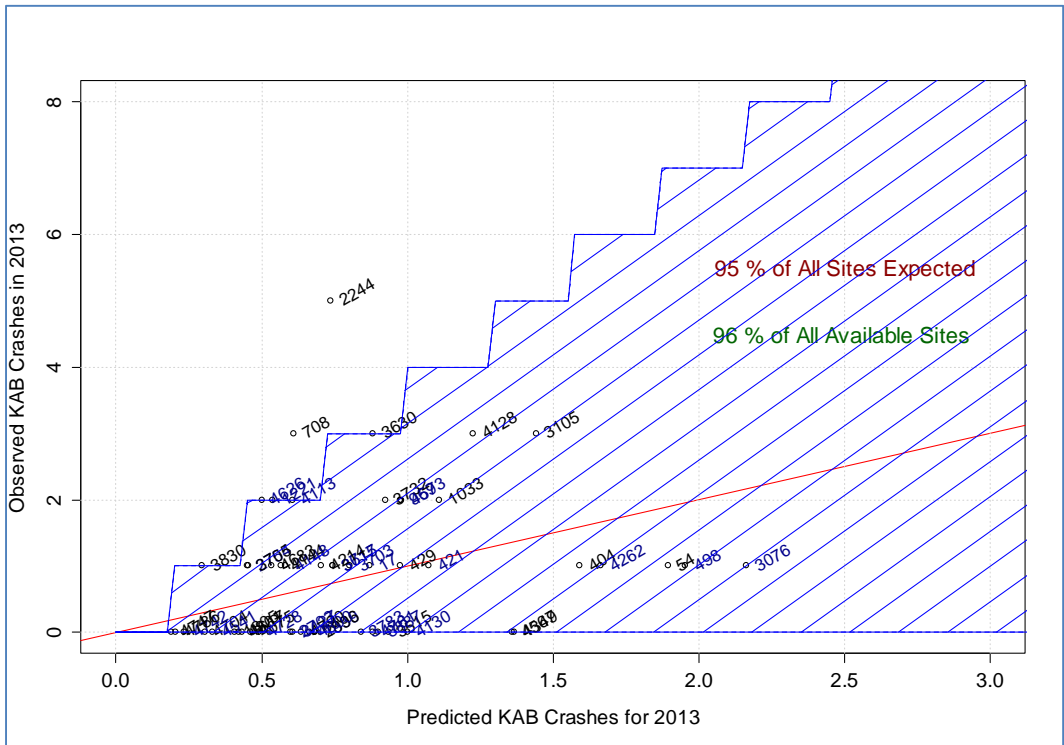


Figure D.6: Observed vs. Predicted KAB Crash Frequencies by Site for 2013

Figure D.6 shows that the deviations of actual number of crashes per site in 2013 are as expected when assessing the KAB SPF predictions. That is, only two sites had crash frequencies outside of the shaded zone. This observation indicates that 96 percent of the validation sites have crash frequencies in the zone where 95 percent of sites are expected. However, this figure also shows a limitation of the KAB SPF: a trend to over-predict crashes whenever the prediction exceeds 1.5 KAB crashes per year (i.e. all four sites with predictions larger than this threshold are below the 1:1 slope line). The research team proceeded to construct a similar graphic using predictions derived from the severity model in combination with the SPF for total crashes, the recommended method when the SPFs and severity model were originally developed. For comparison, Figure D.7 shows these new predictions next to the predictions from the KAB SPF already shown in Figure D.6.

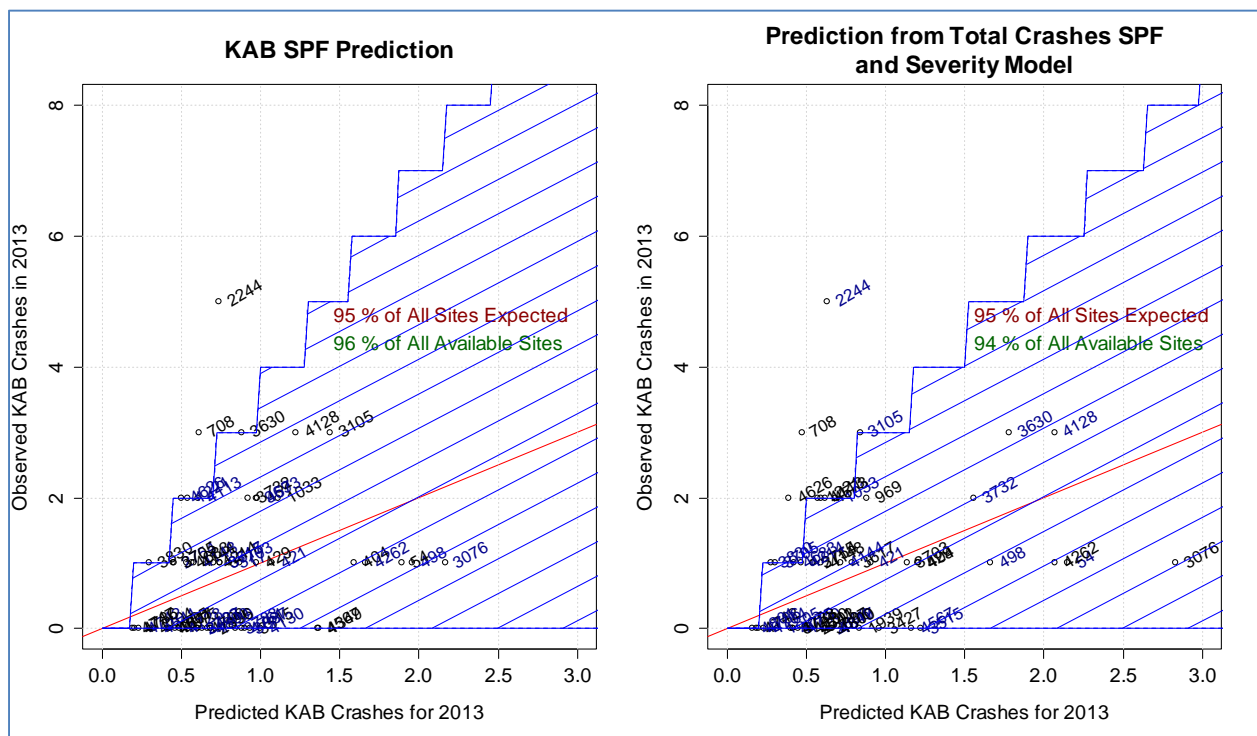


Figure D.7: Comparison of KAB Predictions Using Alternative SPFs

A comparison of the number of sites within the shaded area indicates that both models have very comparable overall prediction capabilities (respectively 96 and 94 percent of all sites within the zone with 95 percent frequency of sites expectation). However, this figure shows two clear advantages of using the Total Crash SPF combined with the Severity Model: (1) the shaded area is narrower than for the KAB SPF alone, which indicates more precision associated with the predictions from the Severity Model and Total SPF; and (2) the over-prediction problem for predictions equal to or greater than 1.5 associated with the KAB SPF is dissipated when using the combined Severity/Total Crashes prediction. Given these advantages, the research team concludes that KAB crashes should be predicted using the Severity Model in combination with the Total Crashes SPF instead of using the KAB SPF alone.

D.2 SPATIAL AND SPATIAL-TEMPORAL TRANSFERABILITY ASSESSMENTS

Similar to the temporal validation, the research team acquired detailed geometric data for a new set of 35 randomly-selected intersections by using the same selection procedure that resulted in the 73 intersections used for SPF development. Appendix F summarizes these individual intersections. The AADT values for these new sites were acquired or estimated in a similar way to the original 73-site sample. The research team collected crash data for years 2010 through 2013. This range of years includes 2013 in addition to the same period used in the SPF development. Therefore, the resulting dataset allows the assessment of spatial and spatial-temporal transferability of the SPF models. Because of the random selection, the validation set includes a variety of characteristics representative of typical conditions for signalized intersections in Oregon. For reference, Figure 3.2 (in Section 3.1.3) shows the location of the validation sites.

The research team acquired and matched crash data to the validation intersections in the same way as previously described (using the newly developed IR threshold procedure). The next section briefly describes this procedure.

D.2.1 Preparation of Data for Spatial and Spatial-Transferability Assessments

A total of 1187 crashes occurred from 2010 to 2013 in the vicinity of the 35 intersections in the validation dataset. In this case, the definition of “vicinity” includes a distance equal to or shorter than 600 ft at each intersection (300 ft upstream and 300 ft downstream), since a detailed analysis using Maximum IFAs was not developed for the spatial validation dataset. Out of the 1187 crashes, 712 were located within a radius of 300 ft, leaving 475 crashes to be examined for TCD indicators. After querying the 475 crashes for TCD indicators, only 171 crashes had codes indicating signalized-intersection TCDs (i.e. Advanced Flashing Beacons, Left or Right turn Signal, or Traffic Signal). However, most of these crashes were related to other signalized intersections/driveways in the vicinity of the study sites. The research team could identify only 11 additional applicable crashes out of the 171 crashes evaluated that were located beyond 300 ft of the study sites. In total, there were 723 crashes available for the spatial and spatial-temporal transferability evaluation.

D.2.2 Characteristics of Filtered Dataset for Spatial-Transferability and Spatial-Temporal-Transferability Assessments

Similar to the modelling phase, data completeness varied depending on the variables to be evaluated for each function under evaluation (i.e. the same variables used in the recommended SPFs and severity model). The largest dataset containing all the variables in any of the functions developed (both SPFs and the severity model) consisted of 80 site-years from 20 intersections. Table D.2 shows the summary statistics for this complete dataset.

As shown in Table D.2, the yearly average of total crashes in the validation subset was 5.36, very close to the 5.74 crashes per year in the complete dataset in the modelling stage. There was also a very similar proportion of MV crashes (394 MV crashes out of 429 total crashes). The

descriptive statistics are similar to those shown in Table 5.4; however, the range of minor AADT is limited in the validation dataset by the maximum value of 9898 vpd. In the modelling dataset, the maximum AADT for the minor road was 23,316 vpd. However, this is not a serious issue, as the validation range is contained in the range represented in the modelling dataset, suggesting that the models should have predicting power over the validation dataset. The only limitation is that the analysis will not be representative of the spatial and spatial-temporal transferability for sites with minor road AADT values larger than 10,000 vpd. Figure D.8 shows the correlations between the variables of interest and the different types of crashes.

Table D.2: Yearly Statistics for Complete 2010-2013 Dataset for Spatial and Spatial-Temporal Validations

Variable	Description	Mean	Std.Dev	Min	Max	Total	N
Total Crashes	All crashes	5.36	3.26	0	15	429	80
MV_Crashes	Multiple vehicle crashes	4.93	3.17	0	12	394	80
KAB_Crashes	Fatal and serious injury crashes	0.7	0.82	0	3	56	80
MV_KAB_Crashes	Severe crashes with multiple vehicles	0.46	0.75	0	3	37	80
MjAADT	Major AADT (vpd)	18,186.46	8136.85	6501	38,266	-	80
MnAADT	Minor AADT (vpd)	5780.60	2298.69	1750	9898	-	80
MjSpLimMax	Major Speed Limit (mph)	33.5	8.73	20	45	-	80
MnSpLimMin	Minor Speed Limit (mph)	28	7.70	15	45	-	80

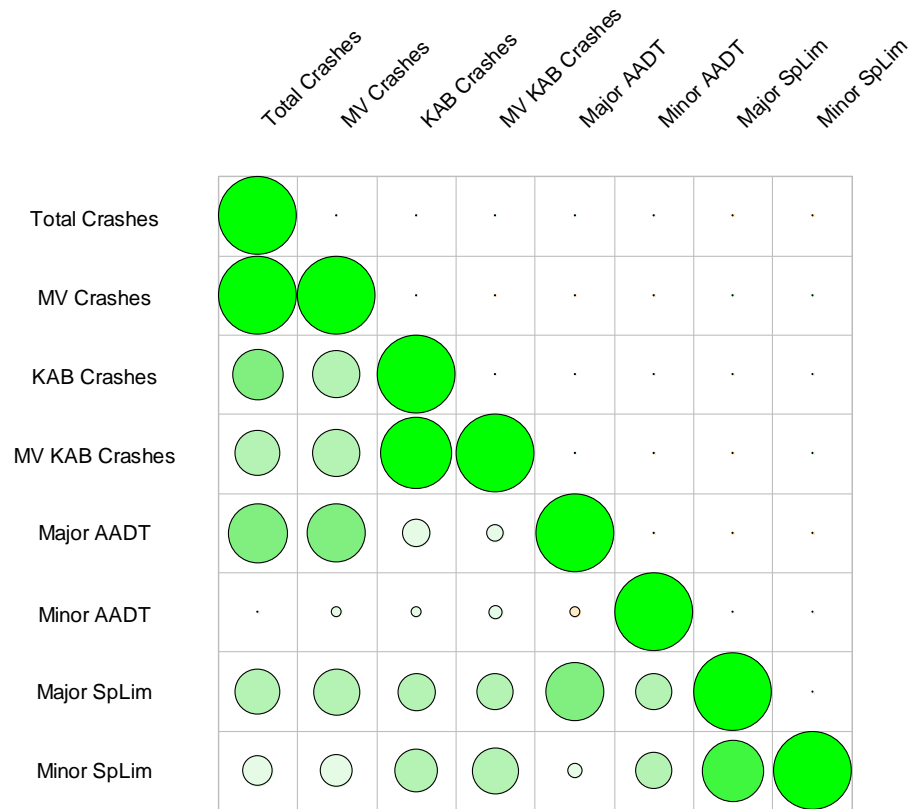


Figure D.8: Correlations Between Variables in Complete 2013 Dataset

With an exception of the minor road AADT, the correlations depicted in Figure D.8 demonstrate very similar relationships to those observed in the initial modelling dataset. The next section describes the spatial transferability evaluations of the SPFs and Severity model for the new dataset for the period 2010-2012.

D.2.3 Spatial Transferability of Total Crashes SPF

In a manner similar to the temporal transferability assessment, the research team calculated the SPF predictions for 2010-2013 at each site in the database of new sites and constructed the expected marginal distribution of crashes from these predictions. Figure D.9 shows a comparison between the theoretical and observed marginal distributions of crashes for the new set of sites. A Chi-Squared Goodness-of-Fit test indicates that the distribution of sites by their crash frequencies for 2010-2012 corresponds very well to what would be expected from the developed SPF for total crashes (at a 0.05 significance level).

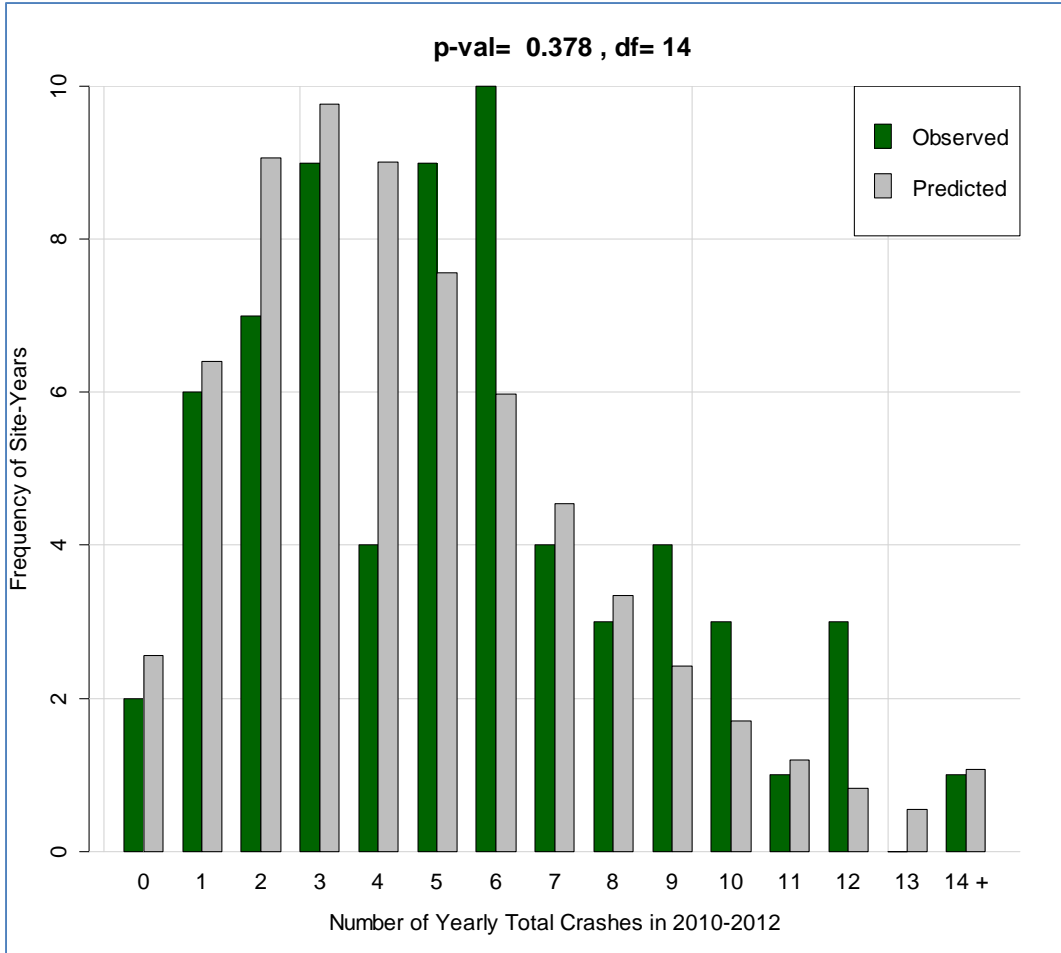


Figure D.9: Theoretical and Observed Marginal Distributions of Sites by Total Crash Frequencies: Spatial Validation Sample for 2010-2012

The research team then examined the spatial validation to determine the difference between the model predictions and the corresponding crash frequencies. Figure D.10 demonstrates this comparison graphically.

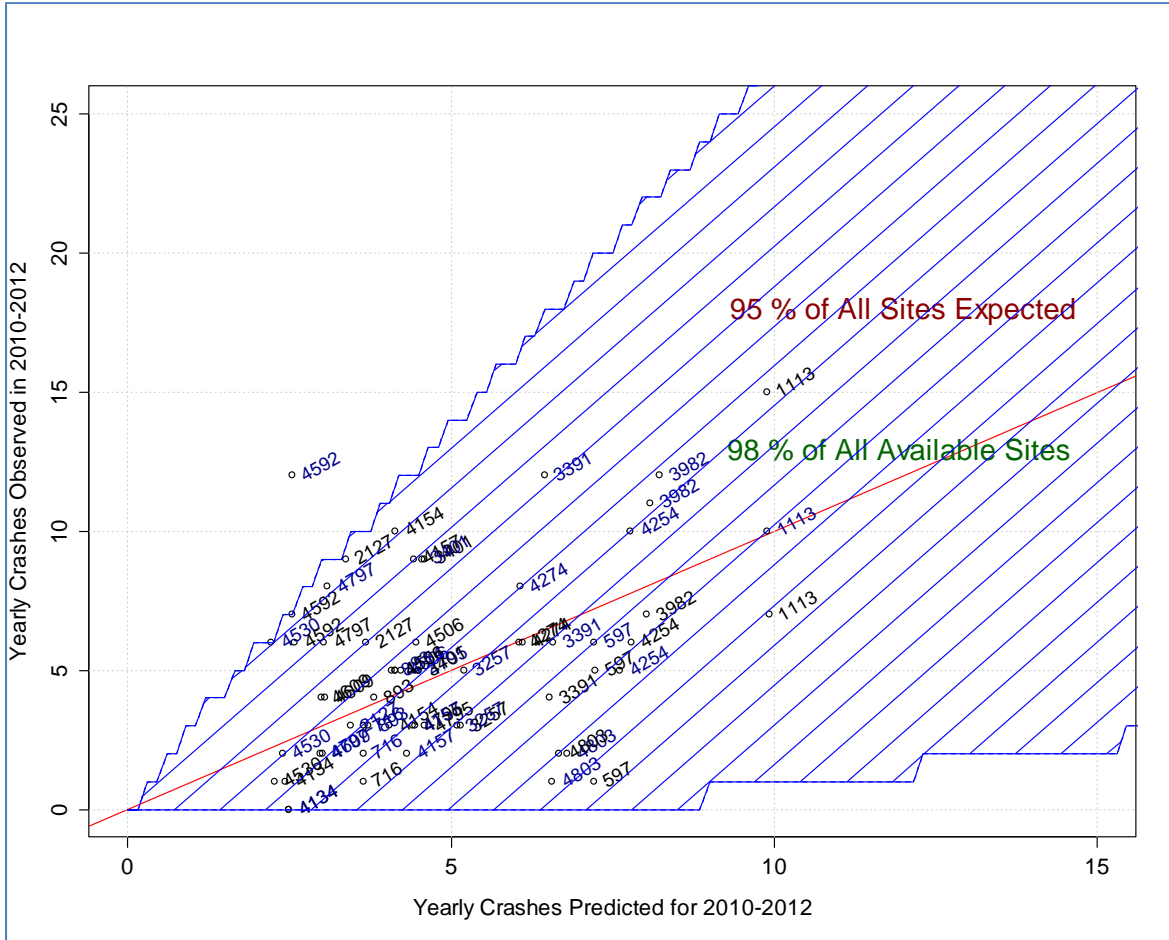


Figure D.10: Observed vs. Predicted Yearly Crash Frequencies for 2010-2012 at Spatial-Validation Sample

As before, the shaded region defines an area where 95 percent of all site-years are expected to have their observed crash frequencies. Figure D.10 demonstrates that 98 percent of all site-years have frequencies in this region. This result indicates that the Total Crash SPF predicts adequately the crash frequencies of additional sites for years 2010-2012.

D.2.4 Spatial Transferability of KAB Crashes SPF

Figure D.11 shows the first evaluation for the KAB SPF. This figure represents the comparison between the actual marginal distributions of KAB crashes in 2010-2012 for the spatial validation sample to the distribution of frequencies predicted by the KAB SPF.

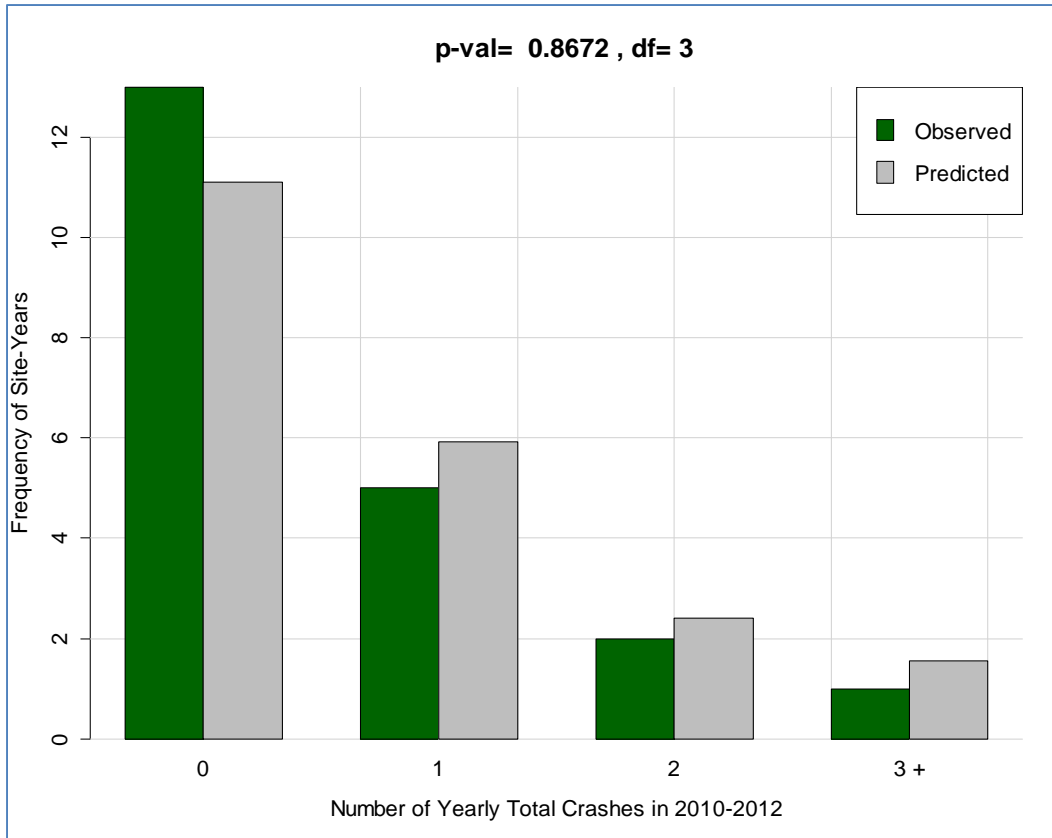


Figure D.11: Theoretical and Observed Marginal Distributions of Sites by KAB Crash Frequencies: Spatial Validation Sample for 2010-2012

This figure indicates a good correspondence between the sites in the spatial validation sample and the sites used for developing the KAB SPF in terms of their crash frequencies. The research team then examined the difference between individual model predictions and the corresponding crash frequencies, similar to the comparisons for total crashes (see Figure D.12).

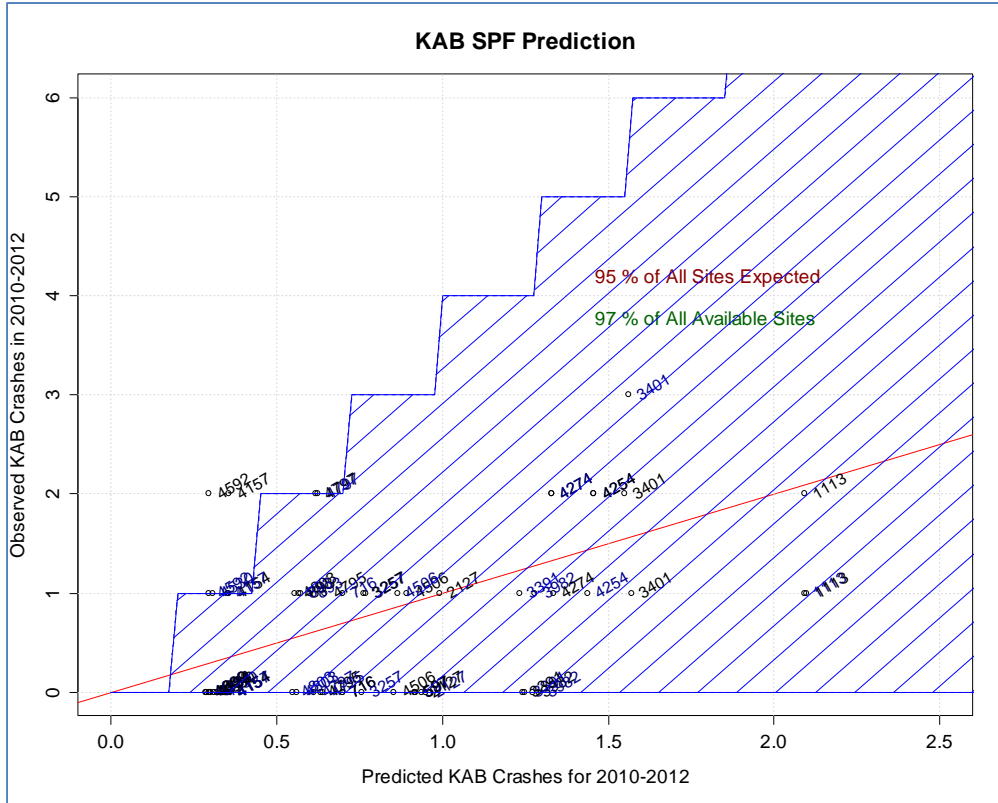


Figure D.12: Observed KAB Crash Frequencies vs. KAB SPF Predicted Frequencies for 2010-2012

This figure shows the same limitation of the KAB SPF identified in the temporal transferability: a trend to over-predict crashes after a certain threshold. In this case, the approximate threshold is a prediction greater than or equal to 1.6 KAB crashes per year. The research team computed the predictions derived from the severity model in combination with the SPF for total crashes for comparison, similar to the previous temporal transferability. Figure D.13 shows a comparison of how this method performs, as well as the same result shown in Figure D.12.

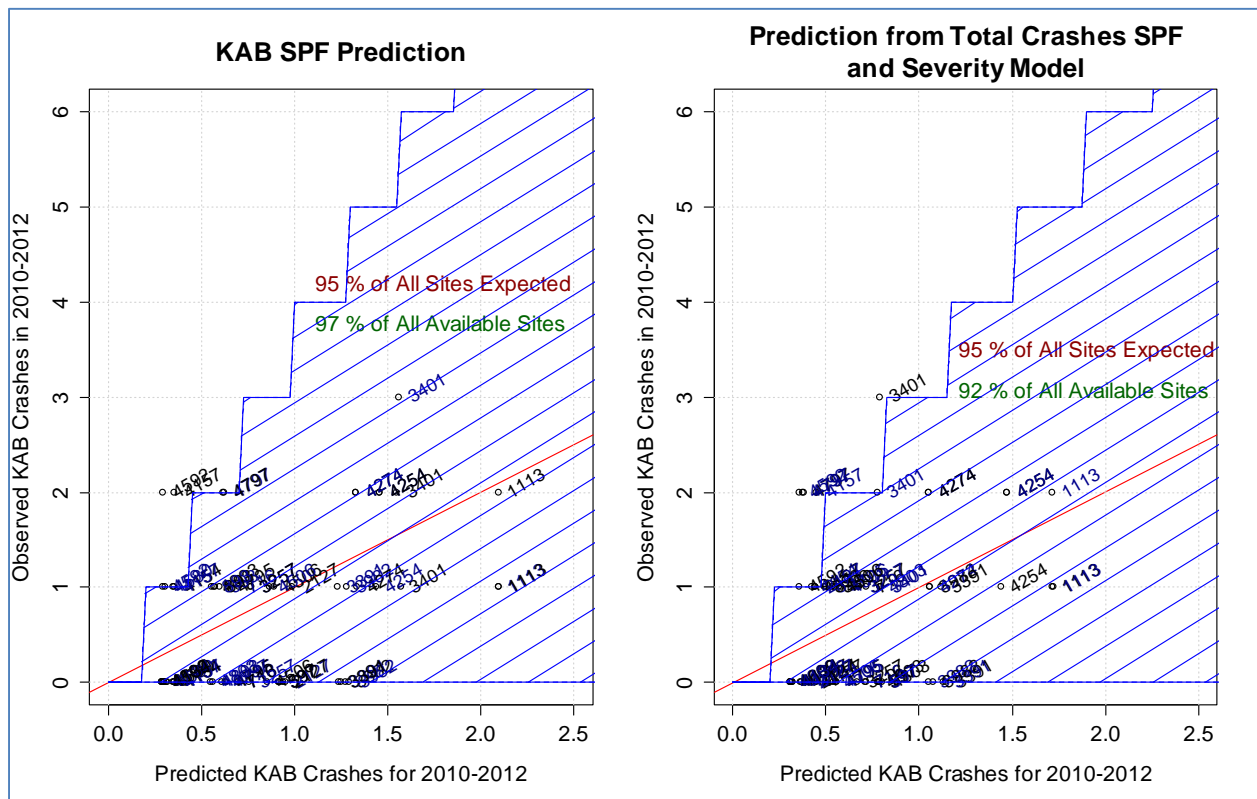


Figure D.13: Comparison of KAB Predictions Using KAB SPF and the Probability-Based Severity Model

The conclusions one can extract from Figure D.13 are similar to those that can be extracted from Figure D.7. There are two clear advantages of using the Total Crash SPF in combination with the Severity Model: (1) more precision associated with these predictions; and (2) the over-prediction problem associated with the predictions of the KAB SPF tends to disappear.

D.2.5 Spatial-Temporal Transferability of Total Crashes SPF

The final validation analyses performed by the research team compared the predictions of the SPFs and Severity Model to the 2013 crashes collected as part of the new validation dataset. These comparisons are expected to yield the largest deviations from the predictions since the crashes and the predictions have no spatial or temporal commonality (i.e. crashes come from different sites for a different time period).

Although Figure D.14 shows a certain degree of discrepancy, a Chi-Squared Goodness-of-Fit test fails to reject the hypothesis that the observed and predicted distributions are equal (p-value of 0.9154 on 12 degrees of freedom).

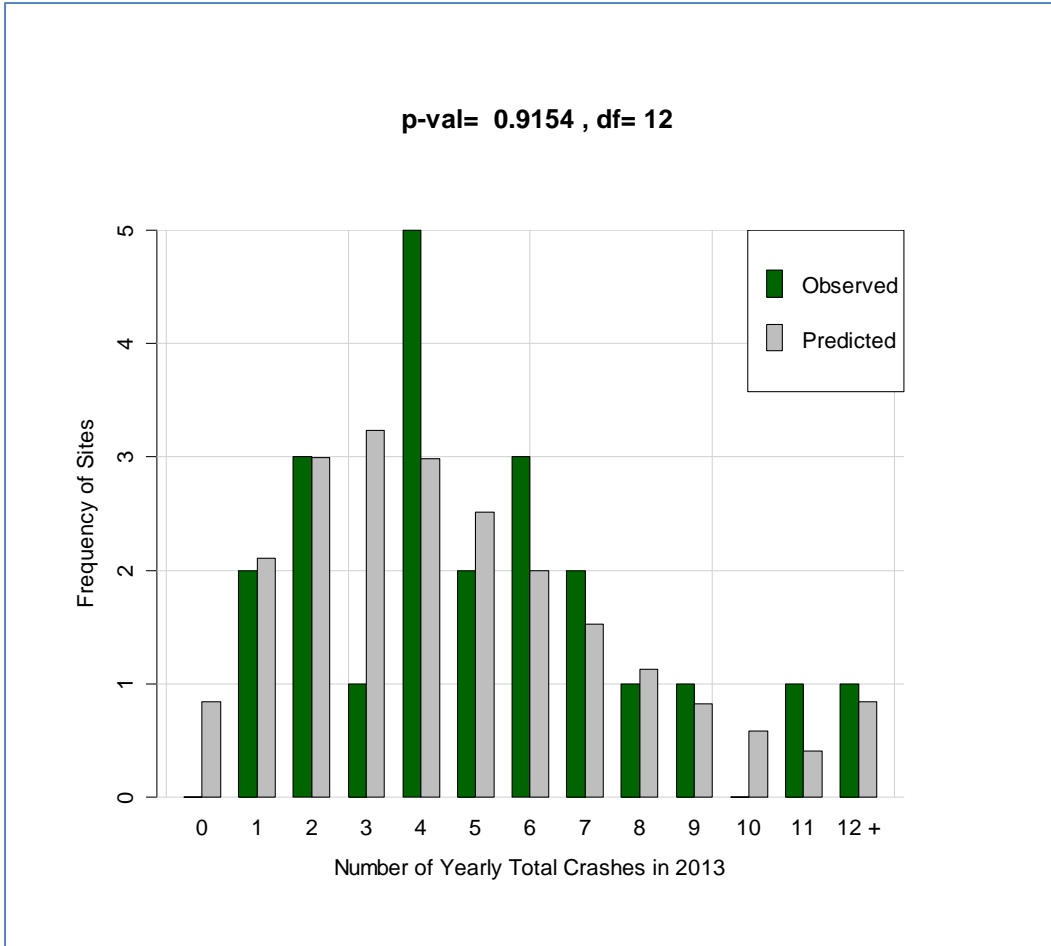


Figure D.14: Theoretical and Observed Marginal Distributions of Sites by Total Crash Frequencies: Spatial-Temporal Validation Sample 2013

Figure D.15 examines the difference between the model predictions and the corresponding crash frequencies at each site. It is clear from this figure that crash frequencies are within the area of 95 percent of expected frequencies. This demonstrates that the initial Total Crash regression model performed well for different time periods as well as for different locations.

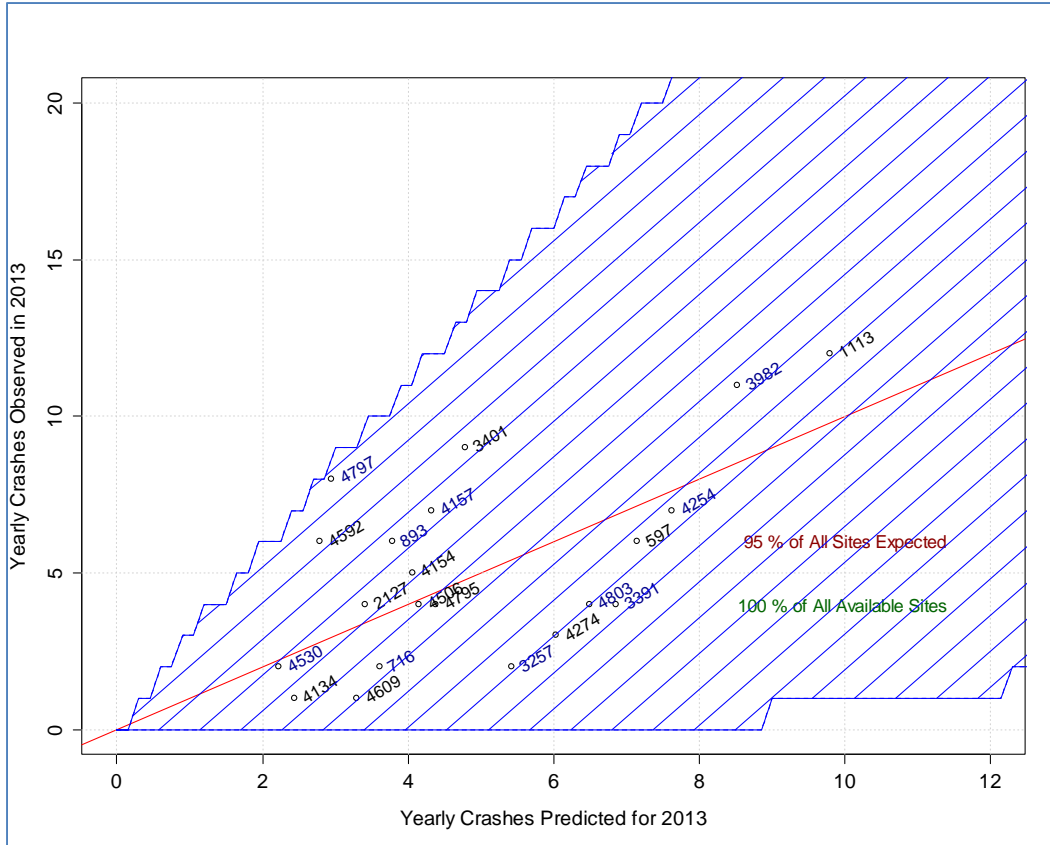


Figure D.15: Observed vs. Predicted Yearly Crash Frequencies for 2013 at Spatial-Temporal-Validation Sample

The next section describes the findings for the spatial-temporal validation of the alternative models to predict KAB Crashes.

D.2.6 Spatial-Temporal Transferability of KAB Crashes SPF

A comparison between the marginal distribution of site frequencies predicted from the KAB SPF and the distribution of KAB crashes in the spatial-Temporal validation sample for 2013 reveals a very close correspondence (see Figure D.16).

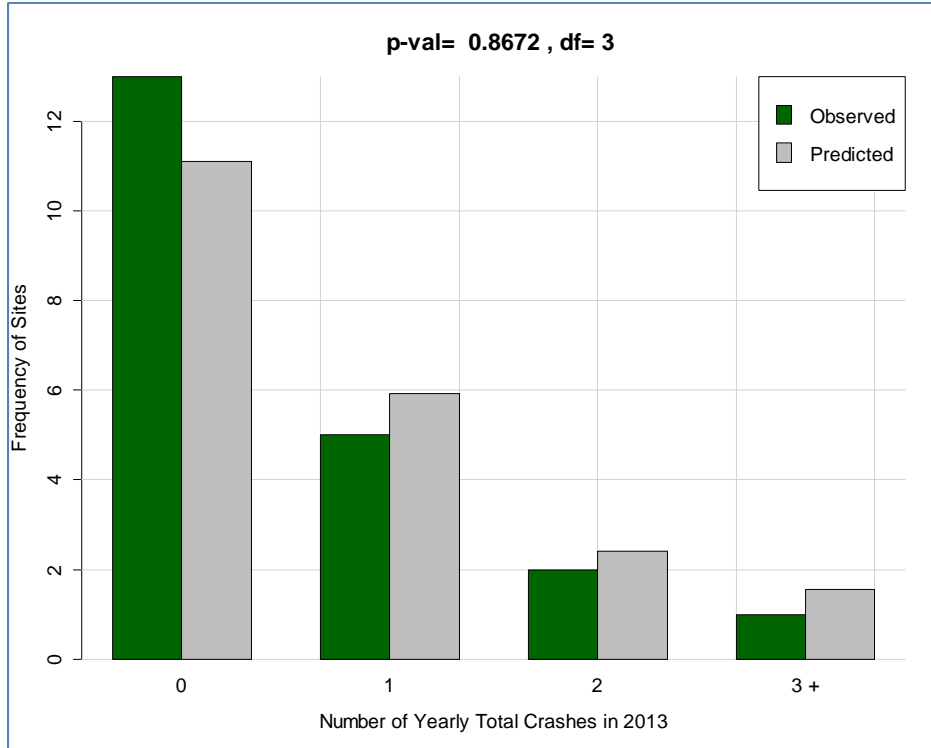


Figure D.16: Theoretical and Observed Marginal Distributions of Sites by KAB Crash Frequencies: Spatial-Temporal-Validation Sample for 2013

A Chi-Squared test fails to reject the hypothesis that the sites in the spatial-temporal validation dataset are associated with a different population than that described by the KAB SPF predictions (0.8672 p-value on three degrees of freedom). Next, the research team examined the differences between the individual predictions and observed crash frequencies at each site (see Figure D.17).

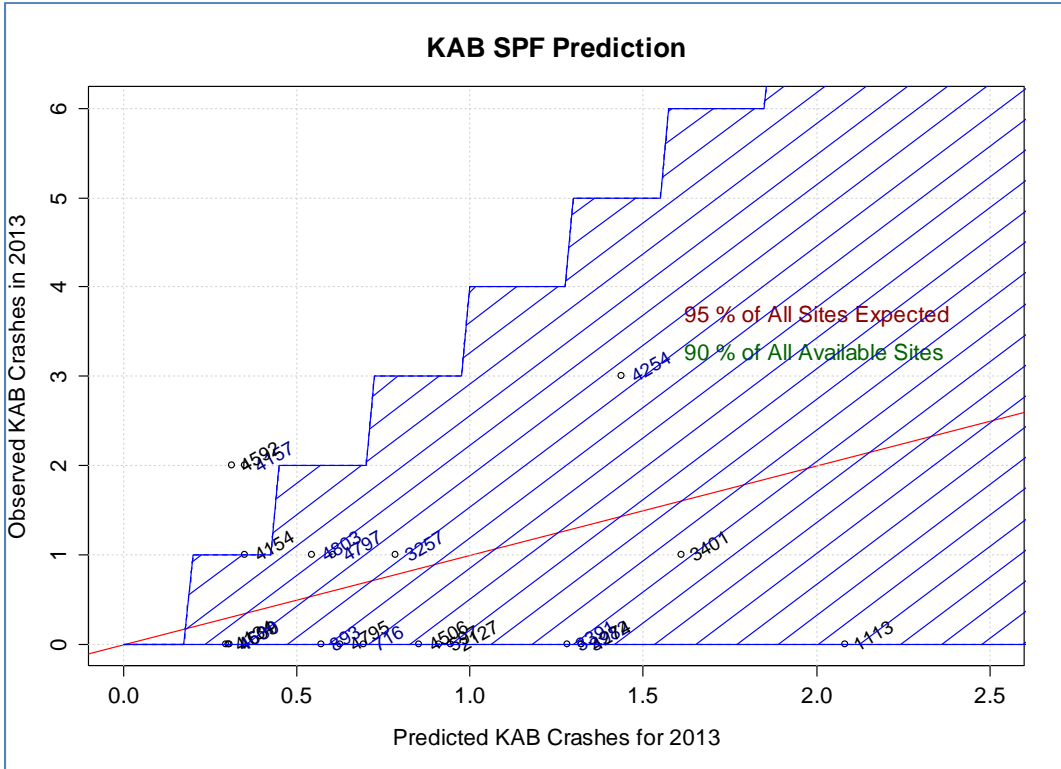


Figure D.17: Observed KAB Crash Frequencies vs. KAB SPF Predicted Frequencies for 2013

The number of sites with frequencies that would be considered typical, based on the KAB SPF predictions, is the lowest for this test (i.e. 90 percent actual frequency, compared to 95 percent expected frequency). This proportion, though it performed worse than the previous models, is still an acceptable threshold for the intended use of the KAB SPF. Additionally, it appears that the overprediction issue found in other tests is not so prominent in this case.

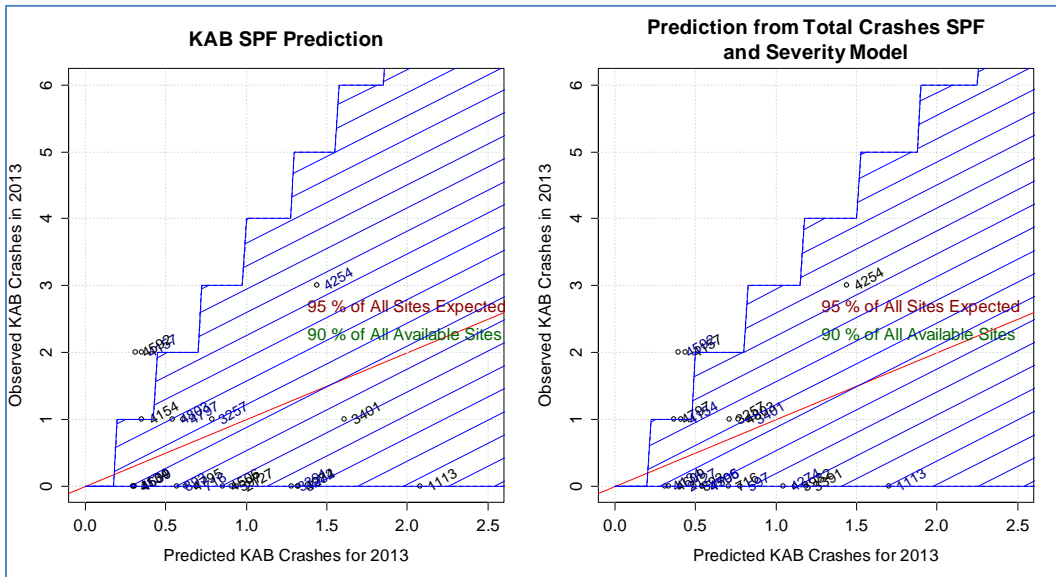


Figure D.18: Comparison of KAB Predictions Using KAB SPF and Severity Model on Spatial-Temporal-Validation Sample

The comparison in Figure D.18 shows the same trends observed in previous comparisons: it is preferable to predict KAB Crashes using a combination of the Total Crashes SPF and the Severity Model, because the predictions tend to be more precise. However, in terms of Spatial-Temporal Transferability, the performance of both this method and the use of the KAB SPF seem to be untarnished by the overprediction issue detected in previous analyses.

